Arenavirus-Host Interactions: Roles of Viral Glycoprotein and Nucleoprotein in Mediating Cell Entry and Host Immune Suppression

A DISSERTATION

SUBMITTED TO THE FACULTY OF

UNIVERSITY OF MINNESOTA

BY

JUNJIE SHAO

IN PARTIAL FULFILLMENT OF THE REQUIREMENTS

FOR THE DEGREE OF

DOCTOR OF PHILOSOPHY

ADVISOR: YUYING LIANG

CO-ADVISOR: HINH LY

JUNE 2018

Copyright

Acknowledgements

Firstly, I am indebted to the instruction and advisement I received from my advisors, Dr. Yuying Liang and Dr. Hinh Ly. I thank them for their indispensable technical knowledge, instruction on writing manuscript, advice on my career path, and for their encouragement and patience.

I would like to thank my wife and colleague, Dr. Xiaoying Liu, and our co-workers, for supporting my Ph.D. study.

I would like to express my gratitude to my peers and friends in the Liang-Ly Lab, including Dr. Qinfeng Huang, Dr. Vikram Verma, Dr. Rekha Dhanwani, Dr. Bjoem Meyer, Dr. Mythili Dileepan, Dr. Xi Kang, Dr. Junji Xing, Dr. Zheng Cai, and Dr. Xintao Zhang for their friendships, guidance and mentoring.

I would like to thank the Veterinary Medicine Ph.D. program (VMED) and its coordinators, Ms. Lisa Hubinger, Ms. Kate Barry, and faculty members for their supports.

Finally, I would like to acknowledge the funding source, NIH and Doctoral Dissertation Fellowship from the University of Minnesota.

Dedication

This thesis is dedicated to my family, my wife (Xiaoying Liu), son (Zhenghao Justin Shao), and daughter (Yuhao Kathleen Shao).

Abstract

Several mammalian arenaviruses can infect humans and non-human primates and can cause severe and deadly hemorrhagic fever diseases. There are currently no FDA-approved vaccines available for the prevention of infection by any of these pathogenic arenaviruses and treatment options for the infections are extremely limited. Arenavirus is an enveloped, bi-segmented, single-stranded RNA virus. Its genome encodes four viral proteins: the RNA-dependent RNA polymerase L, the nucleoprotein NP, the glycoprotein complex GPC, and the matrix protein Z. Arenaviral GPC plays critical roles in the first step of virus infection (i.e, cell entry), which involves receptor recognition and virus-host membrane fusion activity. Arenaviral NP is a multifunctional protein, which is involved in the formation of the viral ribonucleoprotein (RNP) complex needed for viral genome replication and transcription, and in host immunosuppression. Arenaviral L protein, together with NP, is responsible for genome replication and transcription. Arenaviral Z protein is the driving force of virion budding from the membrane of the infected cells and is also involved in mediating immune suppression. My study focused on the roles of arenaviral GPC and NP in mediating cell entry and host immune suppression. Arenaviral GPC is synthesized as a single polypeptide and is post-translationally processed by the cellular signal peptidase and S1P cellular protease into stable signal peptide (SSP), the receptor-binding GP1 and transmembrane GP2 subunits. My thesis focused on characterizing (1) the role of the glycoprotein SSP in mediating entry of the Pichinde virus (PICV) into cells in culture and its role in disease pathogenesis in guinea pigs, (2) the role of several conserved amino acids residues in the glycoprotein GP2 C-terminal domain (CTD) of PICV in mediating virus entry in vitro, and (3) the role of NP in mediating immune suppression via the PACT-RIG-I innate immune pathway.

Table of Contents

List of Tables

List of Figures

Chapter I

Introduction

Arenaviruses are ambisense RNA viruses that are divided into the Old World (OW) and New World (NW) virus groups based on their phylogenetic, serological, and geographical differences. While the prototypic OW arenavirus LCMV with worldwide distribution causes only mild illness in immunocompetent individuals, two other known OW arenaviruses (LASV and LUJV, both found in Africa) can cause severe hemorrhagic fever (HF) in humans. In addition, several of the NW arenaviruses in South America (e.g., JUNV, MACV, SABV, GTOV, and CHPV) can also cause severe hemorrhagic fevers (HF). There are currently limited preventative and therapeutic options for patients infected with these highly pathogenic viruses. Candid #1 is the only vaccine currently available against JUNV infection (1) but is only licensed for the endemic areas in Argentina. Ribavirin, a nucleoside analog, has been used for the treatment of arenavirus infections but it has had mixed success and significant toxicity (2).

Besides the aforementioned pathogenic human arenaviruses, there are many other known and emerging arenaviruses that have no known causal roles in humans (3, 4), including but not necessarily limited to a new group of snake-borne arenaviruses in the Reptarenavirus genus of the Arenaviridae family(5) An important question is why some arenaviruses cause severe disease in humans, while others do not. Recent studies using viral reverse genetics, cell-based assays, animal models, and human genome-wide association analyses have revealed several potential mechanisms of arenaviral

pathogenicity. We will summarize current understanding of the roles of the different viral and cellular factors that contribute to the degrees of arenavirus virulence in humans.

1. Human diseases caused by OW and NW arenaviruses

LASV is responsible for up to 300,000 infections and 5,000-10,000 deaths annually in endemic areas of West Africa (2). LASV infection, which is often misdiagnosed, can result in a wide range of disease symptoms ranging from non-symptomatic to multi-organ failure and death. Some general symptoms include fever, cough, sore throat, malaise, severe headache, nausea, vomiting, diarrhea, and can develop into petechial hemorrhage, facial swelling (edema) (6). More severe symptoms include pleural effusion, thrombocytopenia, leukopenia, sensorineural hearing loss that occurs in up to one-third of patients encephalopathy, seizures, coma, mucosal bleeding, pulmonary edema, respiratory distress, and shock that culminates in the death of the patients (6, 7). The only other known hemorrhagic fever-causing OW arenavirus LUJV was identified during an outbreak of the disease in Lusaka (Zambia) and Johannesburg (Republic of South Africa) in 2008 (8). LUJV-infected patients experienced fever, diarrhea, vomiting, chest pain, sore throat, rash, myalgia, facial and/or cerebral edema, mild bleeding, respiratory distress, elevated liver transaminases, and thrombocytopenia (9).

The OW LCMV virus is found worldwide because its natural host (mus muculus) has a wide distribution. While most acquired LCMV infections are either asymptomatic or mild (e.g., fever, sore throat, cough, headache, muscle aches, malaise, photophobia, nausea, vomiting, thrombocytopenia and leukopenia) (10, 11) , LCMV infections have also been shown to cause neurological symptoms, such as aseptic meningitis or

meningoencephalitis (10, 11). Patients with meningitis may experience fever, headache, myalgia, stiff neck, malaise, and nausea, while those with meningoencephalitis can present with more severe neurological symptoms such as confusion and motor-sensory abnormalities. While acquired LCMV infection does not pose a serious threat to immune-competent adults, congenital infection with LCMV can be quite serious. Congenital LCMV infection can result in spontaneous abortion and fetal death, or leave infants with permanent visual and/or neurological impairments. While 35% of reported cases of congenital LCMV infection are fatal (12), we do not know the exact incidence of congenital LCMV infections since infants are not commonly tested for the infection and that only serious cases have been reported (13). In recent years, LCMV has shown to be an important pathogen that can cause severe symptoms in solid organs transplanted recipients, including but not necessarily limited to encephalopathy, coagulopathy, thrombocytopenia, leukocytosis, and graft dysfunction. Fourteen cases of LCMV infection in transplant recipients have so far been identified, eleven of which have proven fatal (14-16). Another OW arenavirus (Dandenong virus) was isolated from fatal organ-transplant patients (9).

Several South American NW arenaviruses (e.g., JUNV, MACV, GTOV, CHPV, and SABV) can cause HF with high rates of mortality in humans. While only small numbers of human infections with SABV and CHPV are known (17, 18), many cases of human disease have been reported for JUNV, MACV or GTOV (19-25). JUNV is the causative agent of Argentine hemorrhagic fever. JUNV-infected patients may show mild symptoms such as fever, myalgia, mild hypotension, conjunctivitis, petechial hemorrhage of the soft

tissues, lethargy, and irritability. However, in severe cases, patients can experience hemorrhagic fever, leukopenia, thrombocytopenia, shock and seizures (24). Other pathogenic NW arenaviruses (e.g., MACV, SABV, GTOV, and CHPV) can also cause a wide range of symptoms, ranging from fever, sore throat, headache, myalgia, nausea, abdominal pain, vomiting, diarrhea, mucosal and/or conjuntival petechia to more severe symptoms, such as thrombocytopenia, leukopenia, hematuria, tremors, pulmonary edema, respiratory distress, coma, shock, and hepatic and gastrointestinal hemorrhages and necrosis. While hepatitis is common in severe cases of Lassa fever, it is unusual or mild in South American hemorrhagic fevers. Neurologic symptoms, hemorrhaging, leukopenia, and thrombocytopenia are more common in JUNV, GTOV, or MACV infections than LASV infections (26).

2. Basic biology of arenaviruses

2.1. Genome structure

The arenavirus genome is composed of two single-stranded negative-sense RNAs of about 7.2 kb and 3.5 kb (**Fig. 1**). Each of genomic segments codes for two proteins from opposite orientation known as ambisense coding strategy. The large (L) segment encodes the RNA-dependent RNA polymerase (RdRp) L protein and matrix protein Z. The small (S) segment encodes the nucleoprotein (NP) and glycoprotein precursor (GP) (27). Arenavirus genomic RNA segments do not serve as the template for translation directly. Due to the ambisense coding strategy (**Fig. 2**), the NP and L mRNAs are transcribed from genomic RNAs, whereas the GP and Z viral mRNA are transcribed from the anti-

Fig. 1

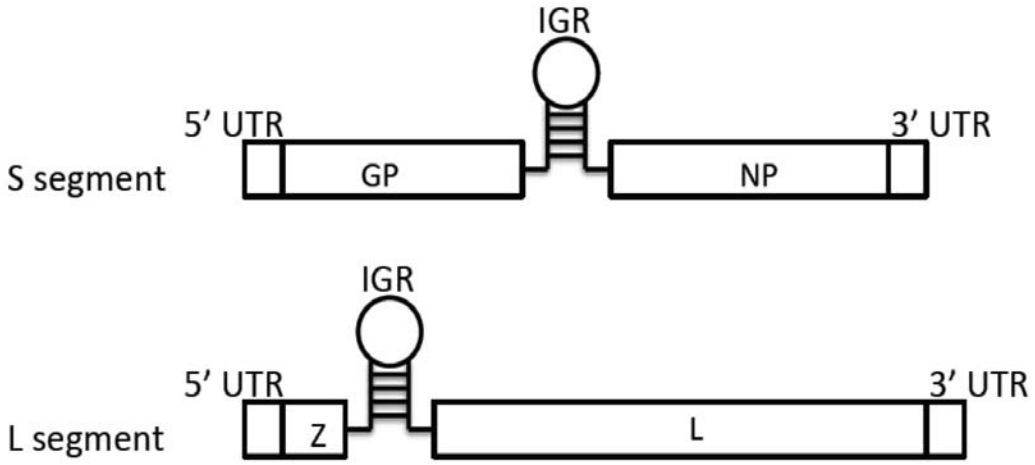

Fig. 1. Arenavirus genome structure: Arenaviruses are enveloped RNA viruses with a single-stranded ambisense genome that is composed of two segments. The genomic L (large) segment encodes the Z matrix protein and the L polymerase protein, and the S (small) segment encodes the glycoprotein (GP) and nucleoprotein (NP). The genes encoded on each segment are separated by noncoding intergenic regions (IGR). The linear genomes are flanked by the conserved 5' and 3' untranslated regions (UTRs).

genomic RNAs. The intergenic region (IGR) separates the two genes on each RNA segment, and the hairpin structure of IGR is believed to provide the termination signal of transcription.

The untranslated regions (UTRs) at the 5' and 3' termini of each RNA segment are conserved among arenaviruses. Like other negative-strand RNA viruses, these UTRs are complementary to each other and therefore can form panhandle structures (28). The UTRs also play an important role in viral nucleocapsid formation and favor the viral

Fig. 2

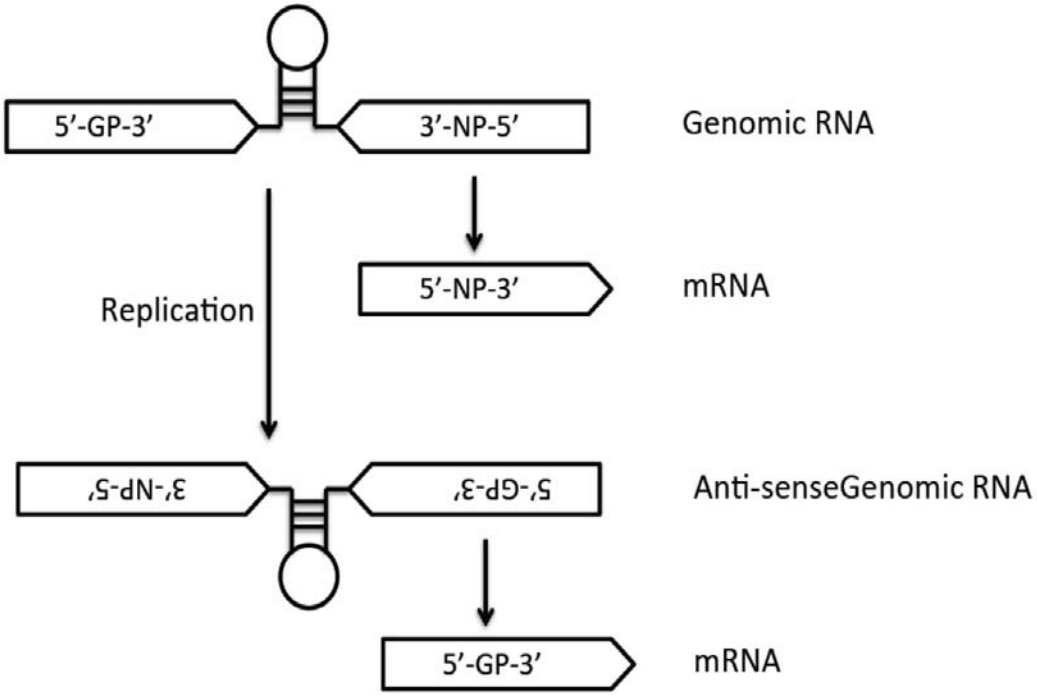

Fig. 2. Arenaviral ambisense-genome replication strategy: due to the ambisense coding strategy of the arenaviruses, the NP (and L) genes are transcribed directly from the viral genomic segments into mRNAs, whereas the GP (and Z) mRNAs must be transcribed from the antigenomic strands after genome replication.

polymerase recognition of the viral termini to initiate replication and transcription (28).

2.2. Virus entry mechanisms

The life cycle of arenaviruses starts with virus attachment and entry into cells (**Fig. 3**). The OW and NW clade C arenaviruses use α-dystroglycan (αDG) as their primary receptor (29, 30). Dystroglycan is a ubiquitously expressed glycoprotein that links cells to the extracellular matrix (ECM). It contains two non-covalently associated subunits, αDG, and βDG, which play different roles in virus attachment and cellular function. αDG is an

extracellular subunit that associates with ECM proteins such as laminin, agrin, perlecan, and neurxins. Upon virus infection, the viral glycoprotein 1 subunit (GP1) mediates attachment to the αDG, which allows the viral particles to internalize and deliver to the late endosomes. βDG is a transmembrane protein that binds to the cytoskeletal adaptor proteins and signaling molecules, but is not required for arenaviral binding and infection (31).

Fig. 3.

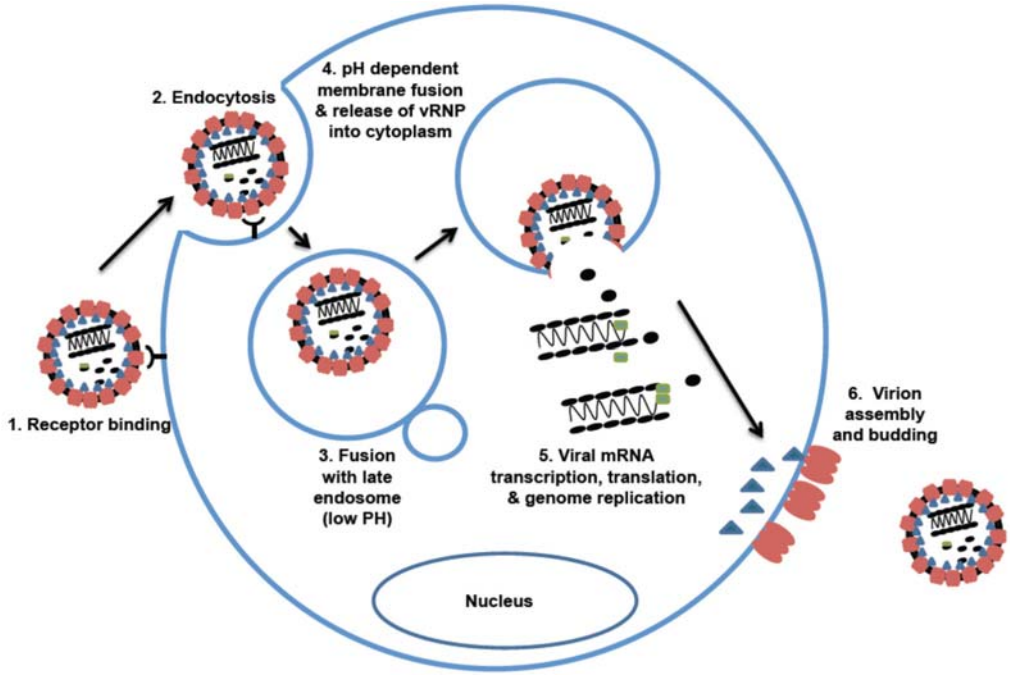

Fig. 3. Arenavirus life cycle. 1. Cellular entry is mediated by different cellular receptors (αDG for OW and NW clade C arenaviruses; TfR1 for NW Clade B). Entry of some viruses (e.g., LASV) may also involve a pH-dependent switch to an intracellular receptor (LAMP1) located in the lysosomes. 2. Virus uptake into cells is mediated by endocytosis (OW arenaviruses: clathrin-independent, NW: clathrin-dependent). 3. Virus fusion occurs with the late endosome. 4. Viral RNP is released into the cytoplasm via a pH-

dependent membrane fusion mechanism. 5. Viral genome replication, transcription, and protein expression strictly occur in the cytoplasm. 6. Virion assembly and budding occur at the plasma membrane.

αDG is a highly glycosylated protein, and studies have shown that post-translational modification of αDG is essential for viral binding (31). Many cellular enzymes are involved in these modification processes, including the cellular like-acetylglucosaminyltransferase (LARGE), LARGE2, putative glycosyltransferases protein O-mannosyltransferase 1/2 (POMT 1/2), protein O-mannose β1,2-N-GlcNAc transferase 1(POMGnT1), fukutin and fukutin-related protein (FKRP) (32). An in vivo study has shown that glycosylation is not critical for LCMV infection (33). However, this may be due to the in vivo compensation mechanism or the use of an alternate receptor.

LCMV and LASV bind to the N-terminal and C-terminal domains of αDG in regions overlapping the binding site of laminin (34), which suggests that these viruses compete with laminin for αDG binding (35). Small peptides based on the binding site residues of laminin have been designed and shown to efficiently neutralize these viruses (36). Interestingly, upon infection by the OW arenaviruses, αDG is down-regulated from the cell membrane while the expression of the precursor DG remains unaffected. This is mediated by the viral GP, which targets the interaction between DG and LARGE in the Golgi and thereby disrupts the proper glycosylation of αDG. However, this process may play an important role in viral release and not necessarily at the entry step (32, 37).

Animal studies and human clinical data have demonstrated high viral titers in the liver despite the fact that hepatocytes are not known to express αDG (38). Several cellular factors, including Axl, Tyro3, DC-SIGN, and LSECtin have been shown to play a role in LASV entry (39). While a recent study has shown that Axl does not necessarily play a major role for the establishment and maintenance of a persistent LCMV-ARM infection in mice (40), its expression is highly up-regulated in mice infected with the LCMV-WE strain that can induce transient liver pathology (41). It is also interesting to note that skeletal muscle expresses high levels of αDG without any evidence of virus replication (42). A recent study has demonstrated that LCMV can replicate in myotubes, but that its entry is restricted in a similar manner as what has been known for avian cells that also express high levels of αDG but are resistant to arenavirus infection(43). More recently, the cellular lysosomal-associated membrane protein 1 (LAMP1) has been demonstrated as an intracellular receptor for LASV, and that a single glycosylation site of LAMP1 is critical for viral binding, which is absent in the birds (44). Therefore, entry of some viruses (e.g., LASV) may also involve a pH-dependent switch to an intracellular receptor (LAMP1) located in the lysosomes of human and mouse cells (44). It remains to be determined whether LAMP1 is required for the entry of other arenaviruses.

The NW clade B arenaviruses use transferrin receptor 1 (TfR1) as their receptor (45). Five viruses in this clade, JUNV, MACV, GTOV, SABV, and CHAPV can cause HF infections due partly to their ability to bind to the human TfR1 receptor (45-48). In contrast, three other viruses in this clade, Tacaribe virus (TCRV), Amapari virus (AMAV) and Cupixi virus (CPXV) are non-pathogenic partly because they cannot bind

to hTfR1 but can still use TfR1 orthologs for entry (49). A recent study has demonstrated that the NW clade A/B arenaviruses use rodent TfR1 as viral receptor, but that some members of this arenavirus clade may also have the potential to use hTfR1 for entry (50-52). Therefore, hTfR1 receptor usage alone is not the primary determinant of pathogenesis for NW arenaviruses. TfR1 is an iron-transferrin receptor that is regulated by the cytosolic level of iron. Upon transferrin binding to the TfR1, the complex is internalized and delivered to the acidic endosome via the clathrin-mediated pathway. At least three different viral families use TfR1 as host receptors (53, 54). These viruses use a similar strategy to gain the entry into cells (55). Under the low iron dietary condition in some endemic areas, in which TfR1 gene expression can be up-regulated, resulting in a suspected worse disease prognosis (56). Some NW clade B arenaviruses may use alternative receptors for entry. For example, JUNV has been shown to use DC-SIGN and L-SIGN for virus binding and entry (57).

Upon binding to the cellular receptor arenaviruses are internalized by vesicles, and are then released into the cytoplasm through a pH-dependent membrane fusion step that is accomplished by the transmembrane portion of the viral glycoprotein GP2 (58). The arenaviral glycoprotein subunit 2 (GP2) is a class I fusion protein (59). However, different from other class I transmembrane proteins, the arenaviral glycoproteins (GPs) remain associated with the unusually long stable signal peptide (SSP) on the membrane. The interaction between SSP and GPs is required for the GP2 membrane-fusion function (60). The SSP helps keep the GP pre-fusion conformation in the natural environment and to facilitate the GP2 response to the acidified environment of the endosome. Interestingly,

some studies have shown that LCMV and LASV do not pass through the early endosome. Instead, these OW arenaviruses directly go into the late endosomes, thereby avoiding recognition by the host endosomal immune sensors in the early endosome. As such, infection by the OW arenaviruses, such as LASV, is able to suppress the innate immune response and produce significantly low levels of type I interferons (IFNs) at the early stage of the infection.

Many studies have focused on the process of internalization of the virion particles into the late endosome. By gold labeling LCMV and visualizing it in a transmission electron microscope (TEM), LCMV has been found to locate in smooth and uncoated plasma membranes, close to the primary endocytic vesicles (61). Few viral particles are found to be associated with clathrin-coated structures. However, a separate study has demonstrated that LCMV infection is independent of clathrin, dynamin-2, actin, Arf6, flotillin-1, caveolae, and lipid rafts. The pathway to deliver LCMV and LASV into acidified endosomes is Rab5-independent but microtubular-dependent (61, 62). This pathway is associated with the cellular endosomal sorting complex required for transport (ESCRT) (62). This unusual pathway of virus internalization is related to the process of αDG receptor degradation (62).

2.3. Viral genome replication and transcription

Arenaviral genome replication and transcription occur in the cytoplasm of the infected cells (Figure 3). Arenaviruses produce 3 types of RNA species: genomic RNA (gRNA), anti-genomic RNA (agRNA), and viral mRNA. While gRNAs and agRNAs are replicated as full-length RNAs, the mRNAs are transcribed from the promoter and

terminated by the highly structured IGRs (Figure 2). Because of the ambisense coding strategy, the NP and L mRNAs are directly transcribed from the gRNAs, but the GP and Z mRNAs can only be transcribed from the agRNAs. The NP and L proteins are necessary and sufficient to mediate viral RNA transcription and replication (63-65).

The arenaviral L protein contains the viral RdRp, which can be divided into three or four domains based on different types of analysis (66-68). The four conserved RdRp residues are located in the central domain, which mediates viral gene transcription and replication(69). The C terminal domain of the L protein may be involved in viral mRNA synthesis process, the exact mechanism of which is unknown (70). The N terminal domain of the L protein has endonuclease activity (71, 72), which has been shown to be essential for viral gene transcription but not replication (71). Arenaviruses employ a "cap snatching" process to obtain the 5' cap structure from cellular mRNAs for use to prime viral mRNA transcription (73). We and other researchers have recently determined the 3-dimensional structures of the endonuclease domain of the LASV and LCMV L proteins (71, 72, 74). Both arenaviral NP and L proteins may be involved in this cap-snatching process. The N terminal domain of NP has a deep groove that can potentially bind the m7GpppN cap structure from the cellular mRNAs (74). This cap binding function of NP is believed to provide some arenaviruses (e.g., JUNV, TCRV, and PICV) with the ability to translate viral genes independently of the cellular eIF4E protein subunit of the eIF4F complex (75). The NP-NP and NP-L interactions also play an important role in mediating viral mRNA synthesis (76). Arenaviral matrix Z protein has also been shown to play an important regulatory role in viral RNA replication process (64, 77-79). Z can directly

interact with the viral L polymerase at the terminal panhandle RNA structure and thereby locking the polymerase in a promoter-bound catalytically inactive state to inhibit viral RNA synthesis (80).

2.4. Post-translational protein processing

The nascent viral GP precursor polypeptides are cleaved into the stable signal peptide (SSP) and the G1/G2 peptide in the endoplasmic reticulum (ER) by the cell signal peptidase (60, 81). The GP1/GP2 peptide remains associated with SSP in the ER until it is being cleaved further by the cellular protease subtilisin/kexin isozyme-1 (SKI-1)/site 1 protease (S1P) into GP1 and GP2 subunits (81, 82). This process can take place in either the ER or Golgi (82-85). Both GP1 and GP2 contain several N-glycosylation sites, which are important for the correct glycoprotein complex (GPC) cleavage, maturation, and transportation. The LASV GPC contains six N-glycosylation sites that are essential for GPC cleavage, but other glycosylation sites do not seem to be directly involved in the proteolytic process (86). The myristoylation site on the G2 residue of the Z protein is important for the virus budding process due to Z homo-oligomerization (87).

2.5. Virion assembly

Like most enveloped negative-strand RNA viruses, the matrix protein mediates the virion assembly process, which depends in part on its late domain motifs (PPxY, PT/SAP, YxxL, θPxV, where x is any amino acid and θ is a hydrophobic amino acid) (88-90). Sequence analysis shows that most of the arenaviral Z proteins contain both the PT/SAP and YxxL motifs with most of the OW arenaviral Z proteins containing the PPxY motif.

The interactions between Z and other viral and cellular proteins are important for the viral assembly and budding process (91). Several studies have revealed some important domains or residues that are important for these interactions. The myristoylation on the G2 residue is required for the membrane association of Z with GPC (92). The RING domain and the L79 residue of the TCRV Z protein are required for the interaction between NP and Z (93). The Z-NP interaction has also been shown for LCMV and LASV (94) and is mediated by the C terminal domain of NP (93, 95). We have confirmed that the G2 myristoylation site, the conserved cysteine and histidine residues of the RING domain, as well as the L79 and P80 residues in the C terminal domain, are essential for Pichinde arenavirus (PICV) replication(96). The interaction between Z and L has also been demonstrated (80, 87) as described above. The homo-oligomerization of Z has been shown to be important for virion budding (97). Finally, the interactions between the late domain motifs of the Z protein with the cellular ESCRT and/or ESCRT associated ubiquitin ligase help drive the virus budding process (98). The LCMV IRG has also been shown to be important for the viral assembly and budding process (99).

3. Molecular mechanisms contributing to virus virulence and HF disease pathogenesis

3.1. Roles of the glycoprotein (GP) and of the host cell receptors in HF disease susceptibility and pathogenesis

The ability of virus binding to the different cellular receptors via its glycoprotein makes GP an important pathogenic factor. OW and NW clade C arenaviruses use alpha-

dystroglycan (αDG) as their receptor for cell entry. The differences in affinity of GP binding to αDG may contribute to differences in the disease outcome. Two strains of LCMV, clone 13 (Cl 13) and Armstrong (ARM), can induce different disease outcomes in mouse models. The Cl 13 strain causes chronic infection, whereas the ARM strain causes acute infection. Studies showed that LCMV with high affinity for αDG, such as the Cl 13 strain, is able to infiltrate the white pulp of the spleen and abolish the cytotoxic T lymphocytes, therefore inducing a persistent infection. During the infection of αDG low-affinity strain, ARM strain, the viruses are mainly restricted in the red pulp and are quickly cleared by the strong cytotoxic T lymphocyte (CTL) response (34, 100).

A recent analysis of over 3 million human genomic polymorphisms by the International HapMap Project has suggested a natural positive selection in a Nigerian population for allele variants of several human genes, including LARGE, interleukin 21 (IL21), and dystrophin (DMD), which is a cytosolic adaptor protein that is required for the proper function of αDG (101, 102). A high proportion of individuals in this population (21%) have shown evidence of prior exposure to LASV, which may apply selective pressure on the allelic frequencies of these human genes giving rise to their differential gene expressions that would confer natural resistance to Lassa fever. These polymorphisms in LARGE and DMD, for example, may have hindered binding and entry of LASV, and thereby protecting these individuals from severe LASV infection (101, 102).

NW clade B arenaviruses include both pathogenic and non-pathogenic viruses. Among this group of viruses, JUNV, MACV, GTOV, SABV, and CHPV can cause severe and lethal HF in humans (17, 18, 21, 25, 103, 104). All five of these pathogenic NW clade B

arenaviruses use human transferrin receptor 1 (hTfR1) as their receptor for cellular entry (3). In contrast, the known NW clade B non-pathogenic viruses can only use the rodent version of TfR1 as their receptor. Likewise, the NW clade A/B viruses also use the host-species specific TfR1 as their receptors (3). Virion RNAs with sequence homology to the Whitewater Arroyo virus (WWAV), a clade A/B virus, has been detected in several human cases, suggesting that WWAV might be associated with human infections. While some studies have shown that this virus is unable to use hTfR1 as an entry receptor (105, 106), WWAV-like viruses have been shown to potentially use hTfR1 as a receptor (3). However, it is not clear whether usage of hTfR1 plays any role in disease pathogenesis, as WWAV has not directly been shown to be a causative HF agent.

Further evidence for the involvement of GPC as an important determinant of arenavirus virulence has been demonstrated in the guinea pig model for PICV infection (107). Two strains of PICV (P2 and P18) can cause vastly different disease outcomes in infected animals (108, 109). Mutational analysis of the virulent (P18) and avirulent (P2) strains has revealed that sequence differences between the GPCs may contribute to the different disease outcomes. Substituting a single amino acid residue at position 140 of GPC from the avirulent P2 into the virulent P18 genome can increase the survival rate of infected animals from 0% to 33%, suggesting that GPC plays an important role in the disease outcomes (107). A separate study has shown that mutational analysis at residue 427 of the GPC of the attenuated Candid #1 strain of JUNV is largely responsible for the attenuation of this vaccine strain in suckling mice (110). That the residue change at this site results in increased virus-cell fusion at neutral pH of the Candid #1 strain and also in

increased dependence on hTfR1 for entry demonstrates its role in contributing to virus attenuation in humans (111). The study of the ML29 vaccine, a reassortant virus consisting of the LASV S genomic RNA segment and the Mopeia (MOPV) L genomic RNA segment, shows the attenuated phenotype of this reassortant virus in non-human primates and guinea pigs (112, 113). This data suggests that the major virulence factor(s) of LASV is located on the L segment. Other virus reassortant studies using LCMV or PICV have also implicated the contribution of the L genomic RNA segment in viral pathogenesis (114-116). While the L polymerase gene, encoded on the L segment may play an important role, it is important to note that the L segment also encodes the Z protein with known roles in regulating RNA synthesis and host innate immunity that can participate in disease pathogenesis (77, 80, 117, 118). Interestingly, sequence analysis of the ML29 viruses isolated from infected animals reveals several important mutations on the S segment, especially within the GP coding sequence. The K272E mutation located between the SKI-1/S1P cleavage site and GP2 fusion domain is one such mutation (119). It remains to be determined whether this and perhaps other mutations within the GP gene or elsewhere on the S segment of the ML29 vaccine virus contribute to the reduced pathogenic phenotype observed for this reassortant virus.

3.2. Role of the polymerase (L) protein in viral virulence

A hallmark of severe and lethal arenavirus-induced HF is the high level of viremia. It has been shown that individuals who can control the level of viremia are able to recover from the infection, while those who cannot typically succumb to the disease (120). A single amino acid in the L polymerase (L1079) of the LCMV Cl13 has been shown to enhance

the levels of intracellular viral replication, which can account for the difference of viral replication rates between the ARM and Cl 13 strains (121). This residue has also been shown to be responsible for generalized immune suppression, which is likely a result of T cell exhaustion caused by the high viral loads, and therefore may be responsible for the difference in acute versus chronic infection by the ARM and Cl 13 strains. A separate study has shown that this same residue is responsible for enhanced viral replication and tropism in macrophages (122). Using reverse genetics technology, we and other researchers have also demonstrated the role of the L polymerases of LASV and PICV in increasing viral replication and virulence in infected animals (123, 124). We show that the C terminal domain of L polymerase is the virulence determinants of PICV P18 strain. In particular, three residues (N1906, N1889, and L1839) in the C terminal domain are associated with increased viral replication and pathogenesis in infected animals (124). It is important to note that all naturally occurring residues found to enhance virus replication in LCMV, LASV, and PICV do not map to the known catalytic domains of the polymerase, and therefore their exact contributions to increased viral RNA synthesis and disease pathogenesis have yet to be determined.

3.3. Role of the nucleoprotein (NP) in innate immune suppression

Host immune responses to infection have a profound and direct influence on the disease course and outcomes. One of the hallmarks of severe and lethal arenavirus-induced HF is generalized immune suppression, the mechanisms of which are still under intense investigation. The nucleoproteins (NPs) of several arenaviruses have been shown to be capable of inhibiting the host innate immune responses. Specifically, the NPs of the OW

arenaviruses LCMV, LASV and the NW arenaviruses JUNV, MACV, WWAV, PICV, TCRV, and LATV have been shown to inhibit the production of interferon-beta (IFNβ) (125, 126).

Using x-ray crystallography and various functional assays, we and other researchers have demonstrated that the C terminus of the NPs of LASV, TCRV, and PICV contains a functional 3'-5' exoribonuclease (RNase) domain that degrades dsRNA in vitro (74, 126, 127). We have therefore proposed that NP inhibits type I IFNs by degrading viral pattern-associated molecular pattern (PAMP) molecules that would otherwise be recognized by cellular pattern recognition receptors (PRRs). The fact that the DEDDH catalytic residues are conserved among all known arenaviruses and that its function to suppress IFNβ production has been demonstrated for both pathogenic (e.g., LASV and LCMV) and non-pathogenic arenaviruses (e.g., TCRV and MOPV) suggests that this is a general mechanism of innate immune suppression by these viruses allowing them to replicate in either their natural hosts (e.g., rodents) or in infected humans.

Amino acid substitutions of the conserved RNase catalytic residues (DEDDH) significantly reduce NP's ability to inhibit IFNβ production in virus-infected cell cultures and in animals, directly implicating the exoribonuclease function in innate immune suppression (74, 126) We have recently generated recombinant PICVs carrying individual NP RNase catalytic mutations (D380, E382, D457, D525, or H520) (128). In vitro studies of these mutant PICVs show that these viruses induce high levels of IFNβ and grow poorly in the IFN competent A549 cells, but they can grow to similarly high titers as that of the wild-type PICV in IFN-defective Vero cells. All the RNase catalytic

mutant viruses show an attenuated phenotype in infected guinea pigs, but show reversion to the wild-type NP sequence in isolates from moribund animals, providing strong genetic evidence for the important role of the NP RNase function in suppressing innate immunity and allowing the virus to replicate in the infected animals. This is consistent with another study in which a recombinant LASV carrying a double-point mutation of the NP RNase catalytic residues (D389 and G392) replicates to lower titers than the wild-type virus partly because it is unable to suppress type I IFNs (129). The same group of investigators has also recently demonstrated that the LASV NP RNase domain is required to mount an effective antigen-presenting-cell-mediated response in NK cells against virus infection (130). Other studies have suggested that when NP is overexpressed in cells, they can either prevent activation of the Nuclear Factor Kappa B (NF□B) or directly associate with RIG-I or IKKε in order to inhibit the phosphorylation the IKKε or of the IFN-responsive gene (IRF3) and its translocation into the nucleus and thereby negatively regulates type I IFN production (131-133). Taken together, these data confirm the critical role of the arenaviral NP in mediating innate immune suppressive function that would then allow the virus to replicate unchecked. While the generalized immunosuppression and high viremia are important factors in arenavirus-induced HF pathogenesis, it is important to note that many individuals infected with pathogenic arenaviruses (e.g., LASV) do recover from the infection as a result of a robust cell-mediated immunity (4, 6).

3.4. Roles of the Z protein in innate immune suppression and viral pathogenicity

In addition to mediating viral budding and regulating viral RNA synthesis (see above), the Z protein also has immune suppressive function. A previous study has shown that the Z proteins of NW arenaviruses (JUNV, MACV, TCRV, and SABV), but not OW arenaviruses LASV and LCMV, can interact with the cytoplasmic pathogen-recognition-receptor RIG-I to inhibit the type I IFN induction (118). We have recently conducted a comprehensive analysis of the Z proteins from many known arenaviruses and have found that the Z proteins of all 9 known pathogenic arenaviruses, including LASV, LCMV, LUJV, JUNV, MACV, TCRV, SABV, and DANV, can effectively suppress the RIG-I-like receptor (RLR)-induced IFNβ responses (117). This Z-mediated RLR inhibition is strongly associated with arenavirus pathogenicity, as only the Z proteins of all known pathogenic arenaviruses, but not any of the 14 non-pathogens, can inhibit human RLRs (117). The inhibition is mediated by the interaction between the flexible N-terminal domain (NTD) of the pathogenic Z proteins and N-terminal tandem CARD domains of RIG-I/MDA5, and thus disrupting the association of the RLRs and the mitochondrial antiviral signaling protein MAVS. Swapping of the 31-residue Z NTD from LCMV into a nonpathogenic PICV genome has led to the inhibition of type I IFN responses and increased viral replication in human macrophages – the early target cells of arenavirus infections. This study indicates that the pathogenic Z-mediated RLR inhibition by arenaviruses may be a common pathogenic mechanism underlying the diverse arenavirus family to cause diseases in humans. While each arenavirus pathogen may have its unique pathogenesis leading to variable disease symptoms in humans, all of them encode a Z protein that can inhibit the RLR signaling and thus, the induction of type-I IFNs.

4. In vivo and in vitro primary cell-culture models of arenavirus-induced HF disease pathogenesis

4.1 Human primary cell-culture models

Macrophages and dendritic cells (DCs) are known early target cells of arenavirus infection. Several studies have suggested that pathogenic arenaviruses (e.g., LASV and JUNV) and non-pathogenic viruses (e.g., MOPV and TCRV) can differentially inhibit human macrophages but they all can inhibit DCs (117, 134-138), the molecular mechanism of which is not yet clearly understood. Both LASV and MOPV have shown to be capable of infecting primary human macrophages and DCs, but intriguingly the pathogenic LASV does not activate these cells upon infection. In sharp contrast, infection of macrophages by the non-pathogenic MOPV activate these cells as demonstrated by increased expression levels of activation markers CD86, CD80 and IFNβ (137). Similarly, primary human macrophages show higher IL-6, IL-10 and TNF□ production upon infection by the nonpathogenic TCRV as compared to the pathogenic JUNV infection (138). Consistent with these data, our laboratory has recently shown that the Z proteins of all known pathogenic arenaviruses are able to inhibit activation of macrophages, unlike those Z proteins from most known non-pathogenic arenaviruses (117). Since macrophages and DCs are professional antigen-presenting cells that offer the first line of defense against viral infections, inhibition of these immune cells can induce a general immune suppression of both the innate and adaptive arms of immunity that undoubtedly impact HF disease pathogenesis. Additional studies to investigate the mechanism(s) of immune responses of macrophages and DCs to pathogenic and

nonpathogenic arenaviruses are therefore warranted in order to elucidate the interplays between these virus pathogens and host immunity in driving HF disease pathogenesis.

4.2. Surrogate and non-human primate models

Although the pathogenesis of Lassa fever is still not clearly understood, severe LASV infection in humans often results in high levels of viremia, lymphopenia, functional liver damage, vascular abnormalities and profound suppression of both innate and adaptive immune responses (6) Different laboratory animal species have been used to mimic key pathophysiological features of human HF diseases (139-141). For example, guinea pigs have been used to study arenavirus-induced lung pathology (142, 143), while common marmosets (144) and LCMV-WE-infected rhesus macaques have been used to study arenavirus-induced liver pathology. Due to the strict requirement to work with the highly pathogenic arenaviruses (e.g., LASV) in the high biocontainment (BSL-4) facilities, surrogate animal models of arenaviral HF that involve infection of guinea pigs with the PICV, a risk group 2 pathogen, has been established in outbred Hartley as well as inbred strain 13 guinea pigs to study some mechanisms of Lassa fever-like disease pathogenesis (108, 145, 146). When outbred Hartley guinea pigs were infected with a low passage 2 (P2) strain of PICV, it induced a mild disease, whereas a highly adapted P18 strain (passaged 18 strain) of PICV caused a fatal disease with symptoms mimicking some features of Lassa fever, including but not necessarily limited to suppression of proinflammatory cytokines that was associated with terminal shock and death. While these surrogate animal models can serve as a relatively inexpensive and safe alternative for studying HF disease pathogenesis, the immune system of these rodents can be

fundamentally different from those of humans and non-human primates (NHPs). LASV-infected rhesus and cynomolgus monkeys are therefore considered the gold-standard models to study Lassa HF disease pathogenesis (147-154). Recent studies focusing on early stages of Lassa fever in NHPs and immune responses (152, 155) have confirmed previous observations on several factors important in HF disease pathogenesis, including high viremia, elevated liver enzymes, low or undetectable levels of proinflammatory cytokines (IL-1β, TNF-α, IL-8 and IP-10), and low and/or ineffective T-cell activation. These studies also show that early and strong T-cell responses are associated with effective control of virus replication and recovery. However, much work still needs to be done in order to understand the molecular mechanism(s) underlying HF disease pathogenesis in these animal models.

5. Conclusions

Arenaviruses are RNA viruses with a relatively simple genomic structure but with a complex biology and pathogenic mechanisms. The genome of the viruses encodes for only four genes, but each viral protein has multiple functions to mediate optimal viral replication and is possibly involved in the determination of different disease outcomes in humans. Studies have suggested that arenaviruses can gain virulence in the hosts by increasing viral cell entry and replication capacity and by effectively suppressing host innate immune responses. The recent identification of the Z protein as a pathogenicity-associated factor has shed important insights into a common pathogenic mechanism underlying the diverse human arenavirus pathogens. Nevertheless, different human arenavirus pathogens exhibit unique features in basic viral replication mechanisms and

disease manifestations(4), suggesting that further studies are warranted in order to understand the virus-specific pathogenic mechanisms for individual arenavirus pathogens. Important insights from recent studies on this group of important human pathogens can be exploited for the development of effective preventative and/or therapeutic modalities that can be tested in some established animal models of arenaviral HF.

This work has been published in the Pathogens journal (Pathogens 2015, 4, 283-306; doi:10.3390/pathogens4020283)

Chapter II

Characterization of the Glycoprotein Stable Signal Peptide in Mediating Pichinde Viral Replication and Virulence

Introduction

Arenaviruses can cause neurologic or hemorrhagic fever diseases in humans with limited preventive or therapeutic measures (156, 157). The most significant arenavirus pathogen is Lassa fever virus (LASV), which causes endemic infections in many countries in West Africa with estimated 500,000 cases resulting in ~5000 deaths annually (158). Except for Junin virus (JUNV), which has a vaccine Candid#1 used only in Argentina, no licensed vaccine for human usage is currently available for any other arenaviruses. Therapeutic options are limited and depend mainly on supportive cares. Ribavirin, a non-specific antiviral compound, has shown some efficacy only if it is administered at an early stage of viral infection when the symptoms are insidious (159). Development of effective vaccines and antivirals against arenavirus pathogens is therefore urgently needed.

Arenaviruses are enveloped, bi-segmented ambisense RNA viruses (160). Each viral genomic segment encodes two viral gene products. The large RNA segment (L) encodes viral RNA-dependent RNA polymerase L protein and the multifunctional protein Z. The small RNA segment (S) encodes nucleoprotein (NP) and glycoprotein (GPC). GPC is expressed as a single polypeptide with a long stable signal peptide (SSP) and is post-translationally processed by the S1P cellular protease into the receptor-binding GP1 and transmembrane GP2 subunits (161, 162). The 58-aa conserved SSP contains an N-terminal G2 myristoylation site, two hydrophobic domains (h1 and h2) separated by an

ectodomain, and a C-terminal SP cleavage site (**Fig. 4A**) (163), although the exact boundaries of these domains have not been well defined (164, 165). SSP is an essential component of the envelope glycoprotein complex and plays important roles not only in regulating the intracellular trafficking and proteolytic maturation of GPC, but also in the pH-induced membrane-fusion reaction (166, 167). However, the biological roles of SSP in arenavirus infection in vitro and in vivo have not been investigated.

Pichinde virus (PICV) is a non-pathogenic BSL2 agent and its infection of guinea pigs has been used as a safe, convenient, and economic small animal model for Lassa fever (168, 169). A low passaged strain of PICV (i.e., P2) causes a brief febrile reaction in guinea pigs, while a high passaged strain (i.e., P18) causes a severe Lassa fever-like disease in guinea pigs with high mortality (158, 168-172). We have developed the infectious clones for both the non-virulent P2 strain and the virulent P18 strain of PICV (173), and characterized the virulence determinants at the molecular level (107, 124, 146).

In this study, we investigate the biological roles of the conserved residues of the SSP in vitro and in vivo by using the PICV reverse genetics system. Many of these residues have been previously characterized in the context of GPC expression and pseudotyped viruses (163, 165, 174-177), however, their biological roles have not been investigated. Here, we show that multiple SSP conserved residues are essential or critical for viral infection of cell culture and/or guinea pigs by participating in the membrane fusion reaction, and that two residues N37 and R55 are required for viral virulence by a yet-to-be-determined mechanism.

Results

Effects of SSP mutations on GPC expression and processing.

Sequence alignment of SSPs among 22 different arenaviruses identified 8 residues that are either completely or highly conserved (**Fig. 4A**): two at the N-terminal end (G2 and Q3), one within the h1 domain (N20), one in the loop region (K33), two within h2 domain (N37 and F49), and two at the C-terminal end (R55 and C57). We introduced alanine substitutions at each of these conserved residues in the PICV GPC expression vector pCAGGS-PICV-GPC. We first examined whether each GPC mutant was expressed and processed properly after transfecting 1 μg of each plasmid into 293T cells and conducting a Western blot analysis with guinea pig anti-PICV antiserum, which detects both the polyprotein precursor GPC and the cleaved products GP1/GP2 but not SSP. The cleavage efficiency of each construct was calculated by dividing the amount of the cleaved products (GP1/GP2 subunits) over the total amount of the proteins (GPC precursor and GP1/GP2). Mutants G2A, Q3A, K33A, N37A, and R55A showed similar levels of expression and cleavage efficiency as the WT GPC (**Fig. 4B**, left panel). While N20A GPC precursor was expressed at a relatively high level, the GP1/GP2 cleavage was significantly reduced (**Fig. 4B**, left panel). Both F49A and C57A GPC precursors were expressed at much lower levels and their GP1/GP2 processing was undetectable (**Fig. 4B**, left panel). Even after transfecting 4x more of the F49A or C57A plasmid (at 4 μg each), we could not detect any significant GP1/GP2 cleavage products (**Fig. 4B**, right panel), suggesting that these two mutations severely impaired GPC processing. In summary,

among all conserved residues within the SSP, residues N20, F49, and C57 play an important role in regulating GP1/GP2 cleavage activity.

We next detected GPC assembly at the cell membrane by staining the transfected 293T cells with anti-PICV antiserum and FITC-conjugated secondary antibody without permeabilization. Representative histograms of empty vector- and WT GPC-expressing cells are shown in **Fig. 4C** (left panel). Using this method, we showed that, with the exception of F49A and C57A, there was no statistical significance in the surface expression levels of GPCs between WT and GPC mutants (**Fig. 4C**, right panel). In particular, N20A had a similar level of surface expression as WT (Fig. **4C**) even though it was defective in the GP1/GP2 cleavage activity (**Fig. 4B**). For F49A and C57A, the reduced surface levels (~ 25% of WT) (Fig. 1C) were most likely due to the diminished total protein expression levels (~ 20% of WT) (**Fig. 4B**) and not because of any block(s) in the intracellular trafficking. The differential effects of F49A and C57A on the GPC trafficking between our results of the PICV GPC and other published studies on JUNV and LCMV GPC (176, 178) may reflect the potential topological and/or biological differences between the GPCs. In summary, our data suggest that most (six out of eight) of the SSP conserved residues do not affect the intracellular transport or surface expression of the glycoprotein complex.

Fig.4

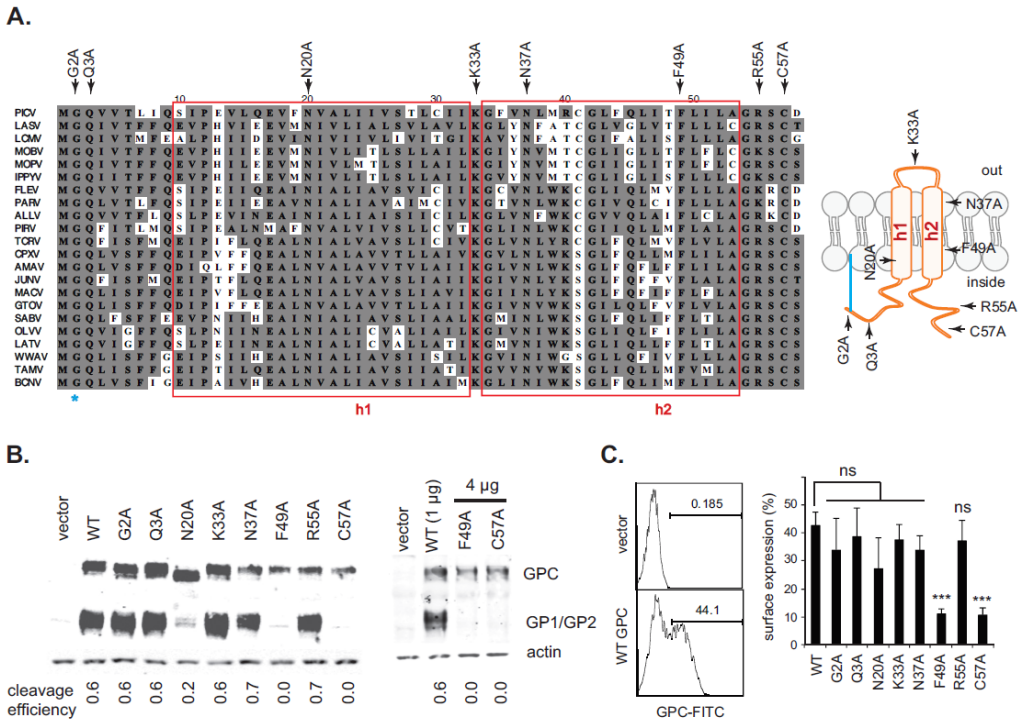

FIG. 4. Effects of SSP mutations on GPC expression, GP1/2 cleavage, and cell surface expression. (A) Sequence alignment of arenavirus GPC SSP regions (left) and the topology of SSP with two transmembrane domains, h1 and h2, shown (right). Conserved residues are indicated by arrows. Abbreviations: MOBV, Mobala virus; IPPYV, Ippy virus; FLEV, Flexal virus; PARV, Parana virus; ALLV, Allpahuayo virus; PIRV, Pirital virus; TCRV, Tacaribe virus; CPXV, Cupixi virus; AMAV, Amapari virus; MACV, Machupo virus; GTOV, Guanarito virus; SABV, Sabia virus; LATV, Latino virus; WWAV, Whitewater Arroyo virus; TAMV, Tamiami virus; BCNV, Bear Canyon virus. (B) Expression and processing of wild-type (WT) and mutant PICV GPCs. Expression vectors of WT or SSP mutants (1 µg of plasmid DNA unless otherwise indicated) were transfected into 293T cells. Cell lysates were analyzed by Western blotting with guinea

*pig anti-PICV antisera. Actin expression was used to monitor equal sample loading efficiency. (C) Cell surface expression of WT and mutant PICV GPCs. Shown on the left are representative FACS histograms for the vector or WT GPC-transfected cells after immunofluorescence staining with anti-PICV antisera. Shown on the right are the averages and standard deviations of GPC surface expression from three independent experiments. Statistical analyses were conducted with Student's t-test. ns, not statistically significant; ***, P<0.001.*

Effects of SSP mutations on GPC-mediated fusion activity

To evaluate the effects of individual SSP mutation on the GPC-mediated membrane fusion activity, we conducted both syncytia formation and luciferase-based (luc-based) fusion assays. For syncytia formation assay, 293T cells were transfected with a GFP expression plasmid, which allows for easy detection of the transfected cells, together with either an empty vector control or the individual GPC plasmid. Cells were exposed to low pH environment and observed for syncytia formation under fluorescence microscopy. Compared to the vector control (negative), WT GPC expression led to the efficient formation of syncytia as evidenced by enlarged cells (**Fig. 5A**). Syncytia formation was also observed for Q3A, N37A, and R55A mutants (albeit to different levels), but not for G2A, N20A, K33A, F49A, and C57A mutants. To quantify the levels of GPC-mediated fusion activities, we used a luc-based fusion assay as described previously (166). GPC-mediated membrane fusion allows for the transfer of the T7 RNA polymerase from BSRT7-5 cells to transcribe the T7 promoter-driven luc reporter gene from the

transfected 293T cells. Luc activity was measured for each of the GPC mutant constructs and normalized to the WT GPC control, which is set as 100% fusion efficiency (**Fig. 5B**). Consistent with the syncytia formations shown in **Fig. 5A**, mutants Q3A, N37A and R55A induced relatively high levels of luc activities as a result of GPC-mediated membrane fusion activities (**Fig. 5B**). The Q3A and R55A mutants appeared to be even more fusogenic than the WT, the reason(s) for which are unknown. In contrast, N20A had a significantly lower level of fusogenic activity, whereas G2A, K33A, F49A, and C57A did not exhibit any obvious fusogenic activity in this assay. Our data are consistent with previous studies, which have demonstrated that K33A, F49A, and C57A lead to a nearly complete loss of fusogenic activity of JUNV GPC (175, 178, 179). K33 has been shown to play a critical role in mediating membrane fusion (175, 180, 181). As F49A and C57A are defective in the GPC processing (**Fig. 4B**), the uncleaved GP1-GP2 precursor may not be able to expose the fusion peptide at the N-terminal GP2 subunit under low pH, which may explain the lack of fusogenic activity of the two mutants.

Fig. 5.

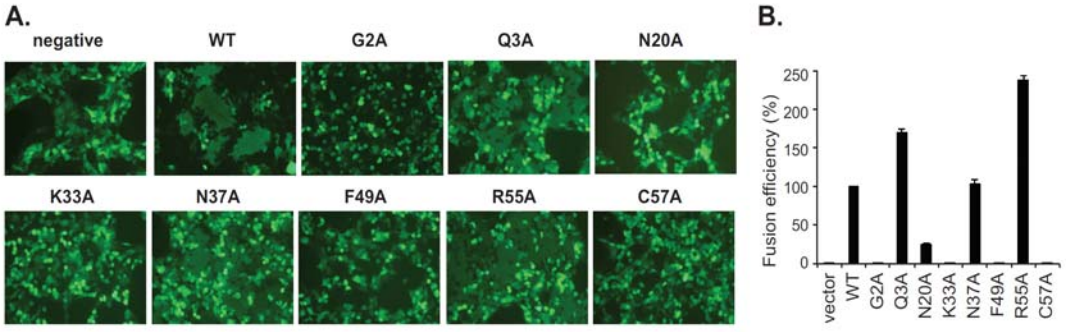

Fig. 5. Effects of SSP mutations on membrane fusion activity. (A) GFP-based fusion assay. Cells were transfected with a plasmid expressing eGFP together with either an

empty vector (negative) or plasmids expressing WT or individual mutant PICV GPCs. Cells were treated with low-pH medium to trigger membrane fusion. (B) Luc-based fusion assay. Luciferase activity mediated by membrane fusion by each of the GPC mutants in the fusion assay was determined and normalized to the activity mediated by the WT GPC, which is set at 100%. Results shown are the averages from three independent experiments with standard deviations.

Effects of SSP mutations on GPC-mediated cell entry

To compare the cell entry efficiency mediated by different GPC mutants, we generated lentivirus-like particles (VLPs) that contain WT or mutant GPC proteins using an established three-plasmid HIV-based system (182). Using the levels of HIV-1 p24 capsid protein on the VLPs for normalization purpose (**Fig. 6A**), similar amounts of GPC-pseudotyped VLPs were used to transduce 293T cells. It is worth to note that F49A and C57A VLPs contained much less GP1/GP2 (**Fig. 6A**), consistent with their defective GPC processing (**Fig. 6B**). As the VLPs encode the eGFP gene, its expression in the VLP-transduced cells was quantitatively evaluated by flow cytometry **(Fig. 6B)**. The G3A and N20A GPC mutants showed similar levels of transduction efficiency (15-20%) as WT, whereas the G2A mutation reduced the entry efficiency by 50%, and the K33A, F59A, and C57A mutations almost completely abolished the cell entry. In contrast, the N37A and R55A mutants led to even higher efficiency in cell entry than the WT GPC, the molecular mechanism(s) for which are unknown. In summary, using the GPC-

pseudotyped VLP system, we have shown that some of the SSP mutations (i.e., K33A, F49A, C57A, and G2A) significantly impair GPC-mediated cell entry.

Fig. 6.

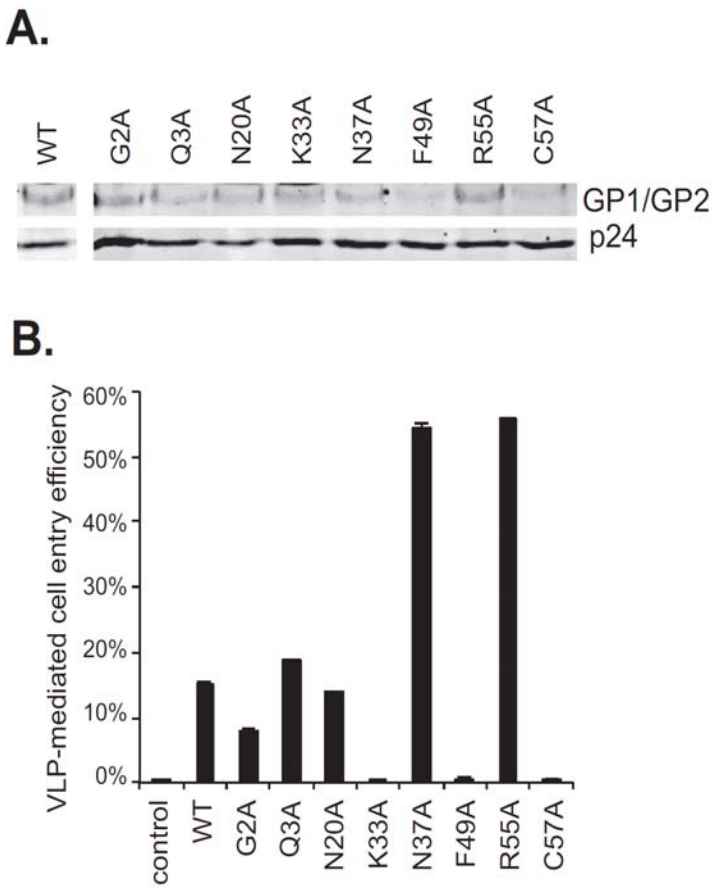

FIG. 6. Effects of SSP mutations on GPC incorporation into VLPs and GPC mediated cell entry. (A) Lentiviral particles pseudotyped with respective GPC constructs were analyzed by Western blotting with guinea pig anti-PICV antiserum and anti-HIV p24 antibody. (B) The percentage of GFP-positive cells after VLP transduction with the respective GPC-pseudotyped VLPs is shown as the average from three independent experiments with standard deviations.

Effects of SSP mutations on viral growth in vitro

To examine the biological roles of the SSP conserved residues in arenavirus replication cycle, we created the same series of alanine substitutions in the GPC gene of the S segment of the PICV (P18 strain) reverse genetics system (173). Together with the L plasmid, each S plasmid expressing WT or mutant SSP was transfected into BSRT7-5 cells in order to rescue recombinant viruses. We successful rescued and amplified recombinant viruses with the individual mutations G2A, Q3A, N20A, N37A, and R55A, but failed to rescue viruses with K33A, F49A, or C57A mutations even after repeated attempts (**Fig. 7A**), suggesting that K33, F49, and C57 are essential for PICV life cycle. We sequenced the viable mutant viruses after passaging four times in cell culture and did not detect WT reversion.

We then compared viral growth ability between the WT and viable mutant viruses in BHK-21 cells at MOI of 0.01 (**Fig. 7B**, left). Four mutants (Q3A, N20A, N37A, and R55A) showed similar growth kinetics as WT, while G2A grew 0.5 - 1 log lower than WT, suggesting that the G2 residue plays an important role in viral replication. Similar results were obtained in human lung epithelial A549 cells (**Fig. 7B**, right). As N20A mutation significantly reduced the GPC processing in a protein expression system (**Fig. 4B**) but did not seem to affect viral growth in vitro (**Fig. 7B**), we wonder whether N20A indeed impaired the GPC processing in the context of viral infection. We infected BHK-21 cells with WT or N20A virus at MOI of 10 for 24 h and analyzed cell lysates by Western blot using the anti-PICV antisera, anti-NP antibody, and anti-actin antibody, respectively (**Fig. 7C**). WT and N20A showed similar levels of NP, consistent with their

similar virus replication levels. The cleavage efficiency, which was calculated as the percentage of the cleaved products (GP1/GP2 subunits) over the total amount of the proteins (GPC precursor and GP1/GP2), was much lower in the N20A- than that in the WT-infected cells (**Fig. 7C**). Our results demonstrate that N20A significantly reduces the GPC processing in both protein expression system (**Fig. 4B**) and viral infection (**Fig. 7C**).

Fig. 7

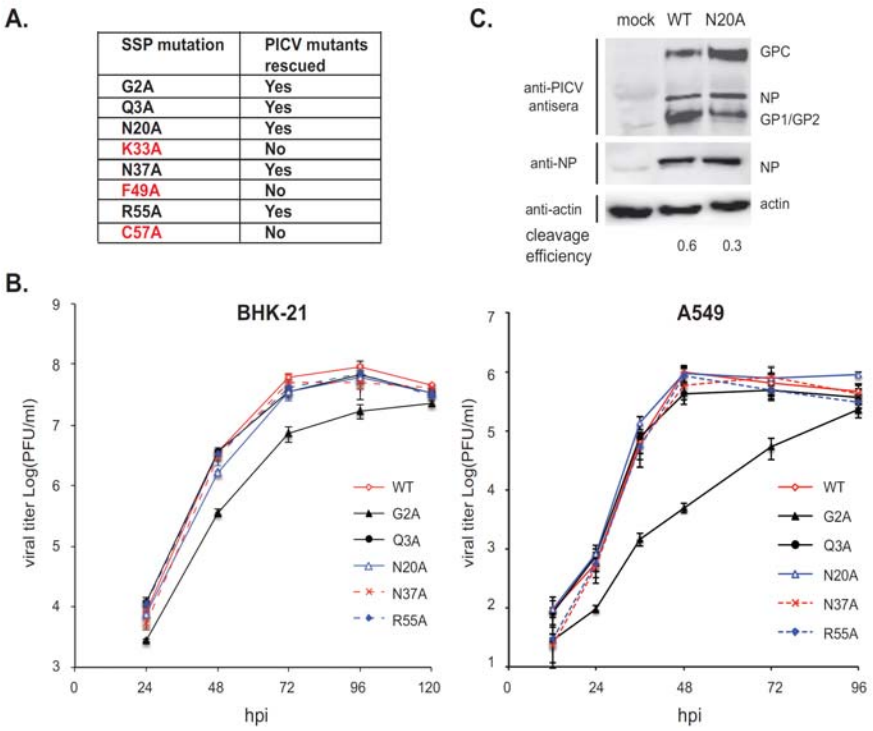

FIG. 7 Rescue of recombinant PICV with WT or mutant SSP. (A) Summary of recombinant virus rescue efforts for each SSP mutant. (B) Viral growth curve analysis in BHK-21 (left) and A549 (right) cells. Vero cells were infected (MOI of 0.01) with WT or recombinant PICV mutants carrying respective SSP mutations. Viral titers in the supernatants at various time points postinfection were quantified by plaque assay. Results shown are averages and standard deviations from three independent experiments.

(C) GPC processing in virus-infected cells. A549 cells were mock infected or infected with the WT or N20A mutant at anMOIof 10. At 24 h postinfection, cell lysates were analyzed by Western blotting with guinea pig anti-PICV antisera, anti-NP antibody, and anti-actin antibody. The GPC processing efficiency is calculated as the percentage of GP1/GP2 over total GPCs.

Effects of SSP mutations on viral virulence in vivo

We determined the degrees of virulence of the recombinant SSP mutants in an established guinea pig model (168, 172, 173). Consistent with our previous observations (173), all animals (n=6) infected with the WT virus experienced a long duration of fever (average of 9 days), significant body weight loss, and reached terminal points by 14 dpi (**Fig. 8)**. In contrast, all animals (n=3) infected with G2A or N20A mutant virus survived the infection with no obvious body weight loss as compared to the PBS control group (**Fig. 8A and 8B**). The G2A-infected animals also experienced significantly less days of fever (average of 3.8 days, **Fig. 8C**) than the WT-infected animals. Similarly, the N20A virus infection led to, on average, a shorter duration of fever than WT virus infection, though the difference is not statistically significant due to the relatively small number of the infected animals (**Fig. 8C**). In summary, both the G2A and N20A mutant viruses almost completely lost virulence in vivo (**Fig. 8A**).

Infection with the Q3A mutant virus (n=7) led to ~ 90% mortality, substantial loss of body weight, and prolonged fever in guinea pigs, without significant difference from the WT virus infection (**Fig. 8**), demonstrating that the Q3A mutation does not greatly

attenuate the virus in vivo. On the other hand, animals (n=6) infected with either the N37A or R55A mutant virus experienced prolonged fever and variable degrees of body weight loss, with a survival rate of 30%-50% that is significantly higher than those infected with the WT virus (**Fig. 8**). Collectively, our data suggest that both the N37A and R55A mutant viruses are attenuated in vivo. It is worth mentioning that, for all mutant viral infections, animals that survived the infection did not contain any trace of infectious virus in the serum while all moribund animals had high viremia as determined by plaque assay, correlating with the previous reports that arenavirus virulence is associated with high levels of viral replication in vivo (124, 158, 183). We also sequenced all mutant viruses isolated from animals and did not detect any WT revertants.

Fig. 8.

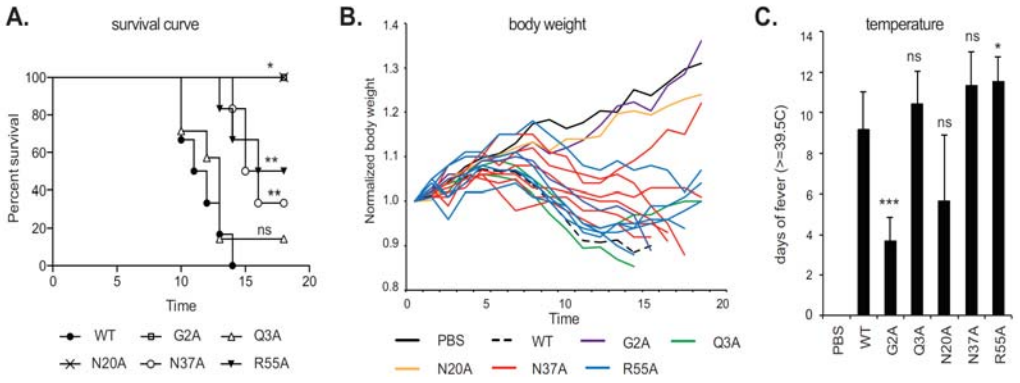

FIG 8 Effects of SSP mutations on PICV virulence in guinea pigs. (A) Survival curve of guinea pigs infected with either the WT or respective SSP mutant viruses. Statistical analyses of the survival curves were performed using the log-rank (Mantel-Cox) χ2 test and/or Fisher's exact test. (B) Daily body weight normalized to day 0 (set at 1.0). For the PBS, WT, G2A, and N20A groups, average body weights of each group are shown because all animals in the same group had similar trends in body weight change. The

*Q3A group had one animal that survived the infection, and its body weight is shown separately from the average for the other 6 animals. The body weights of each animal in the N37A and R55A groups are shown. (C) The average duration of fever (rectal temperature of >39.8°C). Statistical analyses were conducted with Student's t-test. ns, not statistically significant; *, P <0.05; **, P <0.01; ***, P< 0.001.*

Discussion

In this study, we have determined the biological roles of 8 completely conserved residues of GPC SSP among all known arenaviruses, using PICV reverse genetics system. **Table 1** shows the effects of alanine substitution of each conserved SSP residue on the expression and function of GPC as well as on viral infections in vitro and in vivo. Except for N20A, F49A, and C57A, other SSP mutations do not affect the levels of GPC expression, GP1/GP2 cleavage, or surface assembly of the glycoprotein complex (**Fig. 4**). However, multiple SSP conserved residues are essential for viral infection by participating in viral entry, while two residues (N37 and R55) are important for viral virulence by a yet-to-be-determined mechanism(s).

Table 1.

Mutation	Protein expression	GP1/2 cleavage	Surface level	Fusion	VLP entry	Virus rescue[b]	*In vitro* growth	*In vivo* virulence	Virus isolated from animals
None (WT)	+++	+++	+++	+++	+++	+	+++	+++	WT
G2A	+++	+++	+++	−	++	+	+	−	NA
Q3A	+++	+++	+++	++++	+++	+	+++	+++	Q3A
N20A	++	+	+++	+	+++	+	+++	−	NA
K33A	+++	+++	+++	−	−	−	NA	NA	NA
N37A	+++	+++	+++	+++	++++	+	+++	++	N37A
F49A	+	−	+	−	−	−	NA	NA	NA
R55A	+++	+++	+++	++++	++++	+	+++	++	R55A
C57A	+	−	+	−	−	−	NA	NA	NA

a, ++++ higher than the WT level; +++, WT level; ++, significantly less than the WT level; +, minimally detected; -, undetectable; NA, not applicable.

b, Virus rescue is the ability to rescue recombinant mutant virus: + indicates rescue of mutant virus; - indicates inability to rescue mutant virus.

K33, F49, and C57 are required for viral entry and indispensable for PICV life cycle. Our results correlate well with prior studies of other arenaviruses, such as JUNV and the Lymphocytic Choriomeningitis virus (LCMV) (163). The K33 residue has been shown to play an essential role in GPC fusion by interacting with GP2 to prime the complex for pH-induced membrane fusion (163, 175, 177). The F49 residue is located within the recently identified FILL sorting signal motif that is required for glycoprotein processing and surface expression (163, 178). The C57 residue of the GP2 along with its H459, C467, and C469 residues form a zinc-binding center, which provides the structural basis for association with SSP in the glycoprotein complex in order to modulate optimal membrane fusion activity (179, 184).

Another residue critical for viral fusion is the G2 myristoylation site. The myristoylation-defective G2A mutation almost completely abolishes the fusion activity based on the cell-based fusion assay (**Fig. 5**). It is, however, worth to mention that the fusion assay cannot fully reproduce the fusion activity of GPC during viral entry and therefore the result does not exclude the possibility that G2A mutation may retain a low level of fusogenic activity. Indeed we show that G2A GPC-pseudotyped VLPs can still mediate cell entry, albeit at a reduced level (**Fig. 7B**). As such, the G2A mutant virus can be rescued but is

significantly attenuated in vitro and in vivo (**Figs. 7-8**). Previous studies of JUNV and LCMV GPCs have also shown that the G2A mutation can markedly reduce the membrane fusion activity (163, 185). The molecular mechanism by which the G2 myristoylation site is involved in viral membrane fusion remains unknown. Myristoylation plays an important role in membrane targeting and protein-protein interactions (186). We and others have shown that GPC with the G2A substitution is still able to express properly and to assemble at the plasma membrane (**Fig. 4C**) (163, 185), suggesting that this G2 myristoylation site is not essential for membrane targeting, but may be involved in the SSP-GP2 interaction in order to mediate proper membrane fusion. Consistent with previous studies (163, 166), the N20A mutation reduces the membrane fusion activity by ~ 75% (**Fig. 5B**). N20 residue is located within the SSP transmembrane domain 1 (TM1), which has been suggested to directly interact with the GP2 TM domain to affect GPC-mediated membrane fusion (166). The reduced fusion activity of the N20A mutation does not significantly affect VLP-mediated cell entry (**Fig. 5B**) or viral growth in vitro (**Fig. 7B**), but markedly reduces viral virulence in vivo (**Fig. 8**), suggesting that a suboptimal membrane fusion activity could have a major impact on viral infection in vivo.

The N37A and R55A mutations do not reduce the membrane fusion activity (**Fig. 5B**) but rather appear to increase the levels of VLP-mediated cell entry efficacy (**Fig. 8B**). While these mutant viruses grow similarly as the WT virus in cell culture (**Fig. 7B**), they showed reduced degrees of virulence in vivo (**Fig. 8A-B**). It is possible that the seemingly insignificant effects observed in cell culturing conditions can sometimes be

amplified in vivo. The exact molecular mechanism(s) by which N37 and R55 contribute to viral infectivity in vivo remains to be determined, but they do not seem to participate in the membrane fusion and/or cell entry.

Materials and Methods

Cell lines: 293T cells, BHK21, and A549 cells were maintained in Dulbecco's modified Eagle's medium (DMEM) supplemented with 10% fetal bovine serum (FBS, Sigma) and 50 mg penicillin and streptomycin. BSRT7-5 cells, which stably express the T7 RNA polymerase, were obtained from K. Conzelmann (Ludwig-Maximilians-Universität, Germany) and cultured in DMEM supplemented with 10% fetal bovine serum (FBS), 1 mg Geneticin per ml, and 50 mg penicillin and streptomycin per ml. Vero cells were maintained in Eagle's medium (MEM) with 10% FBS plus 50 mg penicillin and streptomycin per ml.

Plasmids and transfection methods: Mutations in the SSP gene were created in the pCAGGS-PICV-GPC plasmid by overlapping PCR mutagenesis reactions, and the mutations were confirmed by sequencing. Plasmids used to rescue the PICV SSP mutant viruses have previously been described (146). A plasmid that contains the T7 promoter-directed firefly luciferase gene has been obtained from J. Nunberg (University of Montana, USA). Plasmid transfection into 293T cells was performed by using the calcium phosphate method (187). Plasmid transfection into BSRT7-5 cells was performed by using the Lipofectamine2000 reagent as per the manufacturer's protocol (Invitrogen).

Western blot: 293T cells were lysed at 48 hrs post transfection by lysis buffer (50 mM Tris-HCl, 150 mM NaCl, 1% NP40, pH=7.4) with protease inhibitor cocktail (Roche). Lysates were assayed by SDS-polyacrylamide gel electrophoresis (SDS-PAGE) and transferred to nitrocellulose membranes (NC membrane). NC membrane was blocked with 5% non-fat powdered milk in Tris-HCl buffer (TBS) for 1 hr at room temperature. The membrane was incubated with anti-PICV guinea pig serum at 4 °C overnight, and washed three times with TBS (50 mM Tris-HCl, pH=7.4) and probed with IRDye 800CW labeled donkey anti-guinea pig antibody and assayed by Odyssey infrared imaging system (LI-COR® Biosciences).

Fusion assay: For eGFP syncytia formation assay, 293T cells were transfected with the eGFP plasmid together with the pCAGGS vector or individual GPC construct. 36 hrs post-transfection, cells were treated with pH-adjusted medium (pH=5) for 5 mins and then replaced with fresh complete DMEM medium for additional 12 hrs of culturing. The cell cultures were visualized by fluorescence microscopy.

For luciferase-based fusion assay, 293T cells were transfected with the T7-promoter-driven firefly luciferase reporter plasmid together with either pCAGGS empty vector or individual GPC construct. 24 hrs post-transfection, the transfected 293T cells were detached by trypsinization, mixed with BSR-T7 cells that constitutively express T7 RNA polymerase. At 36 hrs post-transfection, cells were treated with pH-adjusted medium (pH=5) for 5 mins and then replaced with fresh complete DMEM medium for additional 12 hrs of culturing. Cells were lysed 12 hrs later and analyzed by the luciferase assay kit (Promega).

Cell surface expression of the GPC complex: 293T cells were transfected with either pCAGGS empty vector or individual GPC construct. 48 hrs post-transfection, cells were fixed with 4% PFA for 5 min, washed once with PBS, and blocked with 1% bovine serum albumin (BSA) for 1 hr at 4 °C. Cells were then incubated with guinea pig anti-PICV serum overnight at 4 °C, washed with PBS three times, and incubated with Alexa Fluor® 488- labeled goat anti-guinea pig antibody for 1 hrs at ambient temperature. Cells were washed three times with PBS and analyzed for GPC-positive cells by flow cytometry.

GPC-pseudotyped lentivirus-like particles (VLP) and cell entry assay. As described previously (107), 293T cells were transfected with three plasmids, pCMVRΔ8.91, a plasmid containing the HIV genome except for the packaging signal and envelope gene; pHR'GFP, a plasmid containing a GFP expression cassette and HIV packaging signal; and a pCAGGS expression vector expressing either WT PICV GPC or SSP mutant, using the Lipofectamine2000 (Invitrogen) transfection reagent. Supernatants of the transfected cells were collected at different time points up to 96 hrs post-transfection and filtered through a 0.45 μm filter. After purification through sucrose gradient ultracentrifugation, the pseudotyped VLPs were resuspended in DMEM, aliquoted, and stored at -80ºC. The amount of VLPs was normalized by the HIV-1 p24 levels as determined by Western blot analysis using an anti-HIV-1 p24 antibody, which is kindly provided by E. Hunter (Emory University). For cell entry assay, respective GPC-pseudotyped VLPs were used to transduce 293T cells in the presence of polybrene at 8 μg/ml. 24 hrs post-transduction, GFP-positive cells were analyzed by flow cytometry.

Generation of recombinant PICV mutants and viral growth curve analysis: WT and SSP mutant viruses were rescued as previously described (146). The L plasmid together with the S plasmid containing either WT or mutant SSP was transfected into BSRT7-5 cells. At various time points post-transfection, virus supernatants were collected for plaque assaying to determine whether any infectious virus particles were generated. Individual plaques were then picked and amplified once in BHK-21 cells to prepare virus stocks. Each viral mutant was confirmed by sequence analysis after RT-PCR. For viral growth curve analysis, BHK-21 cells were infected with either WT or mutant virus at MOI of 0.01, each in triplicates. At different time points post infection, supernatants were collected and analyzed for infectious viral particles by plaque assaying in Vero cells as previously described (173).

Animal experiments. Outbred male Hartley guinea pigs of 350-400g were purchased from Charles River laboratories and acclimatized for 3 days before experiments. Animals were administrated intraperitoneally (i.p.) with PBS or 10,000 PFU of respective virus. Body weights and rectal temperatures were monitored daily for up to 18 days. Animals were defined as having reached terminal points either when their body weight decreased by >30% as compared to a nomogram or if the rectal temperature fell below 38 °C in addition to body weight loss. Statistical analyses of the survival curves were performed using the Log-rank (Mantel-Cox) χ^2 Test using GraphPad Prism 5 software. The statistical significance of duration-of-fever was analyzed using the student "t" test.

This work has been published in the Journal of Virology (J Virol. 2016 Oct 28;90(22):10390-10397)

Chapter III

Functional Analysis of the Conserved Amino Acids of Arenaviral Glycoprotein GP2 C-terminal Domain

Introduction

Several arenaviruses cause human hemorrhagic fever diseases, for which preventive or therapeutic measures are limited(188-191). Lassa virus (LASV) causes Lassa fever in West Africa with 300,000 to 500,000 infection cases and ~5,000 deaths annually(158). Junin virus (JUNV) is endemic in South America and causes Argentine hemorrhagic fever. Candid#1 is the only vaccine to prevent JUNV infections and can only be used in Argentina. Except for Candid#1, there is no vaccine for any other arenaviruses (192). Ribavirin is used to treat arenaviral hemorrhagic fever diseases but it only shows some efficacy when it is administered at the early stage of the infection(159). Supportive care is the main treatment for arenaviral hemorrhagic fevers(193). Therefore, effective vaccines and antiviral agents are urgently needed.

Arenavirus is an enveloped ambisense RNA virus(194). Arenaviral genome contains two RNA segments, the large segment (L seg) and small segment (S seg). The L seg encodes viral RNA-dependent RNA polymerase and the viral matrix protein Z. The S seg encodes viral nucleoprotein (NP) and viral glycoprotein complex (GPC). Arenaviral glycoprotein is synthesized as a single polypeptide precursor which is posttranslationally processed into a stable signal peptide (SSP), receptor binding GP1 and transmembrane fusion peptide GP2. GP2 is a type I fusion peptide with its fusion domain located at the N terminal domain, which has been well studied (195, 196). The roles of GP2 C-terminal

domain (CTD) conserved residues in mediating cell entry have not been well understood. Previous studies have identified two zinc-binding domains located at JUNV GP2 CTD: H447, H449, C455, and H485 that formed the first zinc-binding domain, and H459, C467, C469 and C57 of SSP that formed the second zinc-binding domain (179, 184). Mutagenesis study of JUNV GP2 CTD showed that all GP2 CTD zinc-binding residues are essential for glycoprotein processing and GPC functions. The other conserved residues of GP2 CTD, R470, P478, P480, R482, W503, R505, and K508 have not been investigated and the roles of all these conserved amino acids at the CTD of GPC in authentic arenavirus life cycle have not yet been investigated.

In this study, we characterized the roles of GP2 CTD conserved residues in GPC expression, processing, fusion activity and authentic arenaviral lifecycle by using the PICV reverse genetics system (146). Our data indicate that all of the zinc-binding residues, as well as the W503 residue in GP2 CTD, is essential for glycoprotein processing, fusion activity, and viral life cycle and that three residues, R470, P480, and R482, might play important roles in optimizing glycoprotein processing, GPC trafficking, and virus assembly in virus-infected cells.

Results

Effects of GP2 CTD mutations on glycoprotein expression and processing. 13 residues of GP2 CTD are highly conserved among 22 different arenaviruses (**Fig. 9A**), We introduced alanine substitutions at each of these highly conserved residues H469, R470, H471, C477, P478, P480, H481, R482, C489, C491, W503, and G492 that is also highly conserved, as well as R505 and K508, are less conserved, for which we

introduced a double mutation (R505A/K508A). To investigate whether these conserved residues affect glycoprotein complex (GPC) expression and processing, 2 μg of either empty, WT or GP2 CTD mutant plasmid (pCAGGS-GP) was transfected into 293T cells. 48 h post transfection, the cells were lysed and analyzed by Western blot using guinea pig anti-PICV serum. The cleavage efficiency was calculated as the ratio of cleaved products to the total amount of proteins (processed and unprocessed glycoprotein). Mutants P478A and R505A/K508A showed similar cleavage efficiency levels to that of the WT, whereas all other mutants appeared to be defective at processing (**Fig. 9B**), indicating that residues, H469, R470, H471, C477, P480, H481, R482, C489, C491, and W503 are essential for GPC processing. In particular, our data indicate that the zinc-binding residues, H469, H471, C477, H481, C489, and C491 completely impaired GPC processing.

We next detected the levels of GPC cell surface and total expression to evaluate the GPC trafficking efficiency. 2 μg of either empty, WT or GP2 CTD mutant plasmid (pCAGGS-GP) were transfected into 293T cells. 48 h post transfection, cells were analyzed by flow cytometry. Mutants P478A, R505A/K508A showed similar ratios of GPC surface expression positive cell numbers to total GPC expression positive cell numbers (Fig. 10A and 10B). Mutants H469A, P480A, and R482A showed ~30% lower ratios than WT (Fig. 10A and 10B). All other mutants showed significantly lower ratios, ~70% lower than WT, suggesting that these residues, R470, H471, C477, H481, C489, C491, and W503 are essential for GPC trafficking to the cell surface (**Fig. 10A** and **10B**).

Effects of GP2 CTD mutations on GPC mediated-membrane fusion activity. To

Fig. 9.

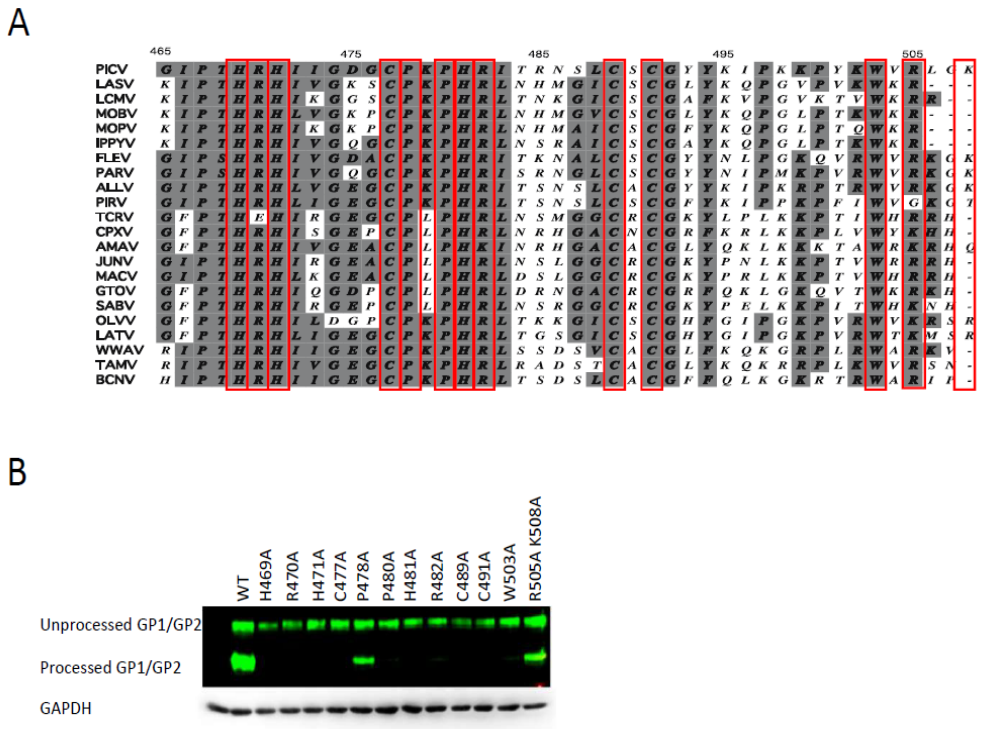

Fig. 9. (A) Sequence alignment of arenavirus glycoprotein GP2 CTD regions. Conserved residues are indicated Red square. Abbreviations: MOBV, Mobala virus; IPPYV, Ippy virus; FLEV, Flexal virus; PARV, Parana virus; ALLV, Allpahuayo virus; PIRV, Pirital virus; TCRV, Tacaribe virus; CPXV, Cupixi virus; AMAV, Amapari virus; MACV, Machupo virus; GTOV, Guanarito virus; SABV, Sabia virus; LATV, Latino virus; WWAV, Whitewater Arroyo virus; TAMV, Tamiami virus; BCNV, Bear Canyon virus. (B) Expression and processing of wild-type (WT) and mutant PICV GPCs. Expression vectors of WT or GP2 CTD mutants (1 μg of plasmid DNA unless otherwise indicated) were transfected into 293T cells. Cell lysates were analyzed by Western blotting with guinea pig anti-PICV antisera. Actin expression was used to monitor equal sample loading efficiency.

Fig. 10.

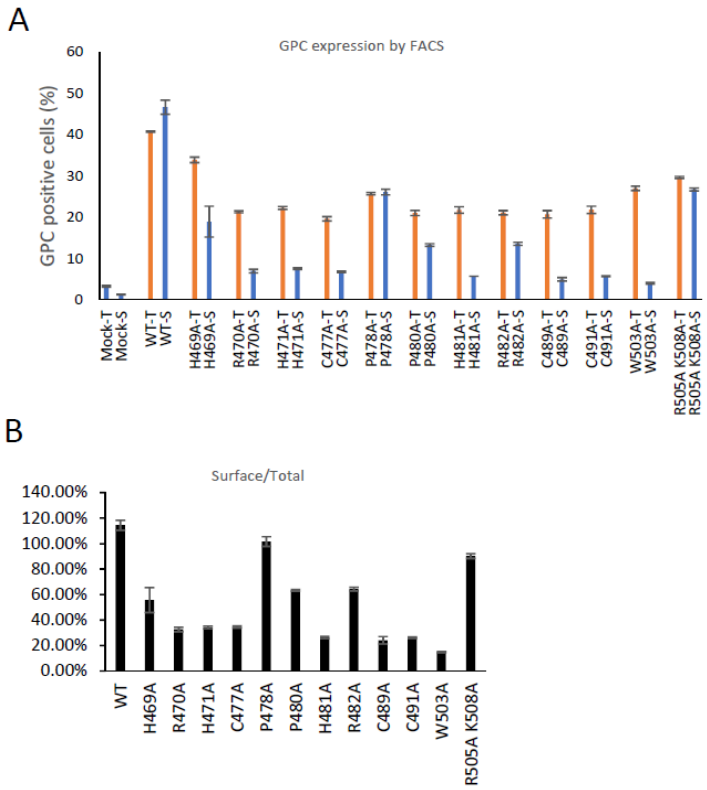

Fig. 10. Cell surface and total expression of WT and GP2 CTD mutant PICV GPCs. (A) Shown the averages deviations of GPC surface and total expression from three independent experiments. (B) shown the ratio of surface/total GPC expression.

evaluate the effects of each GP2 mutation on the GPC mediated membrane fusion activity, we carried out a syncytium formation fusion assay. 1 μg of either empty, WT or each GP2 mutant plasmid together with eGFP expression plasmid were transfected into 293T cells. 36 h post transfection, the cells were treated with low pH medium (pH=4.0) for 5 minutes and replaced with normal complete DMEM for continuing culture for 12 h. Then the cells were analyzed by fluorescence microscopy. WT, P478A, and R505A/K508A GPC expressions led to relatively efficient formations of syncytia (**Fig.**

11). However, we did not observe eGFP syncytia formations from the other GP2 CTD mutants transfected cells, suggesting the critical roles of H469, R470, H471, C477, P480, H481, R482, C489, C491, and W503 play in the GPC mediated membrane fusion (**Fig. 11**).

Fig. 11

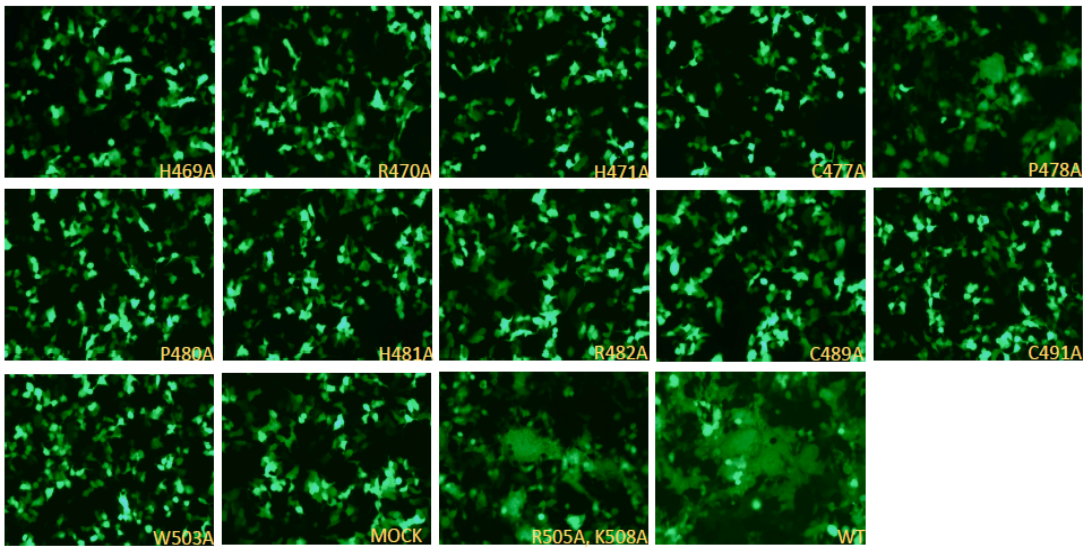

Fig. 11. Effects of GP2 CTD mutations on membrane-membrane fusion activity. Cells were transfected with a plasmid expressing eGFP together with either an empty vector (negative) or plasmids expressing WT or individual mutant PICV GPCs. Cells were treated with low-pH medium to trigger membrane fusion and monitored by fluorescence microscopy.

Effects of GP2 CTD mutations on viral growth. To investigate the biological roles of GP2 CTD conserved residues in the arenaviral life cycle, we created the same series of individual alanine substitutions in the glycoprotein gene encoded on the small segment (S) of the PICV reverse genetics system. Either WT or the individual GP2 CTD mutated

S plasmid together with the large segment (L) containing plasmid were transfected into BSRT7-5 cells in order to rescue recombinant viruses. WT, R470A, P478A, P480A, R482A, and R505A/K508A mutants viruses were successfully rescued (**Fig. 12A**). However, we were not able to rescue viruses in cells transfected with plasmid combinations that carry the individual mutation H469A, H471A, C477A, H481A, C489A, C491A, and W503A on the GPC gene of S segment of the viral genome along with the L segment containing plasmid, despite repeated attempts, suggesting that the zinc-binding residues of GP2 CTD, H469, H471, C477, H481, C489, and C491, as well as the W503 residues, are essential for the PICV life cycle.

To investigate the roles of the GP2 CTD mutants in viral growth kinetics, we infected the BHK21 cells with either WT or the individual GP2 CTD mutant (R470A, P478A, P480A, R482A, and R505A/K508A) at MOI=0.01 and collected the cellular supernatants containing viruses at 24 h, 48 h, 72 h, and 96 h postinfection in order to conduct plaque assaying on Vero cells. The results showed that the GP2 CTD mutants, P478A, P480A, R482A, and R505A/K508A showed WT-like growth kinetics, whereas the R470A mutant grew 1 log less than the WT, suggesting that R470 residue plays an important role in virus replication kinetics (**Fig. 12B**). Viruses from the supernatants used in the growth curve experiments were sequenced to validate the identity of each of the mutants and to confirm that there was no reversion of the mutated GP2 to the WT sequence.

Fig. 12.

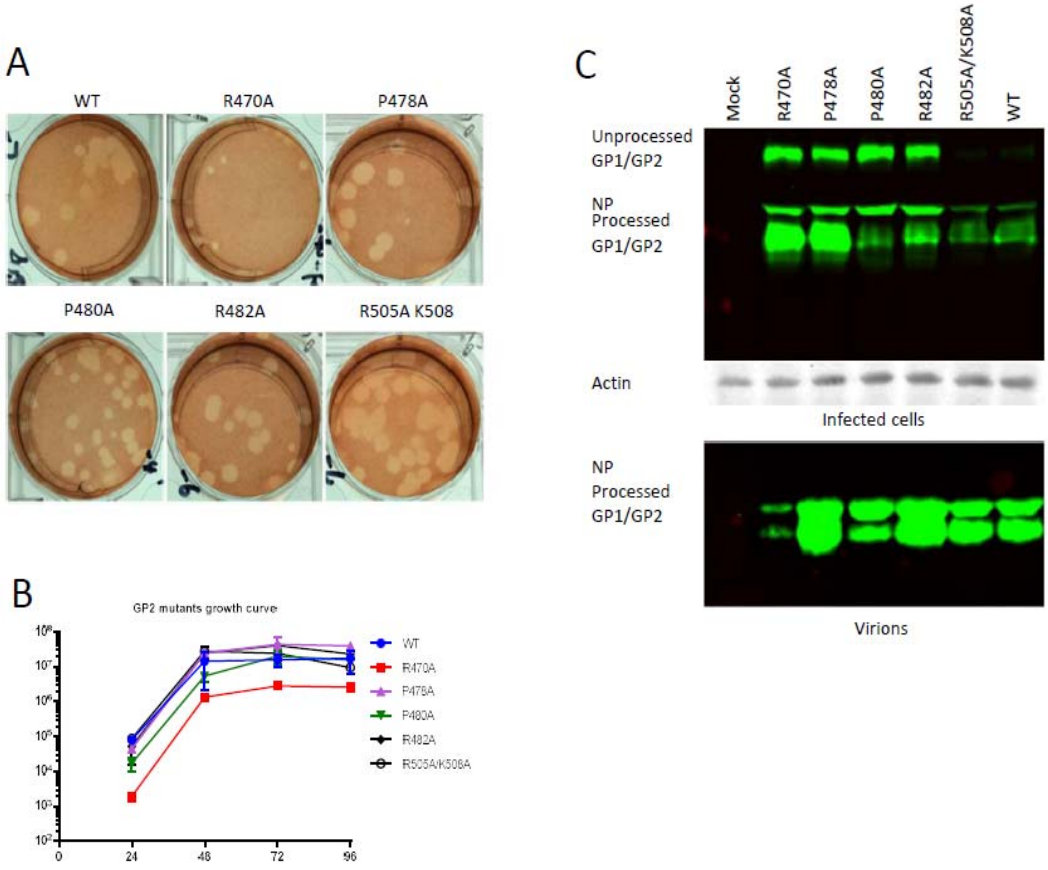

Fig. 12. GP2 CTD mutant viral kinetics. (A) The plaque size of individual GP2 CTD mutant viruses. (B) GP2 mutant viral growth curve. BHK21 cells were infected with either WT or GP2 CTD mutant at an MOI=0.01, the supernatants were collected at indicated time and virus titer was calculated by plaque assay in VERO cells. (C) Glycoprotein processing in the viruses infected cells and virions. For the Western blot for viruses infected cells, BKK21 cells were infected with indicated viruses at a MOI=0.1 and the cells were collected at 48 hrs post-infection. For the Western blot for virions,

BHK21 cells were infected with indicated viruses at an MOI=0.01, supernatants were collected at 24h, 48h, and 72h post infection and concentrated by ultracentrifuge. The samples were analyzed by Western blot with guinea pig anti-PICV serum.

Glycoprotein expression and processing in GP2 CTD mutant virus-infected cells and virions. It was somewhat unexpected that we could rescue the R470A, P480A, and R482A mutant viruses since no cell fusion activity was detected for any of these mutants in the plasmid transfected cells (**Fig. 11**). We, therefore, asked whether GPCs of these mutant viruses were processed in the infected cells and in the virions. To address this question, we infected the BHK21 cells at MOI=0.1 and collected the cell lysates at 48 h post infection. We also infected the BHK21 cells at MOI=0.1 and collected the supernatants at 24 h, 48 h, 72 h, and 96 h postinfection. The supernatants were then concentrated by ultracentrifuge at 27,000 rpm for 2 hrs. The cell lysates and virions were analyzed by Western blot using guinea pig anti-PICV serum. The results showed that all GPCs in both cell lysates and virions of these GP2 CTD mutant viruses, R470A, P480A, and R482A were properly processed (**Fig. 12C**). We also noticed that significantly higher levels of unprocessed GP1/GP2 remained in the R470A, P478A, P480A, and R482A mutant viruses infected cells compared to the WT and R505A/K508A mutant viruses infected cells, suggesting that R470, P478, P480, R482 residues indeed play important roles in glycoprotein trafficking/assembly and especially in glycoprotein processing in the authentic virus-infected cells. The markedly lower levels of processed GP1/GP2 observed with the R470A mutant virus in the virion sample correlated well with its lower

virus titers and plaque sizes as compared to the WT and other GP2 mutant viruses (**Fig. 12B** and **12A**).

Discussion

In this study, we have determined the important roles of the conserved residues of GP2 CTD of the PICV by using both plasmid overexpression system and the PICV reverse genetics system. In particular, our data indicate that the W503 and zinc-binding residues, H469, H471, C477, H481, C489, and C491 are essential for the PICV life cycle.

The roles of H469, H471, C477, H481, C489, and C491 residues have previously been examined for the JUNV (179, 184). These residues formed two zinc-binding domains at the GP2 CTD. Further study on the second zinc domain of GP2 CTD has shown that GP2 CTD forms an intersubunit zinc-binding center that incorporates Cys-57 of SSP, which might act to retain SSP in the GP-C complex and position the ectodomain loop of SSP for its role in modulating membrane fusion activity (184). Our results with PICV confirmed that all the zinc-binding residues are indeed essential for glycoprotein processing and GPC mediated membrane fusion activity (**Fig. 9** and **Fig. 11**). Using the PICV reverse genetics system, we found that all the viruses carrying alanine substitutions in the zinc-binding domain were not able to be rescued, which suggested that the zinc-binding domain at the GP2 CTD was also essential for PICV life cycle.

Interestingly, we found that the R470 residue was required for glycoprotein processing and GPC mediated membrane fusion activity in cells overexpressing PICV GPC carrying this particular R470A mutation (**Fig. 9** and **Fig. 11**). However, we were able to rescue virus carrying the R470A mutation, albeit the viral titer for this mutant virus was about 2-

log lower than the WT PICV, and its growth kinetics were slower and its plaque size was significantly smaller than the WT virus (**Fig. 12A** and **12B**). The Western blot analysis showed that GPC of the R470A mutant virus-infected cells was processed properly, but that its processed levels on the virion was much less than the WT level (**Fig. 12C**), corroborating with the slower growth kinetics and smaller plaque sizes of this particular mutant virus as compared to the WT or other GP2 mutant viruses (**Fig. 12A** and **12B**). It is possible to speculate that viral proteins and/or cellular factors are involved in GPC processing and trafficking during the virus infection, which facilitates the GPC cell surface assembly to form virions.

The virus carrying the P480A mutation was able to be rescued. This virus showed about 1-log lower viral titers at 24h and 48 h compared to the WT. The plaque size seems to be relatively smaller than the WT. Higher levels of unprocessed GP1/GP2 products were observed as compared to that of the WT, suggesting that the P480 residue plays an important role in optimizing glycoprotein processing, GPC trafficking, and virus assembly. The same can be said about viruses that carry the P470A, P478A, or R482A substitution mutation (**Fig. 12C**).

In summary, our data suggest that arenaviral GP2 CTD plays an essential role in glycoprotein processing, GPC mediated membrane-membrane fusion activity, optimizing GPC trafficking and virion particle formation. Knowledge obtained from this study may provide the structure-based targets of GP2 CTD for developing arenaviral therapeutics.

Materials and Methods

Cell line. 293T and BSRT7-5 cells were maintained in Dulbecco's modified Eagle's medium (DMEM, Sigma) plus 10% fetal bovine serum (FBS, Sigma) and 50 mg/ml penicillin and streptomycin (Invitrogen). Vero and BHK21 cells were maintained in Eagles' medium (MEM, Invitrogen) with 10% FBS, 50 mg/ml penicillin and streptomycin.

Plasmids and transfection methods. Mutations in the GP2 CTD gene of pUC18-Seg (plasmid for the PICV reverse genetic system) were created by rolling circle mutagenesis. Mutations in the GP2 CTD gene of pCAGGS-GP (plasmid for GPC overexpression in mammalian cells) were transferred from the plasmids of pUC18-Seg GP2 CTD mutants. Calcium phosphate method was used for 293T cells transfection. Lipofectamine 300 was used for BSRT7-5 cells transfection.

Western blotting. 293T, BHK21 or concentrated virions were lysed by lysis buffer (50mM Tris-HCl, 150mM NaCl, 1% NP-40, pH7.4) with protease inhibitors (Roche). Lysates were assayed by sodium dodecyl sulfate-polyacrylamide gel electrophoresis (SDS-PAGE) and transferred to nitrocellulose membranes (NC membrane, Bio-Rad). The NC membrane was blocked with 5% nonfat powdered milk in Tris-HCl buffer (TBS, pH=7.4) for 1 h at room temperature and incubated with either guinea pig anti-PICV serum or anti-actin antibody (Sigma) at 4°C overnight. The next day, the NC membrane was washed by TBS for three times and incubated with either IRDye 800CW-labeled donkey anti-guinea antibody (LI-COR Biosciences) or HRP labeled goat anti-mouse antibody (PerkinElmer) for 1 h at RT. The NC membrane was washed with TBS for three

times and analyzed by either Odyssey infrared imaging system (LI-COR Biosciences) or MyECL imager system (ThermoFisher).

Fusion Assay. Enhanced green fluorescent protein (eGFP) syncytium formation analysis was used to monitor the GPC induced fusion activity as previously described (197).

Total and Cell surface expression of the GPC. For GPC cell surface expression level analysis, 293T cells were transfected with 2 μg of either empty, wild-type (WT) or GP2 CTD mutation plasmid. 48 hrs post-transfection, the cells were trypsinized and fixed with 4% PFA, cells were then blocked with blocking buffer (1%BSA, 1% normal goat serum, 200mM glycine in PBS, pH=7.4) and stained with guinea pig anti-PICV serum and fluorescein isothiocyanate (FITC)-conjugated goat anti-guinea pig antibody. For the total GPC expression level analysis, the same procedure was carried out plus 0.1% saponin was added into blocking buffer and antibody solutions for permeabilization.

Generation of recombinant PICV mutants and viral growth curve. WT and GP2 CTD mutant viruses were rescued as previously described (197). Viral growth curve analysis was carried out on BHK21 cells as previously described (197).

Glycoprotein expression and processing in virus-infected cells and virions. For the analysis of glycoprotein expression and processing in virus-infected cells, BHK21 cells were infected with either mock, WT or GP2 CTD mutants at MOI=0.1 for 24 h or 48 h. The cell lysates were analyzed by Western blot with guinea pig anti-PICV serum. For the analysis of glycoprotein expression and processing in various, BHK21 cells were infected with either mock, WT or GP2 CTD mutants at MOI=0.1 in 10 cm dishes, supernatants

were collected at 24 h, 48 h, 72 h post infection and concentrated by ultracentrifuge. The concentrated viruses were analyzed by Western blot with guinea pig anti-PICV serum.

Chapter IV

Arenaviral Nucleoproteins Suppress PACT-induced Augmentation of RIG-I Function to Inhibit Type I Interferon Production

Introduction

Mammalian arenaviruses are phylogenetically, serologically and geographically divided into Old World (OW) and New World (NW) subgroups. Several members of the OW and NW-B viruses are known to cause diseases in humans. In addition to Lassa virus (LASV) that causes endemic hemorrhagic fever (HF) infections in West Africa, six other arenaviruses can cause sporadic HF outbreaks in South Africa or South America (156, 157). No vaccine is available for arenavirus pathogens, except for Junín virus (JUNV) vaccine Candid#1, which is licensed for use only in Argentina and offers some cross-protection for another NW arenavirus (Machupo MACV) but not against LASV (198). Therapeutic options are limited and depend mainly on supportive cares. Ribavirin, a nonspecific antiviral compound, has shown some efficacy only if it is administered at an early stage of viral infection when the symptoms are insidious (159). Severe and lethal Lassa HF infections are associated with a generalized immune suppression of the infected hosts, as characterized by the absence of early immune responses, delayed and low levels of neutralizing antibody production and T cell activation, the molecular mechanisms of which have only recently been investigated in some details (199).

RIG-I is a major cytosolic sensor of many RNA viruses (200), including arenaviruses (201). RIG-I recognizes viral dsRNA carrying the 5’ triphosphate (202). Structural and biochemical studies from several laboratories have provided tantalizing evidence for a

multistep model of RIG-I activation via binding to dsRNA (200, 203). In uninfected cells, RIG-I is kept inactive by a closed conformation, in which its N-terminal CARD domains and C-terminal (repression) domain (CTD) are kept close to the centrally located helicase domain, in which specific Thr and Ser residues in the CTD and CARDs are phosphorylated by casein kinase II (CKII) and protein kinase C (PKC)-α/β, respectively (204-207). Upon viral infection, RIG-I binds to RNA ligand to facilitate its conformational changes, dimerization, and multimerization. A series of protein modifications (ubiquitylation and dephosphorylation) of RIG-I help mediate its conformational changes (205-213) and translocation to mitochondria-associated membranes (MAMs), where RIG-I interacts with MAVS to mediate several downstream processes in order to induce type I IFN production (214). ATP hydrolysis via the ATPase function of RIG-I has been shown to be critical for RIG-I activation (215), as RIG-I can translocate on the bound dsRNA in an ATP hydrolysis-driven manner (216, 217).

A cellular factor known as PACT has been shown to greatly enhance RIG-I function by interacting with it (218). PACT is a 313-aa protein that contains 3 conserved dsRNA-binding motifs (dsRBMs), with dsRBM1 and 2 binding to dsRNA and dsRBM3 activating the dsRNA-dependent kinase PKR (219). PACT has been shown to activate RIG-I via interaction with the C-terminal repression domain of RIG-I and activation of the RIG-I's ATPase function to potently enhance type I IFN production (218). The same study shows that the interaction between RIG-I and PACT can be detected endogenously in cells [upon Sendai virus (SeV) infection] and that the enforced expression of PACT alone has no effect on the IFNβ promoter activity, but when co-expressed with RIG-I

with a functional helicase activity, PACT can significantly augment RIG-I activation. PACT potentiates RIG-I function by activating the intrinsic ATPase activity of RIG-I at a level comparable to the preferred RIG-I ligand 5'-triphosphate dsRNA (218).

For a wide range of human pathogenic viruses, such as Ebola (EBOV), influenza A virus (IAV), Middle East Respiratory Syndrome Coronavirus (MERS-CoV), human T-cell leukemia virus (HTLV1), mouse hepatitis virus (MHV), measles virus (MeV), and human simplex virus (HSV1), their viral proteins or defective interfering (DI) RNAs have been shown to modulate PACT-mediated enhancement of RIG-I's function to drive the expression of type I IFN (218, 220-226). Specifically, the EBOV VP35, IAV NS1, HSV1 Us11, MERS-CoV 4a and nucleocapsid (N) proteins, as well as the N protein of MHV, have been shown to directly disrupt the interaction between RIG-I and PACT, and hence block the ability of PACT to activate RIG-I (218, 220-223, 226). We and other researchers have previously shown that arenaviral nucleoproteins (NPs) can efficiently suppress type I IFN production by degrading immunostimulatory RNAs via its intrinsic 3'-5' exoribonuclease activity (126, 227-233). In the current study, we show that LASV NP could effectively block PACT-induced augmentation of RIG-I function and therefore suppressed type I IFN production. We also show that the LASV NP RNase activity is required for inhibition of PACT-induced potentiation of RIG-I function and therefore plays an essential role for arenavirus replication in interferon-competent cells by limiting the functions of PACT and RIG-I.

Results

Arenaviral nucleoproteins (NPs) blocked PACT-augmented RIG-I-induced IFNβ production.

Previous studies have shown that PACT can strongly augment RIG-I-induced activation of the IFNβ promoter (218). To determine whether arenaviral NPs could suppress PACT- and RIG-I-induced IFNβ activation, we conducted the IFNβ promoter-dependent luciferase (LUC) assay. 293T cells were transfected with either an empty vector or a plasmid expressing the WT Lassa virus (LASV) NP gene together with the IFNβ -LUC reporter plasmid, β-gal expressing plasmid (as transfection efficiency control), RIG-I-expression plasmid, and/or PACT expression plasmid. The results showed that RIG-I alone activated the IFNβ promoter activity by 60-fold, and together with PACT, strongly activated the IFNβ promoter activity by 240-fold (**Fig. 13A**), confirming previous studies that PACT can potently enhance RIG-I induced IFNβ production. The inclusion of LASV NP largely suppressed the IFNβ activation induced by either RIG-I or RIG-I/PACT combination. Our data suggest that LASV NP can suppress both RIG-I alone and RIG-I/PACT induced IFNβ activation.

We next asked whether this inhibition was applicable to other arenaviral NPs. Using a similar set up as described in Figure 1A, we examined the impact of NPs from LASV, Junín virus (JUNV), Machupo virus (MACV), Pichinde virus (PICV), and Tacaribe virus (TCRV) on RIG-I or RIG-I/PACT induced IFNβ-promoter activation. The results showed that all arenaviral NPs were able to suppress PACT/RIG-I-induced IFNβ-promoter activation to similar levels (**Fig. 13B**), suggesting that this is a general mechanism of innate immune suppression by arenaviral NPs.

Fig. 13

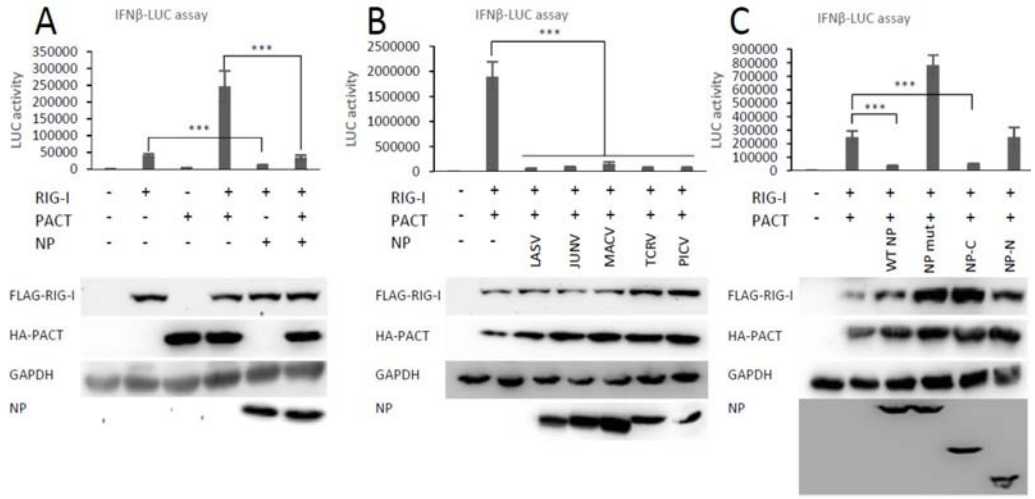

*Fig. 13. 293T cells were transfected with the indicated plasmids together with IFNβ promoter-directed luciferase (LUC) plasmid and β-gal plasmid for normalization of transfection efficiency. (A) LASV NP could inhibit both RIG-I and RIG-I plus PACT induced IFNβ promoter activity. (B) LASV NP, JUNV NP, MACV NP, TCRV NP and PICV NP could inhibit RIG-I and PACT induced IFNβ promoter activity. (C) WT LASV NP, WT LASV NP C-terminal RNase-containing domain (NP-C), but not RNase-defective NP (NP mut) or NP N-terminal domain (NP-N), could inhibit RIG-I and PACT induced IFNβ promoter activity. The experiments that generated data for each of the panels shown had been repeated three times. The results shown are the average of one such experiment (in triplicates). The luciferase (LUC) activities of certain samples were compared to the corresponding controls by the Student's t-test, ***, P<0.01. The western blots shown below the bar graphs confirmed the expression of the transgenes (FLAG-RIG-I, HA-PACT, and NP) as well as of the housekeeping GAPDH gene using the appropriate antibodies.*

The 3'-5' exoribonuclease (RNase) function of NPs was required for inhibition of PACT/RIG-I-induced IFNβ-promoter activation.

We and other researchers have shown that the NP RNase activity was required for its inhibition of type I IFN production (126, 227-233). To determine whether NP's RNase activity was also necessary to inhibit PACT- and RIG-I-induced IFNβ promoter activities, plasmids carrying either the WT LASV NP, LASV NP with a known RNase-defective mutation (D389A) (126, 228), the C-terminal RNase-containing LASV NP (126), or its N terminal domain without enzymatic function was individually transfected into 293T cells with the IFNβ-LUC and β-gal expressing plasmids along with the RIG-I-expressing and PACT-expressing plasmids. The results showed that RNase-containing LASV NP and its C terminal domain strongly suppressed PACT- and RIG-I-induced IFNβ promoter activation, but the RNase-defective D389A mutant and the N-terminal non-RNase containing domain of NP did not exhibit such an inhibitory effect (**Fig. 13C**). The NP D389A RNase-defective mutant appeared to consistently further enhance the levels of RIG-I activation (after repeated assaying), the molecular mechanism of which is not known. These data demonstrate that NP's RNase activity is required for NP inhibition of PACT- and RIG-I-induced IFNβ promoter activities.

NP-mediated inhibition of PACT/RIG-I was not via disruption of PACT and RIG-I interaction.

Recent studies have shown that several viral proteins, such as the EBOV VP35, HSV Us11, and IAV NS1 protein, can suppress PACT- and RIG-I-induced IFNβ activities by disrupting the protein-protein interactions between RIG-I and PACT (220-223, 226). We

wondered whether arenaviral NPs could also suppress PACT- and RIG-I-induced IFNβ promoter activity through a similar mechanism. Since WT NP but not the RNase-deficient NP could suppress the IFNβ promoter, we asked whether there was any difference between WT LASV NP and D389A RNase-defective NP in their interactions with RIG-I and/or PACT. We performed co-immunoprecipitation assays to analyze the interactions among NP, RIG-I, and PACT in lysates of 293T cells transfected with plasmids expressing HA-PACT and FLAG-RIG-I along with a plasmid expressing either the wild-type NP (WT NP-myc) or the RNase-defective NP mutant (NP mut-myc) or an empty plasmid control. Immunoprecipitation (IP) with an anti-HA antibody but not with an anti-IgG control antibody could pull down FLAG-RIG-I (**Fig. 14A**, compare lanes 2, 5, 8 to lanes 3, 6, 9), demonstrating the specific interaction between FLAG-RIG-I and HA-PACT by immunoblotting (IB), which is consistent with a previous study (218) . The immunoprecipitates also contained similar levels of WT and mutant NP when the respective NP plasmid was co-transfected (**Fig. 14A**, lanes 6 and 9, protein bands shown as NP-myc), suggesting that both WT and mutant NP can interact with PACT. Furthermore, the presence of WT or mutant NP reduced but did not completely eliminate the FLAG-RIG-I protein levels in the immunoprecipitates (**Fig. 14A**, compare FLAG-RIG-I levels in lanes 6 and 9 to lane 3), which was partly due to the decreased total RIG-I expression levels in these cell lysates (**Fig. 14A**, compare the FLAG-RIG-I levels of the cellular lysates shown in lanes 1, 4 and 7). Nevertheless, there appeared to be no major differences between WT and NP mut in disrupting the RIG-I/PACT interactions (**Fig. 14A**, compare FLAG-RIG-I levels in lanes 6 and 9), indicating that the NP-mediated

PACT/RIG-I inhibition is not mediated mainly through the abolishment of the PACT-RIG-I interaction, as has previously been demonstrated for other viral proteins (220-223, 226). To address the interaction between PACT and NP in authentic virus infection, we infected HEK293 cells with WT PICV, performed IP assays of the infected cell lysates with an anti-IgG control antibody or an anti-PACT antibody followed by immunoblotting (IB) with either an anti-NP antibody or an anti-PACT antibody. PICV NP was readily detected in the immunoprecipitates pulled down with an anti-PACT antibody but not with an anti-IgG control (**Fig. 14B**), demonstrating the interaction of PICV NP with endogenous PACT during viral infection.

Fig. 14.

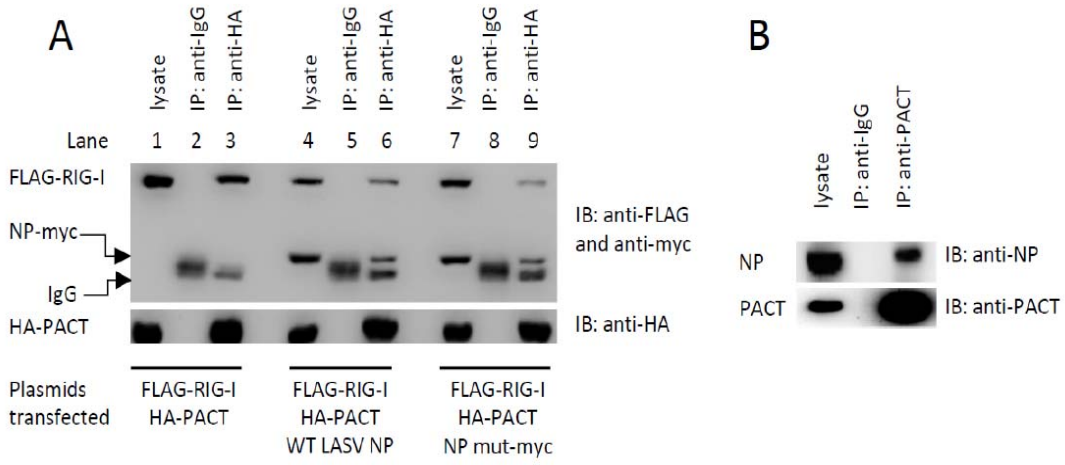

Fig. 14. LASV NP interacts with the RIG-I/PACT complex. (A) 293T cells were transfected with the indicated plasmids shown in the bottom of the gels. 48 hrs post-transfection, cell lysates were immunoprecipitated (IP) with either anti-IgG or anti-HA antibody and analyzed by immunoblotting (IB) with anti-FLAG, anti-myc, or anti-HA antibody. (B) HEK293 cells were infected with WT PICV for 24 hrs. Cell lysates were

pulled down with either anti-IgG or anti-PACT antibody and analyzed by immunoblotting (IB) with antibodies against NP or PACT.

RIG-I and PACT played important roles in restriction of Pichinde virus (PICV) replication.

To understand the roles of RIG-I, PACT and NP in authentic arenavirus infection, we characterized the growth kinetics of recombinant WT and RNase-defective PICV generated from reverse genetics system (173, 231) in normal (WT), RIG-I knockout (KO) or PACT KO mouse embryonic fibroblast (MEF) cells (234, 235). We separately infected these cells with either recombinant WT PICV or the RNase-defective D389A PICV at the multiplicity of infection (MOI) of 0.01. Cellular supernatants were collected at 24 h, 48 h, 72 h and 96 h post infection. The results showed that the WT PICV could replicate in both RIG-I KO and PACT KO cells at levels that were significantly higher than in the WT MEF cells (**Fig. 15A, 15B**), strongly suggesting that these cellular proteins can restrict PICV replication. While the RNase-defective D389A PICV could barely grow in WT MEF cells, it grew to a similar level as that of the WT PICV in the RIG-I KO MEF cells (**Fig. 15A**). It also grew relatively better in the PACT KO MEF cells than in WT MEF cells, but to a level that was less than in the RIG-I KO MEF cells (**Fig. 15A, 15B**). Collectively, these data indicate that both RIG-I and PACT restrict PICV replication and that the viral NP RNase function potently antagonizes these host restriction factors in order to optimize virus replication. These data also implicate RIG-I as a sensor for arenavirus, and PACT plays an enhancing role of host innate immune response to arenavirus infection.

Although the PICV growth kinetics in RIG-I and PACT KO MEFs (**Fig. 15A and 15B**) are consistent with the role of NP RNase activity in the inhibition of RIG-I/PACT signaling, the studies described in Figure 1 and Figure 2 were conducted in human cells with human RIG-I and human PACT proteins. While the human and mouse PACT proteins are highly conserved (>98%), the RIG-I proteins from both species show a higher degree of primary sequence variation (59.5% sequence conservation). We therefore decided to use human PACT and mouse RIG-I (mRIG-I) in a similar IFNβ-LUC assay in an attempt to confirm the role of NP RNase activity in the suppression of PACT-enhanced mRIG-I-dependent IFNβ activation. Similar to the results shown in Figure 1C, WT NP but not RNase-defective NP, strongly suppressed mRIG-I/PACT-induced IFNβ-promoter activation (**Fig. 15C**), suggesting that NP RNase activity plays a similar role to suppress both human and mouse RIG-I's via the highly conserved PACT proteins, validating our choice of using MEFs for further analyses. Our data also demonstrate that mouse RIG-I and human RIG-I proteins are functionally interchangeable and are similarly impacted by the viral NP-mediated inhibition (**Fig. 15A and Fig. 15C**). These data are consistent with the viral growth kinetics in the RIG-I and PACT KO MEF cells (**Fig. 15A, 15B**).

Fig. 15

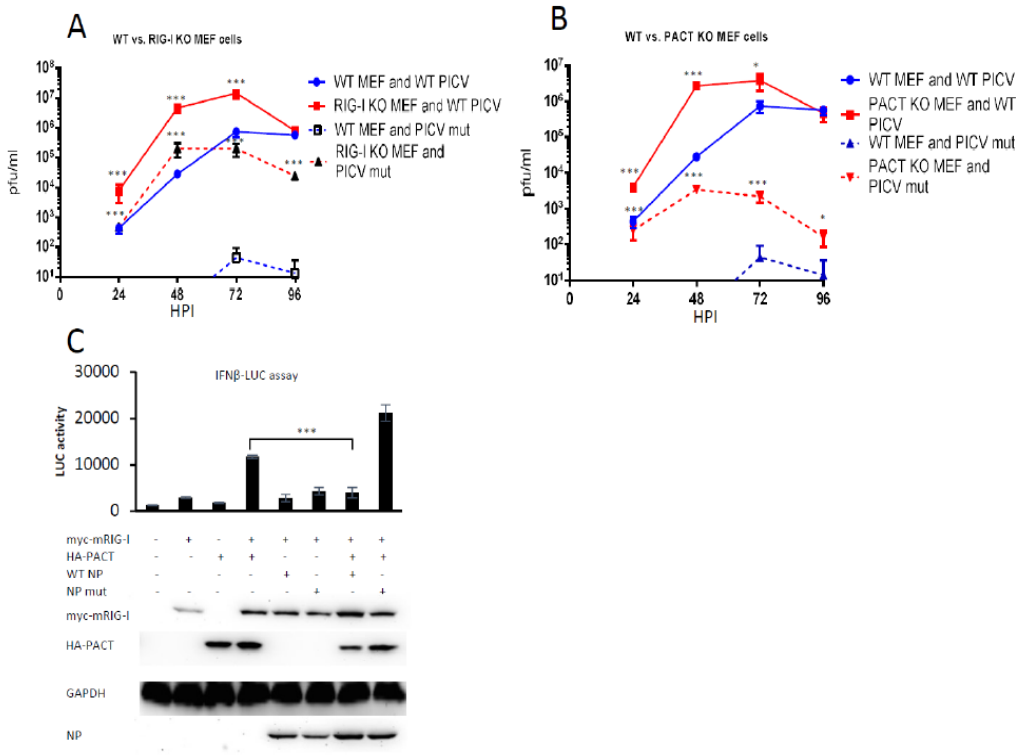

*Fig. 15. Viral growth kinetics of WT and mutant PICV in RIG-I KO (A) and PACT KO (B) mouse embryonic fibroblast (MEF) cells. Cells were infected with either WT or NP RNase-defective PICV mutant (PICV mut) at moi of 0.01. At different time points post infection, virus titers in the supernatants were quantified by plaque assay. WT cells are shown in red lines, whereas KO cells are shown in blue lines. WT PICV is shown in solid line, while mutant PICV is shown in dashed line. The experiments that generated data for each of the panels shown had been repeated three times. The results shown are the average of one such experiment (in triplicates). Titer of each type of virus samples from the KO MEF cells was compared to WT MEF cells by the Student's t-test, ***, P<0.01, *, P<0.05. (C) WT LASV NP, but not RNase-defective NP (NP mut), could inhibit mouse RIG-I (mRIG-I)/PACT-induced IFNβ promoter activity. The experiments that generated*

*data for this panel had been repeated three times. The results shown are the average of one such experiment (in triplicates). The luciferase (LUC) activities of certain samples were compared to the corresponding controls by the Student's t-test, ***, P<0.01. Expression of mRIG-I, PACT, NP, and housekeeping gene GAPDH in each transfection was detected by Western blotting with respective antibodies and shown at the bottom.*

WT and NP RNase-defective PICV infections induced differential IFNβ production in WT, RIG-I KO and PACT KO MEF cells.

We next asked whether the different viral growth kinetics seen in cell cultures would correspond to the different levels of innate-immune gene expressions. To do this, we infected WT, RIG-I KO and PACT KO MEF cells with WT or NP RNase defective D389A PICV at different MOIs (MOI = 0.1, 1.0, and 5.0). The expression levels of the IFNβ, NFκB, ISG56, and IFNβ genes were quantified by either ELISA (**Fig. 16**) or quantitative RT-PCR (**Fig. 17**). The results showed that WT PICV effectively suppressed IFNβ expression in all cell lines tested (**Fig. 16 and Fig. 17A**). On a contrary, the RNase-defective PICV induced significantly higher levels of IFNβ production as compared to the WT PICV virus in all cell lines tested (**Fig. 16 and Fig. 17A**). Significantly higher levels of NFκB and ISG56 mRNA levels were also detected in WT MEF cells infected with the NP RNase-defective PICV when compared to WT PICV infection (**Fig. 17B and 17C**). While there were no obvious IFNβ, NFκB and ISG56 expressions in the RIG-I KO MEFs when they were infected with either the WT or the NP RNase-defective PICV (**Fig. 16, Fig. 17A, 17B and 17C**), these mRNA levels were significantly induced in the PACT KO MEF cells when they were infected with the NP RNase-defective PICV (**Fig.**

17A, 17B, and 17C) but were still lower than those in WT MEF cells infected with the same NP RNase-defective PICV. These data once again implicate that RIG-I acts as a major sensor of arenavirus, whereas PACT plays an enhancing role of host innate immune response to arenavirus infection.

Fig. 16

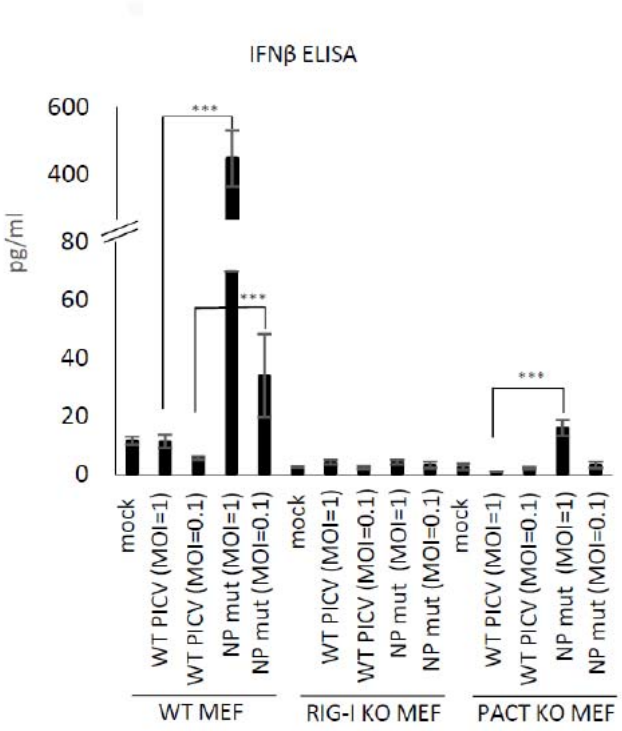

*Fig. 16. IFNβ expression levels from different types of MEF cells stimulated by either WT or RNase defective PICV (NP mut) infection (MOI=1 or MOI=0.1). (A) IFNβ expression levels measured by ELISA. The experiments that produced data for this graph had been repeated three times. The results shown are the average of one such experiment (in triplicates). The IFNβ expression levels for certain samples were compared by Student t-test, ***, P<0.01.*

Fig. 17

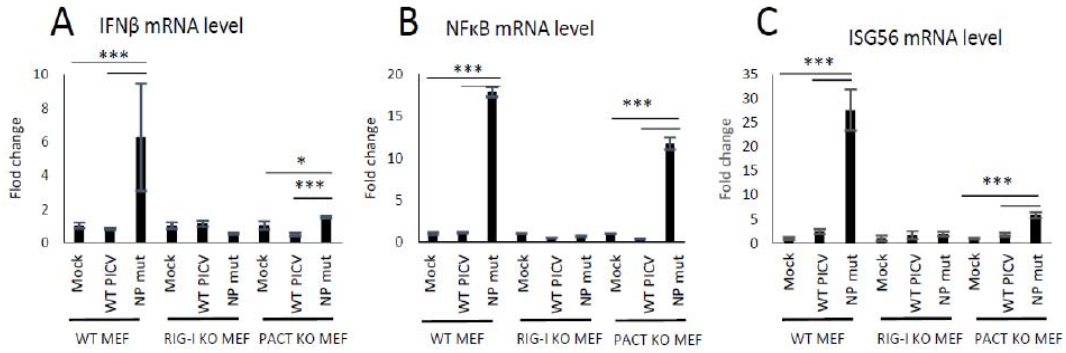

*Fig. 17. IFNβ, NFκB and ISG56 mRNA levels from different types of MEF cells stimulated by infection with either WT or RNase defective PICV (NP mut) (MOI=5). The levels of the IFNβ and NFκB mRNA transcripts were measured at 16 hrs postinfection, whereas the levels of the ISG56 mRNA transcripts was measured at 4 hrs post infection. The house-keeping gene (GAPDH) mRNA levels were also measured to normalize the CT values. Experiments that generated data for each of the panels were repeated at least 3 times. The mRNA levels of certain samples were compared by Student t-test, ***, P<0.01, *, P<0.05.*

Discussion

In this study, we show for the first time that arenavirus NPs can strongly inhibit the RIG-I/PACT activation through its RNase activity and that this inhibition is essential for viral replication in immune-competent cells.

RIG-I is a major cytosolic sensor of RNA viruses that activate the early antiviral responses including the expression of the type I IFN. Recent studies have identified PACT as a positive regulator of the RIG-I signaling (218). PACT can strongly augment RIG-I's function to activate type I IFN production through a direct protein-protein

interaction with RIG-I to stimulate RIG-I's ATPase activity (218). Several viral antagonists, such as EBOV VP35, IAV NS1, HSV1 Us11, and MERS-CoV 4a and N proteins, and MHV N, have been shown to inhibit the PACT-enhanced RIG-I activation by directly disrupting the RIG-I-PACT interaction (220-223, 226). We show here that arenavirus NP can also effectively inhibit the PACT-enhanced RIG-I activation, but that its inhibitory mechanism is not through disrupting the RIG-I-PACT interaction. It is rather dependent on the NP's RNase domain and function (**Fig. 14**), possibly by degrading the RNA ligands of the RIG-I/PACT complex.

Our study suggests an essential role of RNA ligands in the PACT-enhanced RIG-I activation. RIG-I is known to recognize short dsRNA with a 5'-di/triphosphate end (215, 236, 237). Although PACT is a dsRNA-binding protein (219), its physiological ligands and their functional role remain uncharacterized. Previous studies have mostly focused on the direct RIG-I-PACT protein-protein interactions in the activation of RIG-I function (218, 220-223, 226). In particular, when RIG-I and PACT are overexpressed in cells in the absence of viral infections or PAMP RNA transfection, it is generally assumed that PACT can directly activate RIG-I through direct protein-protein interaction. Our data on the NP RNase-dependent inhibition of PACT/RIG-I-induced IFNβ production (**Fig. 13C**) indicate that, even in cell over-expressing PACT and RIG-I without presence of PAMP RNAs, RNA ligands might still be essential for the PACT/RIG-I activation as targeting these RNA ligands by NP RNase effectively inhibits the PACT/RIG-I-induced IFNβ production. The identity of these RNA ligands is unknown but can be originated from both endogenous cellular RNAs (e.g., in the absence of viral infection or PAMP RNA

transfection) and exogenous PAMP RNAs (e.g., in virus-infected cells). It is also unknown whether they are ligands for RIG-I or PACT or both. A recent study by Ho and colleagues shows that a defective interfering (DI) RNA from measles virus vaccine strongly activates IFNβ production through PACT and RIG-I and that this DI RNA is associated with PACT, implicating PACT as another cytoplasmic PAMP RNA sensor. Further studies are necessary to identify the endogenous and exogenous RNA ligands of PACT and RIG-I in order to fully understand the activation mechanism of the PACT/RIG-I complex.

Both PAMP RNA and PACT can activate RIG-I ATPase activity, which is essential for RIG-I function, however, the exact role of ATPase of RIG-I has not been well characterized (217, 238, 239). Several studies have shown that RIG-I ATPase is involved in the discrimination of self-RNA versus nonself-RNA (238, 239), whereas other studies have shown that ATP hydrolysis is critical for RIG-I activation (215) to mediate its translocation on the bound dsRNA (216, 217). Our data show that RNA ligands (self and/or PAMP RNA) are essential for the PACT/RIG-I activation and that NP RNase activity can degrade these RNA ligands and therefore effectively inhibits the PACT/RIG-I pathway. While we have not formally ruled out the involvement of RIG-I's ATPase function, our data collectively indicate that NP mainly affects IFNβ production by degrading the RNA ligands to suppress the PACT/RIG-I pathway.

Our study further demonstrates the restrictive roles of RIG-I and PACT in arenavirus replication. Previous studies have shown that RIG-I is a sensor of arenavirus infections (201). By recognizing the 5' di/triphosphated dsRNA ligands derived from RNA virus

replication, RIG-I recruits the adaptor protein MAVS to activate the downstream protein kinase complexes leading to the activation of several transcriptional factors such as IRF3 and IRF7 that induce the production of type I IFNs and other antiviral genes to restrict viral replication at multiple steps (240-243). As a positive regulator of RIG-I, the functional role of PACT in authentic viral infection, however, is less clear. Previous studies have shown that the IFNβ production is attenuated in the PACT KO cells upon HSV or SeV infection (218, 223), suggesting that PACT plays an important role in IFNβ production upon virus infection. However, no prior studies have addressed whether PACT restricts virus replication. Our study has demonstrated for the first time that both RIG-I and PACT function to restrict arenavirus replication (**Fig. 15**). On the other hand, arenavirus utilizes its NP protein to effectively evade the PACT- and RIG-I-mediated inhibition via its RNase activity, allowing the virus to replicate at high levels in the infected cells. Recombinant PICV with an RNase-defective NP mutation completely lost the ability to grow in WT mouse embryonic cells (**Fig. 15**), consistent with our previous study in human lung epithelial A549 cells (231), demonstrating again that NP RNase-mediated immune evasion is essential for arenavirus replication. This NP RNase-defective mutant virus grows to a much higher level in the RIG-I-KO than in the PACT-KO cells, indicating that RIG-I is the major target of the NP RNase-mediated inhibition during viral infection, consistent with an earlier finding (201).

In summary, our study provides important insight into the role of PACT-enhanced RIG-I activation mechanism, reveals the functions of PACT and RIG-I as restriction factors of arenavirus infection, and demonstrates the essential role of the NP RNase-mediated

PACT/RIG-I inhibition. This new knowledge can be exploited for the development of novel antiviral treatments and/or vaccine development against some arenaviruses that can cause severe and lethal hemorrhagic fever diseases in humans.

Materials and Methods

Plasmids and cells: The LASV, JUNV, MACV, Tacaribe virus (TCRV) and Pichinde virus (PICV) NP genes were cloned into mammalian expression plasmid pCAGGS, respectively, with a C-terminal myc tag, except for PICV NP, which did not have a myc tag. Human RIG-I and PACT expression plasmids were kind gifts of C. Basler (Georgia State University) and G. Amarasinghe (Washington University), respectively. Mouse RIG-I expression plasmid was a kind gift of Dr. Adolfo Garcia-Sastre (Mount Sinai School of Medicine). Single alanine substitution of a conserved RNase catalytic residue (D389A) of the LASV NP protein was generated as described previously (228). Human kidney epithelial cells (293T and 293 cells) and baby hamster kidney cells (BHK21 and BSRT7-5 cells) were grown in Dulbecco's modified Eagle's medium (DMEM, Sigma) supplemented with 10% heat-inactivated fetal bovine serum (FBS, Sigma) and 50 μg/ml penicillin-streptomycin. Vero cells were grown in minimum essential medium (MEM, Invitrogen) supplemented with 10% heat-inactivated FBS and 50 μg/ml penicillin-streptomycin. RIG-I KO MEF cells and PACT KO MEF cells (derived from the C57BL/6 mouse strain) were kind gifts of G. Sen (Cleveland Clinic) (234) and M. Gale, Jr. (University of Washington) (235), and were grown in DMEM supplemented with 10% heat-inactivated FBS and 50 μg/ml penicillin-streptomycin.

Generation of recombinant PICV mutants and viral growth curve analysis: The methods for generating the WT and NP RNase-deficient PICV have been described previously (231). Viral growth curve was carried out as previously described (197).

PICV plaque assay: Vero cells were seeded into six-well plates at 50%-70% confluence and infected with 1 ml of serial 10-fold dilutions of viruses in MEM for 1 h at 37°C. After removal of the medium and washed with phosphate buffer saline (PBS), the cells were incubated in complete fresh MEM supplemented with 0.5% agar and cultured for additional 4 days at 37°C with 5% CO_2. Plaques were stained overnight with a diluted neutral red solution (0.01%) in 0.5% agar–MEM–2% FBS medium.

Coimmunoprecipitation assay: 293T cells were grown overnight to 60%-80% confluence in 10-cm tissue-culture dishes in complete DMEM supplemented with 1% penicillin-streptomycin and 10% FBS. Using a standard calcium phosphate transfection method, cells were transfected with 10 μg of each of the plasmids expressing the RIG-I and PACT along with 10 μg of wild-type (WT) LASV NP or 10 μg of NP RNase-catalytic mutants (D389A). In a control experiment, 10 μg of an empty pCAGGS plasmid was used in place of the NP-expressing plasmid. Forty-eight hours post-transfection, cells were lysed in lysis buffer (50 mM Tris-HCl, pH 7.4, 150 mM NaCl, 1% NP-40, and protein inhibitor cocktail (Roche]). The cell lysates were incubated either with 1 μg of anti-HA or mouse IgG (Genescript), as a negative control, at 4°C for 2 h to 4 h, with constant rotation. Protein A/G beads (Santa Cruz) were added, and the samples were incubated with constant rotation at 4°C overnight. The protein complexes were washed 5 times with lysis buffer, standard 2X Laemmli sample buffer was added, and the samples

were boiled for 5 min and then loaded onto an SDS-PAGE gel for Western blotting using a mouse anti-FLAG, anti-HA or anti-myc monoclonal antibody (Sigma). For the endogenous NP and PACT co-immunoprecipitation assay, 293 cells were seeded in 10 cm dish with 60%-80% confluence for PICV infection. Twenty-four hours post infection, a similar co-IP assay was carried out with 1 μg of anti-PACT antibody (Cell Signaling Technology) and analyzed with the PACT- or NP-specific antibody as previously described (228).

IFNβ promoter-dependent LUC assay: 293T cells were transfected with either an empty vector or the NP expression vector together with 100 ng of IFNβ-LUC reporter plasmid, which expresses the firefly luciferase (Fluc) reporter gene from the IFNβ promoter, and 50 ng of β-gal expressing plasmid for the purpose of transfection efficiency normalization. For RIG-I or RIG-I plus PACT mediated IFNβ induction, 100 ng of a plasmid expressing the FLAG-tagged human RIG-I (FLAG-hRIG-I) or myc-tagged mouse RIG-I (myc-mRIG-I) either alone or with 100ng of the pCAGGS-PACT-HA was included in the transfection reaction. Cell lysates were prepared at 48 hrs post-transfection for Fluc and β-gal assays. Fluc activities were normalized to the β-gal values as previously described (231).

ELISA assay: WT or NP RNase defective PICVs were used to infect WT, PACT KO or RIG-I KO MEF cells at MOI=1 or 0.1. Twenty-four hours post infection, the levels of IFNβ in the supernatants of the virus-infected cells were quantified using a mouse IFNβ enzyme-linked immunosorbent assay (ELISA) kit (LEGEND MAX™ Mouse IFN-β ELISA Kit with Pre-coated Plates) following the manufacturer's instructions.

qRT-PCR assay: WT or NP RNase-defective PICVs were used to infect WT, PACT KO or RIG-I KO MEF cells at MOI=5. Total cellular RNAs were extracted using the TRI reagent (Sigma) according to the manufacturer's instructions. The extracted RNAs were treated with DNase (Promega) to eliminate genomic DNA contamination and re-extracted with Acid-Phenol: Chloroform (Ambion) according to the manufacturer's instructions. Single-stranded cDNAs were generated using an oligo(dT) primer and MMLV reverse transcriptase (Promega) following the manufacturer's protocol. Quantitative PCR was conducted with specific primers designed to detect mouse IFNβ, NFκB, ISG56 and the housekeeping glyceraldehyde-3-phosphate dehydrogenase (GAPDH) gene by using iQ™ SYBR® Green Supermix (Bio-Rad) on a Bio-Rad CFX quantitative PCR machine. The IFNβ and NFκB mRNA levels were quantified at 16 hrs postinfection, whereas the ISG56 mRNA levels were measured at 4 h post infection. The primer sequences were listed in Table 2. The PCR mixtures were incubated at 95°C for 3 min, followed by 40 cycles of amplification at 95°C for 10 s and 55°C for 30 s. The RNA level of each gene from virus-infected cells was first normalized to that of GAPDH gene and then compared to that in mock-treated cells and shown as the fold changes in the graph. Results shown are the averages of one experiment done in triplicates. The experiment has been repeated 4 times.

Table 2: Primers used in qRT-PCR

Primer name	Sequence
mouse IFN beta F	5'CCAGCTCCAAGAAAGGACGA3'
mouse IFN beta R	5'CGCCCTGTAGGTGAGGTTGAT3'
mouse NFkB F	5'GAAATTCCTGATCCAGACAAAAAC3'
mouse NFkB R	5'ATCACTTCAATGGCCTCTGTGTAG3'
mouse ISG56 F	5'ACCATGGGAGAGAATGCTGAT3'
mouse ISG56 R	5'GCCAGGAGGTTGTGC3'
mouse GAPDH F	5'CATCTTGGGCTACACTGAGG3'
mouse GAPDH R	5'ACCACCCTGTTGCTGT3'

This work has been published in the Journal of Virology (J Virol. 2018 Jun 13;92(13). pii: e00482-18. doi: 10.1128/JVI.00482-18)

Chapter V

Discussion and Future Directions

With globalization, human arenavirus-infected cases have been found all over the world by travelers to and from the endemic areas, which also increases the risk of disease outbreaks. The lack of specific FDA-approved arenavirus vaccines and the limitation of treatments highlight arenavirus infection as a significant public health threat. Therefore, understanding the basic biology of arenavirus life cycle and host immune response to arenavirus infection will undoubtedly aid the development of the much-needed vaccines and therapies against these deadly viral pathogens. My studies have filled in the knowledge gap by characterizing the functional mechanisms of viral GPC and NP proteins in arenavirus biology and pathogenesis, and are expected to guide the future development of novel antivirals and vaccines.

My studies have revealed residues within SSP and GP2 CTP regions that are critical for GPC-mediated membrane fusion and viral replication. It has been shown that SSP and GP2 CTD play important roles in GPC processing and membrane-membrane fusion activity (167, 184, 244), but these functions have not been tested in authentic arenavirus infection. Using the PICV reverse genetics system, I have characterized the biological roles of conserved residues of SSP *in vitro* and *in vivo* and GP2 CTD *in vitro*. Some conserved residues (K33, F49 and C57 of SSP and H469, H471, C477, H481, C489, C491, and W503 of GP2 CTD) are essential for arenaviral life cycle and play important roles in regulating membrane-membrane fusion activity. These conserved critical residues could be targeted for developing anti-viral agent. Screening of small molecules

to inhibit GPC-mediated virus entry and membrane-membrane fusion has been reported (166, 245-248). Specific compound that targets K33 has been found to suppress GPC mediated membrane-membrane fusion activity (245). According to my SSP and GP2 CTD study, screening for specific small molecules targeting F49, C57 and other conserved residues of GP2 are also promising. We also have shown the G2A and N20A mutants are attenuated in guinea pig models, suggesting that G2 and N20 could be used to attenuate arenavirus in the development of arenaviral vaccines. Many questions still remain to be addressed on the molecular mechanism of GPC-mediated membrane fusion and virus entry. In particular, the crystal structure of entire GPC is not available, we do not know the exact position of these conserved residues in either pre- or post-fusion form, which limits our understanding of the detailed mechanism of membrane fusion and the roles of these conserved residues play in GPC function.

My arenaviral NP study has demonstrated the important roles of arenaviral NPs in suppressing RIG-I/PACT induced IFNβ production by its 3'-5' exoribonuclease (RNase) activity. As such, screening for compounds that can inhibit the NP RNase activity (as described in the Introduction chapter (Chapter 1) and/or its role in mediating immune suppression in the PACT-RIG-I innate immune pathway as described in Chapter 4) warrants additional studies, especially when structural details of arenavirus NPs have been well studied (126, 228-230, 233, 249, 250). In particular, the RNase domain located at the C-terminal region of NP, which belongs to the DEDD superfamily (126, 228-230, 233, 250) seems like a very good target for drug screening. In addition, the NP RNase activity can also be exploited for arenaviral vaccine development. Several studies have

shown that the NP RNase defective arenaviruses are attenuated in human primary cells and guinea pig models (129, 231). These results not only showed the essential roles NP played in the inhibition of innate immune response in authentic arenavirus infections but also indicated the value of this protein for developing arenaviral vaccines, i.e., by crippling NP ability to suppress immunity in order to enhance host recognition and response immunologically to the vaccines.

My study also reveals novel mechanistic insights into the host innate immunity and virus-mediated immune evasion. However, many questions remain to be addressed.

(1) In Chapter 4, we showed that arenaviral NP can suppress the PACT-mediated enhancement of RIG-I function to produce type I interferon (e.g., IFNβ) in response to virus infection. In our study, we have shown that both RIG-I and PACT play important roles in restricting arenavirus replication in primary mouse fibroblasts. However, it is known that macrophages and dendritic cells (DCs) are the primary target cells for arenavirus infections. It is therefore important in future studies to investigate the roles of RIG-I, PACT, and NP in macrophages and DCs in the setting of arenavirus infection.

(2) In this study, we also provided evidence to suggest that self RNAs could be targeted by arenaviral NPs as it is required for PACT function to enhance RIG-I activity to induce IFNβ production. A recent study has shown that self RNA such as cellular 5S rRNA pseudogene transcripts can activate RIG-I and induce IFNβ production (251). It is therefore important to characterize these self RNA species in future studies because they play important roles in the RLR pathway, especially their potential roles in the virus-infected cells.

(3) LASV is an important human pathogen that causes human viral hemorrhagic fever. Characterization of the roles of PACT, RIG-I and NP in human cells is much more relevant in order to understand the mechanism of LASV-caused human disease. CRISPR/CAS9 system is a powerful tool to knock out genes from cells. We can generate PACT or RIG-I KO human cells such as 293 and A549 cells, and investigate the roles of PACT and RIG-I in LASV infection condition in the BSL4 lab. Since the LASV reverse genetic system is available, both WT and NP RNase defective LASV can be tested in these PACT or RIG-I KO human cells. The viral kinetics and immune response data from these experiments will help us to further understand the roles of PACT and RIG-I in LASV infection.

(4) Animal model is the most important tool to investigate the pathology of the disease. The roles of NP, RIG-I and PACT has not been investigated in animal models in my study. To further address the roles of NP, RIG-I and PACT, PICV/LASV (WT and/or NP RNase defective virus) should be tested in animal models. Mouse models are convenient and cost-effective, however, normal mouse model is not a perfect animal model for arenaviral hemorrhagic fever, since normal mouse does not develop hemorrhagic fever symptoms. But recent studies have shown that some immunodeficient mice, such as IFN receptor KO and STAT KO mouse can be infected with LASV and JUNV and develop some symptoms that mimic LASV and JUNV caused human diseases. The IFN signaling pathway is severely impaired in these KO mice, which suggested the important roles of type I IFN in arenavirus infection mouse models. Our data has already shown that RIG-I and PACT play important roles in IFN production in arenavirus infected cells. PACT KO

and RIG-I KO mice are also available (252). Therefore, it is possible to use them as new mouse models for arenavirus infection studies, and the data obtained from these animal experiments will provide important insight into the mechanism of RIG-I, PACT in arenavirus infection.

Taken together, my studies have characterized biological roles of arenaviral conserved residues of SSP and GP2 CTD, and a novel immunosuppression mechanism of NP. My studies not only provided potential targets for anti-viral agent/vaccine development but also gain insight into the immunosuppression of arenaviral NPs. My studies might help in improving our knowledge of arenaviruses infections and develop new treatment to combat arenaviral hemorrhagic fevers.

References

1. Maiztegui JI, McKee KT, Oro JGB, Harrison LH, Gibbs PH, Feuillade MR, Enria DA, Briggiler AM, Levis SC, Ambrosio AM, Halsey NA, Peters CJ, Group tAS. Protective Efficacy of a Live Attenuated Vaccine against Argentine Hemorrhagic Fever. Journal of Infectious Diseases. 1998;177(2):277-83. doi: 10.1086/514211.
2. Günther S, Lenz O. Lassa Virus. Critical Reviews in Clinical Laboratory Sciences. 2004;41(4):339-90. doi: 10.1080/10408360490497456.
3. Zong M, Fofana I, Choe H. Human and Host Species Transferrin Receptor 1 Use by North American Arenaviruses. Journal of virology. 2014;88(16):9418-28. doi: 10.1128/JVI.01112-14. PubMed PMID: 24920811.
4. McLay L, Liang Y, Ly H. Comparative analysis of disease pathogenesis and molecular mechanisms of New World and Old World arenavirus infections. J Gen Virol. 2014;95(Pt 1):1-15. doi: 10.1099/vir.0.057000-0. PubMed PMID: 24068704.
5. Radoshitzky SR, Bao Y, Buchmeier MJ, Charrel RN, Clawson AN, Clegg CS, DeRisi JL, Emonet S, Gonzalez JP, Kuhn JH, Lukashevich IS, Peters CJ, Romanowski V, Salvato MS, Stenglein MD, de la Torre JC. Past, present, and future of arenavirus taxonomy. Arch Virol. 2015. doi: 10.1007/s00705-015-2418-y. PubMed PMID: 25935216.
6. Moraz M-L, Kunz S. Pathogenesis of arenavirus hemorrhagic fevers. Expert Review of Anti-infective Therapy. 2010;9(1):49-59. doi: 10.1586/eri.10.142.
7. Cummins D MJBBD, et al. ACute sensorineural deafness in lassa fever. JAMA: The Journal of the American Medical Association. 1990;264(16):2093-6. doi: 10.1001/jama.1990.03450160063030.
8. Briese T, Paweska JT, McMullan LK, Hutchison SK, Street C, Palacios G, Khristova ML, Weyer J, Swanepoel R, Egholm M, Nichol ST, Lipkin WI. Genetic Detection and Characterization of Lujo Virus, a New Hemorrhagic Fever–Associated Arenavirus from Southern Africa. PLoS pathogens. 2009;5(5):e1000455. doi: 10.1371/journal.ppat.1000455.
9. Paweska JT, Sewlall NH, Ksiazek TG, Blumberg LH, Hale MJ, Lipkin WI, Weyer J, Nichol ST, Rollin PE, McMullan LK, Paddock CD, Briese T, Mnyaluza J, Dinh T-H, Mukonka V, Ching P, Duse A, Richards G, Jong Gd, Cohen C, Ikalafeng B, Mugero C, Asomugha C, Malotle MM, Nteo DM, Misiani E, Swanepoel R, Zaki SR, Team OCaI. Nosocomial outbreak of novel arenavirus infection, southern Africa. Emerging Infectious Disease. 2009;15(10):1598-602.
10. Peters CJ. Lymphocytic Choriomeningitis Virus — An Old Enemy up to New Tricks. New England Journal of Medicine. 2006;354(21):2208-11. doi: 10.1056/NEJMp068021.
11. Rousseau MC, Saron MF, Brouqui P, Bourgeade A. Lymphocytic choriomeningitis virus in southern France: Four case reports and a review of the literature. European Journal of Epidemiology. 1997;13(7):817-23.

12. Wright R, Johnson D, Neumann M, Ksiazek TG, Rollin P, Keech RV, Bonthius DJ, Hitchon P, Grose CF, Bell WE, Bale JF. Congenital Lymphocytic Choriomeningitis Virus Syndrome: A Disease That Mimics Congenital Toxoplasmosis or Cytomegalovirus Infection. Pediatrics. 1997;100(1):e9. doi: 10.1542/peds.100.1.e9.
13. Bonthius DJ. Lymphocytic Choriomeningitis Virus: An Underrecognized Cause of Neurologic Disease in the Fetus, Child, and Adult. Seminars in Pediatric Neurology. 2012;19(3):89-95. doi: 10.1016/j.spen.2012.02.002.
14. Fischer SA, Graham MB, Kuehnert MJ, Kotton CN, Srinivasan A, Marty FM, Comer JA, Guarner J, Paddock CD, DeMeo DL, Shieh W-J, Erickson BR, Bandy U, DeMaria A, Davis JP, Delmonico FL, Pavlin B, Likos A, Vincent MJ, Sealy TK, Goldsmith CS, Jernigan DB, Rollin PE, Packard MM, Patel M, Rowland C, Helfand RF, Nichol ST, Fishman JA, Ksiazek T, Zaki SR. Transmission of Lymphocytic Choriomeningitis Virus by Organ Transplantation. New England Journal of Medicine. 2006;354(21):2235-49. doi: 10.1056/NEJMoa053240.
15. MacNeil A, Stroher U, Farnon E, Campbell S, Cannon D, Paddock CD, Drew CP, Kuehnert M, Knust B, Gruenenfelder R, Zaki SR, Rollin PE, Nichol ST, team LTI. Solid organ transplant-associated lymphocytic choriomeningitis, United States, 2011. Emerging Infectious Disease. 2012;18(8):1256-62.
16. Prevention CfDCa. Brief Report: lymphocytic choriomeningitis virus transmitted through solid organ transplantation - Massachussetts, 2008. MMWR Morb Mortal Wkly Rep. 2008;57:799-801.
17. Delgado S, Erickson BR, Agudo R, Blair PJ, Vallejo E, Albariño CG, Vargas J, Comer JA, Rollin PE, Ksiazek TG, Olson JG, Nichol ST. Chapare Virus, a Newly Discovered Arenavirus Isolated from a Fatal Hemorrhagic Fever Case in Bolivia. PLoS pathogens. 2008;4(4):e1000047. doi: 10.1371/journal.ppat.1000047.
18. Lisieux T, Coimbra M, Nassar ES, Burattini MN, Souza LTMd, Ferreira IB, Rocco IM, Rosa APATd, Vasconcelos PFC, Pinheiro FP, LeDuc JW, Rico-Hesse R, Gonzalez J-P, Jahrling PB, Tesh RB. New arenavirus isolated in Brazil. Lancet. 1994;343(8894):391-2.
19. Aguilar PV, Camargo W, Vargas J, Guevara C, Roca Y, Felices V, Laguna-Torres VA, Tesh R, Ksiazek TG, Kochel TJ. Reemergence of Bolivian hemorrhagic fever, 2007-2008. Emerging Infectious Disease. 2009;15(9):1526-8.
20. Ambrosio A, Saavedra M, Mariani M, Gamboa G, Maiza A. Argentine hemorrhagic fever vaccines. Human Vaccines. 2011;7(6):694-700.
21. Charrel RN, Lamballerie Xd. Arenaviruses other than Lassa virus. Antiviral Research. 2003;57(1–2):89-100. doi: 10.1016/s0166-3542(02)00202-4.
22. Enria DA, Briggiler AM, Sánchez Z. Treatment of Argentine hemorrhagic fever. Antiviral Research. 2008;78(1):132-9. doi: 10.1016/j.antiviral.2007.10.010.
23. Fulhorst CF, Cajimat MNB, Milazzo ML, Paredes H, de Manzione NMC, Salas RA, Rollin PE, Ksiazek TG. Genetic diversity between and within the arenavirus species indigenous to western Venezuela. Virology. 2008;378(2):205-13. doi: 10.1016/j.virol.2008.05.014.

24. Harrison LH, Halsey NA, McKee KT, Peters CJ, Barrera Oro JG, Briggiler AM, Feuillade MR, Maiztegui JI. Clinical Case Definitions for Argentine Hemorrhagic Fever. Clinical Infectious Diseases. 1999;28(5):1091-4. doi: 10.1086/514749.
25. Manzione Nd, Salas RA, Paredes H, Godoy O, Rojas L, Araoz F, Fulhorst CF, Ksiazek TG, Mills JN, Ellis BA, Peters CJ, Tesh RB. Venezuelan Hemorrhagic Fever: Clinical and Epidemiological Studies of 165 Cases. Clinical Infectious Diseases. 1998;26(2):308-13. doi: 10.1086/516299.
26. Pfau CJ. Arenaviruses. In: Baron S, editor. Medical Microbiology. 4th ed. Galveston, TX: The University of Texas Medical Branch at Galveston; 1996.
27. Meyer BJ, de la Torre JC, Southern PJ. Arenaviruses: genomic RNAs, transcription, and replication. Current topics in microbiology and immunology. 2002;262:139-57. PubMed PMID: 11987804.
28. Knipe DMH, Peter M. Fields Virology, 5th Edition. Buchmeier MJ, Torre J-Cdl, Peters CJ, editors2007.
29. Cao W, Henry MD, Borrow P, Yamada H, Elder JH, Ravkov EV, Nichol ST, Compans RW, Campbell KP, Oldstone MB. Identification of alpha-dystroglycan as a receptor for lymphocytic choriomeningitis virus and Lassa fever virus. Science. 1998;282(5396):2079-81. PubMed PMID: 9851928.
30. Spiropoulou CF, Kunz S, Rollin PE, Campbell KP, Oldstone MB. New World arenavirus clade C, but not clade A and B viruses, utilizes alpha-dystroglycan as its major receptor. Journal of virology. 2002;76(10):5140-6. PubMed PMID: 11967329; PubMed Central PMCID: PMC136162.
31. Kunz S, Campbell KP, Oldstone MB. Alpha-dystroglycan can mediate arenavirus infection in the absence of beta-dystroglycan. Virology. 2003;316(2):213-20. PubMed PMID: 14644604.
32. Rojek JM, Spiropoulou CF, Campbell KP, Kunz S. Old World and Clade C New World Arenaviruses Mimic the Molecular Mechanism of Receptor Recognition Used by α-Dystroglycan's Host-Derived Ligands. Journal of virology. 2007;81(11):5685-95. doi: 10.1128/jvi.02574-06.
33. Imperiali M, Sporri R, Hewitt J, Oxenius A. Post-translational modification of {alpha}-dystroglycan is not critical for lymphocytic choriomeningitis virus receptor function in vivo. J Gen Virol. 2008;89(Pt 11):2713-22. doi: 10.1099/vir.0.2008/004721-0. PubMed PMID: 18931067.
34. Kunz S, Sevilla N, McGavern DB, Campbell KP, Oldstone MB. Molecular analysis of the interaction of LCMV with its cellular receptor [alpha]-dystroglycan. J Cell Biol. 2001;155(2):301-10. doi: 10.1083/jcb.200104103. PubMed PMID: 11604425; PubMed Central PMCID: PMC2198839.
35. Kunz S, Rojek JM, Perez M, Spiropoulou CF, Oldstone MB. Characterization of the interaction of lassa fever virus with its cellular receptor alpha-dystroglycan. Journal of virology. 2005;79(10):5979-87. PubMed PMID: 15857984.
36. Kunz S, Calder L, Oldstone MB. Electron microscopy of an alpha-dystroglycan fragment containing receptor sites for lymphocytic choriomeningitis virus and laminin, and use of the receptoid body as a reagent to neutralize virus. Virology. 2004;325(2):207-15. doi: 10.1016/j.virol.2004.04.044. PubMed PMID: 15246261.

37. Rojek JM, Campbell KP, Oldstone MBA, Kunz S. Old World Arenavirus Infection Interferes with the Expression of Functional α-Dystroglycan in the Host Cell. Molecular biology of the cell. 2007;18(11):4493-507. doi: 10.1091/mbc.E07-04-0374.
38. Yamamoto T, Kato Y, Karita M, Kawaguchi M, Shibata N, Kobayashi M. Expression of genes related to muscular dystrophy with lissencephaly. Pediatric Neurology. 2004;31(3):183-90. doi: 10.1016/j.pediatrneurol.2004.03.020.
39. Shimojima M, Ströher U, Ebihara H, Feldmann H, Kawaoka Y. Identification of Cell Surface Molecules Involved in Dystroglycan-Independent Lassa Virus Cell Entry. Journal of virology. 2012;86(4):2067-78. doi: 10.1128/jvi.06451-11.
40. Sullivan BM, Welch MJ, Lemke G, Oldstone MB. Is the TAM receptor Axl a receptor for lymphocytic choriomeningitis virus? Journal of virology. 2013;87(7):4071-4. doi: 10.1128/JVI.03268-12. PubMed PMID: 23325690; PubMed Central PMCID: PMC3624193.
41. Beier JI, Jokinen JD, Holz GE, Whang PS, Martin AM, Warner NL, Arteel GE, Lukashevich IS. Novel mechanism of arenavirus-induced liver pathology. PLoS One. 2015;10(3):e0122839. doi: 10.1371/journal.pone.0122839. PubMed PMID: 25822203; PubMed Central PMCID: PMC4378851.
42. Ibraghimov-Beskrovnaya O, Milatovich A, Ozcelik T, Yang B, Koepnick K, Francke U, Campbell KP. Human dystroglycan: skeletal muscle cDNA, genomic structure, origin of tissue specific isoforms and chromosomal localization. Hum Mol Genet. 1993;2(10):1651-7. PubMed PMID: 8268918.
43. I. S. Lukashevich. Reproduction of Lassa virus in different cell cultures. Acta Virol. 1983;27. Epub 285.
44. Jae LT, Raaben M, Herbert AS, Kuehne AI, Wirchnianski AS, Soh TK, Stubbs SH, Janssen H, Damme M, Saftig P, Whelan SP, Dye JM, Brummelkamp TR. Virus entry. Lassa virus entry requires a trigger-induced receptor switch. Science. 2014;344(6191):1506-10. doi: 10.1126/science.1252480. PubMed PMID: 24970085; PubMed Central PMCID: PMC4239993.
45. Radoshitzky SR, Abraham J, Spiropoulou CF, Kuhn JH, Nguyen D, Li W, Nagel J, Schmidt PJ, Nunberg JH, Andrews NC, Farzan M, Choe H. Transferrin receptor 1 is a cellular receptor for New World haemorrhagic fever arenaviruses. Nature. 2007;446(7131):92-6. doi: 10.1038/nature05539. PubMed PMID: 17287727; PubMed Central PMCID: PMC3197705.
46. Flanagan ML, Oldenburg J, Reignier T, Holt N, Hamilton GA, Martin VK, Cannon PM. New world clade B arenaviruses can use transferrin receptor 1 (TfR1)-dependent and -independent entry pathways, and glycoproteins from human pathogenic strains are associated with the use of TfR1. Journal of virology. 2008;82(2):938-48. doi: 10.1128/JVI.01397-07. PubMed PMID: 18003730; PubMed Central PMCID: PMC2224602.
47. Rojek JM, Kunz S. Cell entry by human pathogenic arenaviruses. Cell Microbiol. 2008;10(4):828-35. Epub 2008/01/10. doi: 10.1111/j.1462-5822.2007.01113.x. PubMed PMID: 18182084.
48. Helguera G, Jemielity S, Abraham J, Cordo SM, Martinez MG, Rodriguez JA, Bregni C, Wang JJ, Farzan M, Penichet ML, Candurra NA, Choe H. An antibody

recognizing the apical domain of human transferrin receptor 1 efficiently inhibits the entry of all new world hemorrhagic Fever arenaviruses. Journal of virology. 2012;86(7):4024-8. Epub 2012/01/27. doi: 10.1128/JVI.06397-11. PubMed PMID: 22278244; PubMed Central PMCID: PMC3302512.
49. Radoshitzky SR, Kuhn JH, Spiropoulou CF, Albarino CG, Nguyen DP, Salazar-Bravo J, Dorfman T, Lee AS, Wang E, Ross SR, Choe H, Farzan M. Receptor determinants of zoonotic transmission of New World hemorrhagic fever arenaviruses. Proceedings of the National Academy of Sciences of the United States of America. 2008;105(7):2664-9. doi: 10.1073/pnas.0709254105. PubMed PMID: 18268337; PubMed Central PMCID: PMC2268193.
50. Centers for Disease C, Prevention. Fatal illnesses associated with a new world arenavirus--California, 1999-2000. MMWR Morb Mortal Wkly Rep. 2000;49(31):709-11. PubMed PMID: 10958585.
51. Enserink M. Emerging diseases. New arenavirus blamed for recent deaths in California. Science. 2000;289(5481):842-3. PubMed PMID: 10960307.
52. Milazzo ML, Campbell GL, Fulhorst CF. Novel arenavirus infection in humans, United States. Emerg Infect Dis. 2011;17(8):1417-20. doi: 10.3201/eid1708.110285. PubMed PMID: 21801618; PubMed Central PMCID: PMC3381580.
53. Hueffer K, Parker JS, Weichert WS, Geisel RE, Sgro JY, Parrish CR. The natural host range shift and subsequent evolution of canine parvovirus resulted from virus-specific binding to the canine transferrin receptor. Journal of virology. 2003;77(3):1718-26. PubMed PMID: 12525605; PubMed Central PMCID: PMC140992.
54. Ross SR, Schofield JJ, Farr CJ, Bucan M. Mouse transferrin receptor 1 is the cell entry receptor for mouse mammary tumor virus. Proceedings of the National Academy of Sciences of the United States of America. 2002;99(19):12386-90. doi: 10.1073/pnas.192360099. PubMed PMID: 12218182; PubMed Central PMCID: PMC129454.
55. Demogines A, Abraham J, Choe H, Farzan M, Sawyer SL. Dual host-virus arms races shape an essential housekeeping protein. PLoS biology. 2013;11(5):e1001571. doi: 10.1371/journal.pbio.1001571. PubMed PMID: 23723737; PubMed Central PMCID: PMC3665890.
56. Choe H, Jemielity S, Abraham J, Radoshitzky SR, Farzan M. Transferrin receptor 1 in the zoonosis and pathogenesis of New World hemorrhagic fever arenaviruses. Curr Opin Microbiol. 2011;14(4):476-82. doi: 10.1016/j.mib.2011.07.014. PubMed PMID: 21807555; PubMed Central PMCID: PMC3159852.
57. Martinez MG, Bialecki MA, Belouzard S, Cordo SM, Candurra NA, Whittaker GR. Utilization of human DC-SIGN and L-SIGN for entry and infection of host cells by the New World arenavirus, Junin virus. Biochem Biophys Res Commun. 2013;441(3):612-7. doi: 10.1016/j.bbrc.2013.10.106. PubMed PMID: 24183720; PubMed Central PMCID: PMC4096786.
58. Eschli B, Quirin K, Wepf A, Weber J, Zinkernagel R, Hengartner H. Identification of an N-Terminal Trimeric Coiled-Coil Core within Arenavirus Glycoprotein 2 Permits Assignment to Class I Viral Fusion Proteins. Journal of virology. 2006;80(12):5897-907. doi: 10.1128/jvi.00008-06.

59. Gallaher WR, DiSimone C, Buchmeier MJ. The viral transmembrane superfamily: possible divergence of Arenavirus and Filovirus glycoproteins from a common RNA virus ancestor. BMC Microbiol. 2001;1:1. PubMed PMID: 11208257.
60. York J, Nunberg JH. Distinct requirements for signal peptidase processing and function in the stable signal peptide subunit of the Junín virus envelope glycoprotein. Virology. 2007;359(1):72-81. doi: 10.1016/j.virol.2006.08.048.
61. Quirin K, Eschli B, Scheu I, Poort L, Kartenbeck J, Helenius A. Lymphocytic choriomeningitis virus uses a novel endocytic pathway for infectious entry via late endosomes. Virology. 2008;378(1):21-33. doi: 10.1016/j.virol.2008.04.046. PubMed PMID: 18554681.
62. Pasqual G, Rojek JM, Masin M, Chatton J-Y, Kunz S. Old World Arenaviruses Enter the Host Cell via the Multivesicular Body and Depend on the Endosomal Sorting Complex Required for Transport. PLoS pathogens. 2011;7(9):e1002232. doi: 10.1371/journal.ppat.1002232.
63. Hass M, Gölnitz U, Müller S, Becker-Ziaja B, Günther S. Replicon System for Lassa Virus. Journal of virology. 2004;78(24):13793-803. doi: 10.1128/jvi.78.24.13793-13803.2004.
64. Lee KJ, Novella IS, Teng MN, Oldstone MBA, de la Torre JC. NP and L Proteins of Lymphocytic Choriomeningitis Virus (LCMV) Are Sufficient for Efficient Transcription and Replication of LCMV Genomic RNA Analogs. Journal of virology. 2000;74(8):3470-7. doi: 10.1128/jvi.74.8.3470-3477.2000.
65. López N, Jácamo R, Franze-Fernández MaT. Transcription and RNA Replication of Tacaribe Virus Genome and Antigenome Analogs Require N and L Proteins: Z Protein Is an Inhibitor of These Processes. Journal of virology. 2001;75(24):12241-51. doi: 10.1128/jvi.75.24.12241-12251.2001.
66. Vieth S, Torda AE, Asper M, Schmitz H, Günther S. Sequence analysis of L RNA of Lassa virus. Virology. 2004;318(1):153-68. doi: 10.1016/j.virol.2003.09.009.
67. Brunotte L, Lelke M, Hass M, Kleinsteuber K, Becker-Ziaja B, Günther S. Domain Structure of Lassa Virus L Protein. Journal of virology. 2011;85(1):324-33. doi: 10.1128/jvi.00721-10.
68. Brunotte L, Kerber R, Shang W, Hauer F, Hass M, Gabriel M, Lelke M, Busch C, Stark H, Svergun DI, Betzel C, Perbandt M, Günther S. Structure of the Lassa Virus Nucleoprotein Revealed by X-ray Crystallography, Small-angle X-ray Scattering, and Electron Microscopy. Journal of Biological Chemistry. 2011;286(44):38748-56. doi: 10.1074/jbc.M111.278838.
69. Poch O, Sauvaget I, Delarue M, Tordo N. Identification of four conserved motifs among the RNA-dependent polymerase encoding elements. Embo J. 1989;8(12):3867-74. PubMed PMID: 2555175.
70. Lehmann M, Pahlmann M, Jerome H, Busch C, Lelke M, Gunther S. Role of the C terminus of Lassa virus L protein in viral mRNA synthesis. Journal of virology. 2014;88(15):8713-7. doi: 10.1128/JVI.00652-14. PubMed PMID: 24829349; PubMed Central PMCID: PMC4135956.
71. Morin B, Coutard B, Lelke M, Ferron F, Kerber R, Jamal S, Frangeul A, Baronti C, Charrel R, de Lamballerie X, Vonrhein C, Lescar J, Bricogne G, Günther S, Canard B.

The N-Terminal Domain of the Arenavirus L Protein Is an RNA Endonuclease Essential in mRNA Transcription. PLoS pathogens. 2010;6(9):e1001038. doi: 10.1371/journal.ppat.1001038.
72. Wallat GD, Huang Q, Wang W, Dong H, Ly H, Liang Y, Dong C. High-resolution structure of the N-terminal endonuclease domain of the Lassa virus L polymerase in complex with magnesium ions. PLoS One. 2014;9(2):e87577. doi: 10.1371/journal.pone.0087577. PubMed PMID: 24516554; PubMed Central PMCID: PMC3917842.
73. Raju R, Raju L, Hacker D, Garcin D, Compans R, Kolakofsky D. Nontemplated bases at the 5' ends of Tacaribe virus mRNAs. Virology. 1990;74(1):53-9.
74. Qi X, Lan S, Wang W, Schelde LM, Dong H, Wallat GD, Ly H, Liang Y, Dong C. Cap binding and immune evasion revealed by Lassa nucleoprotein structure. Nature. 2010;468(7325):779-83.
75. Linero F, Welnowska E, Carrasco L, Scolaro L. Participation of eIF4F complex in Junin virus infection: blockage of eIF4E does not impair virus replication. Cell Microbiol. 2013;15(10):1766-82. doi: 10.1111/cmi.12149. PubMed PMID: 23601822.
76. D'Antuono A, Loureiro ME, Foscaldi S, Marino-Buslje C, Lopez N. Differential contributions of tacaribe arenavirus nucleoprotein N-terminal and C-terminal residues to nucleocapsid functional activity. Journal of virology. 2014;88(11):6492-505. doi: 10.1128/JVI.00321-14. PubMed PMID: 24696466; PubMed Central PMCID: PMC4093893.
77. Cornu TI, de la Torre JC. RING Finger Z Protein of Lymphocytic Choriomeningitis Virus (LCMV) Inhibits Transcription and RNA Replication of an LCMV S-Segment Minigenome. Journal of virology. 2001;75(19):9415-26. doi: 10.1128/jvi.75.19.9415-9426.2001.
78. Cornu TI, Feldmann H, de la Torre JC. Cells expressing the RING finger Z protein are resistant to arenavirus infection. Journal of virology. 2004;78(6):2979-83. Epub 2004/03/03. PubMed PMID: 14990716; PubMed Central PMCID: PMC353761.
79. Cornu TI, de la Torre JC. Characterization of the arenavirus RING finger Z protein regions required for Z-mediated inhibition of viral RNA synthesis. Journal of virology. 2002;76(13):6678-88. Epub 2002/06/07. PubMed PMID: 12050381; PubMed Central PMCID: PMC136245.
80. Kranzusch PJ, Whelan SPJ. Arenavirus Z protein controls viral RNA synthesis by locking a polymerase–promoter complex. Proceedings of the National Academy of Sciences. 2011;108(49):19743-8. doi: 10.1073/pnas.1112742108.
81. Eichler R, Lenz O, Strecker T, Garten W. Signal peptide of Lassa virus glycoprotein GP-C exhibits an unusual length. FEBS Letters. 2003;538(1–3):203-6. doi: 10.1016/s0014-5793(03)00160-1.
82. Beyer WR, Pöpplau D, Garten W, von Laer D, Lenz O. Endoproteolytic Processing of the Lymphocytic Choriomeningitis Virus Glycoprotein by the Subtilase SKI-1/S1P. Journal of virology. 2003;77(5):2866-72. doi: 10.1128/jvi.77.5.2866-2872.2003.
83. Burri DJ, Pasqual G, Rochat C, Seidah NG, Pasquato A, Kunz S. Molecular Characterization of the Processing of Arenavirus Envelope Glycoprotein Precursors by

Subtilisin Kexin Isozyme-1/Site-1 Protease. Journal of virology. 2012;86(9):4935-46. doi: 10.1128/jvi.00024-12.
84. Lenz O, ter Meulen J, Klenk H-D, Seidah NG, Garten W. The Lassa virus glycoprotein precursor GP-C is proteolytically processed by subtilase SKI-1/S1P. Proceedings of the National Academy of Sciences. 2001;98(22):12701-5. doi: 10.1073/pnas.221447598.
85. Wright KE, Spiro RC, Burns JW, Buchmeier MJ. Post-translational processing of the glycoproteins of lymphocytic choriomeningitis virus. Virology. 1990;177(1):175-83.
86. Eichler R, Lenz O, Garten W, Strecker T. The role of single N-glycans in proteolytic processing and cell surface transport of the Lassa virus glycoprotein GP-C. Virology Journal. 2006;3(1):41. PubMed PMID: doi:10.1186/1743-422X-3-41.
87. Loureiro ME, Wilda M, Levingston Macleod JM, D'Antuono A, Foscaldi S, Buslje CM, Lopez N. Molecular Determinants of Arenavirus Z Protein Homo-Oligomerization and L Polymerase Binding. Journal of virology. 2011;85(23):12304-14. doi: 10.1128/jvi.05691-11.
88. Bieniasz PD. Late budding domains and host proteins in enveloped virus release. Virology. 2006;344(1):55-63. doi: 10.1016/j.virol.2005.09.044. PubMed PMID: 16364736.
89. Im YJ, Kuo L, Ren X, Burgos PV, Zhao XZ, Liu F, Burke TR, Jr., Bonifacino JS, Freed EO, Hurley JH. Crystallographic and functional analysis of the ESCRT-I /HIV-1 Gag PTAP interaction. Structure. 2010;18(11):1536-47. doi: 10.1016/j.str.2010.08.010. PubMed PMID: 21070952; PubMed Central PMCID: PMC3124085.
90. Freed EO. Viral late domains. Journal of virology. 2002;76(10):4679-87. PubMed PMID: 11967285.
91. Loureiro ME, D'Antuono A, Levingston Macleod JM, López N. Uncovering Viral Protein-Protein Interactions and their Role in Arenavirus Life Cycle. Viruses. 2012;4(9):1651-67. PubMed PMID: doi:10.3390/v4091651.
92. Capul AA, Perez M, Burke E, Kunz S, Buchmeier MJ, de la Torre JC. Arenavirus Z-Glycoprotein Association Requires Z Myristoylation but Not Functional RING or Late Domains. Journal of virology. 2007;81(17):9451-60. doi: 10.1128/jvi.00499-07.
93. Casabona JC, Levingston Macleod JM, Loureiro ME, Gomez GA, Lopez N. The RING Domain and the L79 Residue of Z Protein Are Involved in both the Rescue of Nucleocapsids and the Incorporation of Glycoproteins into Infectious Chimeric Arenavirus-Like Particles. Journal of virology. 2009;83(14):7029-39. doi: 10.1128/jvi.00329-09.
94. Ortiz-Riaño E, Cheng BYH, de la Torre JC, Martínez-Sobrido L. The C-Terminal Region of Lymphocytic Choriomeningitis Virus Nucleoprotein Contains Distinct and Segregable Functional Domains Involved in NP-Z Interaction and Counteraction of the Type I Interferon Response. Journal of virology. 2011;85(24):13038-48. doi: 10.1128/jvi.05834-11.
95. Levingston Macleod JM, D'Antuono A, Loureiro ME, Casabona JC, Gomez GA, Lopez N. Identification of Two Functional Domains within the Arenavirus Nucleoprotein. Journal of virology. 2011;85(5):2012-23. doi: 10.1128/jvi.01875-10.

96. Wang J, Danzy S, Kumar N, Ly H, Liang Y. Biological roles and functional mechanisms of arenavirus Z protein in viral replication. Journal of virology. 2012;86(18):9794-801. doi: 10.1128/JVI.00385-12. PubMed PMID: 22761375; PubMed Central PMCID: PMC3446593.
97. Kentsis A, Gordon RE, Borden KLB. Self-assembly properties of a model RING domain. Proceedings of the National Academy of Sciences. 2002;99(2):667-72. doi: 10.1073/pnas.012317299.
98. Wolff S, Ebihara H, Groseth A. Arenavirus budding: a common pathway with mechanistic differences. Viruses. 2013;5(2):528-49. doi: 10.3390/v5020528. PubMed PMID: 23435234; PubMed Central PMCID: PMC3640512.
99. Pinschewer DD, Perez M, de la Torre JC. Dual Role of the Lymphocytic Choriomeningitis Virus Intergenic Region in Transcription Termination and Virus Propagation. Journal of virology. 2005;79(7):4519-26. doi: 10.1128/jvi.79.7.4519-4526.2005.
100. Smelt SC, Borrow P, Kunz S, Cao W, Tishon A, Lewicki H, Campbell KP, Oldstone MBA. Differences in Affinity of Binding of Lymphocytic Choriomeningitis Virus Strains to the Cellular Receptor α-Dystroglycan Correlate with Viral Tropism and Disease Kinetics. Journal of virology. 2001;75(1):448-57. doi: 10.1128/jvi.75.1.448-457.2001.
101. Andersen KG, Shylakhter I, Tabrizi S, Grossman SR, Happi CT, Sabeti PC. Genome-wide scans provide evidence for positive selection of genes implicated in Lassa fever. Philosophical Transactions of the Royal Society B: Biological Sciences. 2012;367(1590):868-77. doi: 10.1098/rstb.2011.0299.
102. Sabeti PC, Varilly P, Fry B, Lohmueller J, Hostetter E, Cotsapas C, Xie X, Byrne EH, McCarroll SA, Gaudet R, Schaffner SF, Lander ES. Genome-wide detection and characterization of positive selection in human populations. Nature. 2007;449(7164):913-8
103. Peters CJ. Human infection with arenaviruses in the Americas. Current topics in microbiology and immunology. 2002;262:65-74. Epub 2002/05/04. PubMed PMID: 11987808.
104. Maiztegui JI. Clinical and epidemiological patterns of Argentine haemorrhagic fever. Bull World Health Organ. 1975;52(4-6):567-75. PubMed PMID: 1085212; PubMed Central PMCID: PMC2366633.
105. Abraham J, Kwong JA, Albariño CG, Lu JG, Radoshitzky SR, Salazar-Bravo J, Farzan M, Spiropoulou CF, Choe H. Host-Species Transferrin Receptor 1 Orthologs Are Cellular Receptors for Nonpathogenic New World Clade B Arenaviruses. PLoS pathogens. 2009;5(4):e1000358. doi: 10.1371/journal.ppat.1000358.
106. Reignier T, Oldenburg J, Flanagan ML, Hamilton GA, Martin VK, Cannon PM. Receptor use by the Whitewater Arroyo virus glycoprotein. Virology. 2008;371(2):439-46. doi: 10.1016/j.virol.2007.10.004.
107. Kumar N, Wang J, Lan S, Danzy S, McLay Schelde L, Seladi-Schulman J, Ly H, Liang Y. Characterization of virulence-associated determinants in the envelope glycoprotein of Pichinde virus. Virology. 2012;433(1):97-103. doi:

10.1016/j.virol.2012.07.009. PubMed PMID: 22877842; PubMed Central PMCID: PMC3444631.
108. Aronson J, Herzog N, Jerrells T. Pathological and virological features of arenavirus disease in guinea pigs. Comparison of two Pichinde virus strains. Am J Pathol. 1994;145:228-35.
109. Jahrling PB, Hesse RA, Rhoderick JB, Elwell MA, Moe JB. Pathogenesis of a Pichinde Virus Strain Adapted to Produce Lethal Infections in Guinea Pigs. Infection and Immunity. 1981;32(2):872-80.
110. Albariño CG, Bird BH, Chakrabarti AK, Dodd KA, Flint M, Bergeron É, White DM, Nichol ST. The Major Determinant of Attenuation in Mice of the Candid1 Vaccine for Argentine Hemorrhagic Fever Is Located in the G2 Glycoprotein Transmembrane Domain. Journal of virology. 2011;85(19):10404-8. doi: 10.1128/jvi.00856-11.
111. Droniou-Bonzom ME, Reignier T, Oldenburg JE, Cox AU, Exline CM, Rathbun JY, Cannon PM. Substitutions in the Glycoprotein (GP) of the Candid#1 Vaccine Strain of Junin Virus Increase Dependence on Human Transferrin Receptor 1 for Entry and Destabilize the Metastable Conformation of GP. Journal of virology. 2011;85(24):13457-62. doi: 10.1128/jvi.05616-11.
112. Lukashevich IS, Carrion R, Jr., Salvato MS, Mansfield K, Brasky K, Zapata J, Cairo C, Goicochea M, Hoosien GE, Ticer A, Bryant J, Davis H, Hammamieh R, Mayda M, Jett M, Patterson J. Safety, immunogenicity, and efficacy of the ML29 reassortant vaccine for Lassa fever in small non-human primates. Vaccine. 2008;26(41):5246-54. Epub 2008/08/12. doi: 10.1016/j.vaccine.2008.07.057. PubMed PMID: 18692539; PubMed Central PMCID: PMC2582173.
113. Carrion R, Jr., Patterson JL, Johnson C, Gonzales M, Moreira CR, Ticer A, Brasky K, Hubbard GB, Moshkoff D, Zapata J, Salvato MS, Lukashevich IS. A ML29 reassortant virus protects guinea pigs against a distantly related Nigerian strain of Lassa virus and can provide sterilizing immunity. Vaccine. 2007;25(20):4093-102. PubMed PMID: 17360080.
114. Harnish DG, Dimock K, Bishop DH, Rawls WE. Gene mapping in Pichinde virus: assignment of viral polypeptides to genomic L and S RNAs. Journal of virology. 1983;46(2):638-41. PubMed PMID: 6302325; PubMed Central PMCID: PMC255169.
115. Riviere Y, Oldstone MB. Genetic reassortants of lymphocytic choriomeningitis virus: unexpected disease and mechanism of pathogenesis. Journal of virology. 1986;59(2):363-8. PubMed PMID: 2426464; PubMed Central PMCID: PMC253085.
116. Lukashevich IS, Carrion Jr R, Salvato MS, Mansfield K, Brasky K, Zapata J, Cairo C, Goicochea M, Hoosien GE, Ticer A, Bryant J, Davis H, Hammamieh R, Mayda M, Jett M, Patterson J. Safety, immunogenicity, and efficacy of the ML29 reassortant vaccine for Lassa fever in small non-human primates. Vaccine. 2008;26(41):5246-54. doi: 10.1016/j.vaccine.2008.07.057.
117. Xing J, Ly H, Liang Y. The Z proteins of pathogenic but not nonpathogenic arenaviruses inhibit RIG-I-like receptor-dependent interferon production. Journal of virology. 2015;89(5):2944-55. doi: 10.1128/JVI.03349-14. PubMed PMID: 25552708; PubMed Central PMCID: PMC4325705.

118. Fan L, Briese T, Lipkin WI. Z Proteins of New World Arenaviruses Bind RIG-I and Interfere with Type I Interferon Induction. Journal of virology. 2010;84(4):1785-91. doi: 10.1128/jvi.01362-09.
119. Moshkoff DA, Salvato MS, Lukashevich IS. Molecular characterization of a reassortant virus derived from Lassa and Mopeia viruses. Virus genes. 2007;34(2):169-76. Epub 2006/12/05. doi: 10.1007/s11262-006-0050-3. PubMed PMID: 17143722; PubMed Central PMCID: PMC1892610.
120. Johnson KM, McCormick JB, Webb PA, Smith ES, Elliott LH, King IJ. Clinical Virology of Lassa Fever in Hospitalized Patients. Journal of Infectious Diseases. 1987;155(3):456-64. doi: 10.1093/infdis/155.3.456.
121. Bergthaler A, Flatz L, Hegazy AN, Johnson S, Horvath E, Löhning M, Pinschewer DD. Viral replicative capacity is the primary determinant of lymphocytic choriomeningitis virus persistence and immunosuppression. Proceedings of the National Academy of Sciences. 2010;107(50):21641-6. doi: 10.1073/pnas.1011998107.
122. Matloubian M, Kolhekar SR, Somasundaram T, Ahmed R. Molecular determinants of macrophage tropism and viral persistence: importance of single amino acid changes in the polymerase and glycoprotein of lymphocytic choriomeningitis virus. Journal of virology. 1993;67(12):7340-9.
123. Albariño CG, Bird BH, Chakrabarti AK, Dodd KA, Erickson BR, Nichol ST. Efficient Rescue of Recombinant Lassa Virus Reveals the Influence of S Segment Noncoding Regions on Virus Replication and Virulence. Journal of virology. 2011;85(8):4020-4. doi: 10.1128/jvi.02556-10.
124. McLay L, Lan S, Ansari A, Liang Y, Ly H. Identification of virulence determinants within the L genomic segment of the pichinde arenavirus. Journal of virology. 2013;87(12):6635-43. doi: 10.1128/JVI.00044-13. PubMed PMID: 23552411; PubMed Central PMCID: PMC3676128.
125. Martínez-Sobrido L, Zúñiga EI, Rosario D, García-Sastre A, de la Torre JC. Inhibition of the Type I Interferon Response by the Nucleoprotein of the Prototypic Arenavirus Lymphocytic Choriomeningitis Virus. Journal of virology. 2006;80(18):9192-9. doi: 10.1128/jvi.00555-06.
126. Jiang X, Huang Q, Wang W, Dong H, Ly H, Liang Y, Dong C. Structures of arenaviral nucleoproteins with triphosphate dsRNA reveal a unique mechanism of immune suppression. The Journal of biological chemistry. 2013;288(23):16949-59. doi: 10.1074/jbc.M112.420521. PubMed PMID: 23615902; PubMed Central PMCID: PMC3675627.
127. Hastie KM, Kimberlin CR, Zandonatti MA, MacRae IJ, Saphire EO. Structure of the Lassa virus nucleoprotein reveals a dsRNA-specific 3′ to 5′ exonuclease activity essential for immune suppression. Proceedings of the National Academy of Sciences. 2011;108(6):2396-401. doi: 10.1073/pnas.1016404108.
128. Qinfeng Huang JS, Shuiyun Lan, Yanqin Zhou, Junji Xing, Changjiang Dong, Yuying Liang, Hinh Ly. In vitro and in vivo characterizations of the Pichinde viral NP exoribonuclease function. Journal of virology. 2015.
129. Carnec X, Baize S, Reynard S, Diancourt L, Caro V, Tordo N, Bouloy M. Lassa virus nucleoprotein mutants generated by reverse genetics induce a robust type I

interferon response in human dendritic cells and macrophages. Journal of virology. 2011;85(22):12093-7. Epub 2011/09/02. doi: 10.1128/JVI.00429-11. PubMed PMID: 21880754; PubMed Central PMCID: PMC3209271.
130. Russier M, Reynard S, Carnec X, Baize S. The exonuclease domain of Lassa virus nucleoprotein is involved in antigen-presenting-cell-mediated NK cell responses. Journal of virology. 2014;88(23):13811-20. doi: 10.1128/JVI.01908-14. PubMed PMID: 25253342; PubMed Central PMCID: PMC4248958.
131. Pythoud C, Rodrigo WWSI, Pasqual G, Rothenberger S, Martínez-Sobrido L, de la Torre JC, Kunz S. Arenavirus Nucleoprotein Targets Interferon Regulatory Factor-Activating Kinase IKKε. Journal of virology. 2012;86(15):7728-38. doi: 10.1128/jvi.00187-12.
132. Rodrigo WWSI, Ortiz-Riaño E, Pythoud C, Kunz S, de la Torre JC, Martínez-Sobrido L. Arenavirus Nucleoproteins Prevent Activation of Nuclear Factor Kappa B. Journal of virology. 2012;86(15):8185-97. doi: 10.1128/jvi.07240-11.
133. Zhou S, Cerny AM, Zacharia A, Fitzgerald KA, Kurt-Jones EA, Finberg RW. Induction and Inhibition of Type I Interferon Responses by Distinct Components of Lymphocytic Choriomeningitis Virus. Journal of virology. 2010;84(18):9452-62. doi: 10.1128/jvi.00155-10.
134. Mahanty S, Hutchinson K, Agarwal S, Mcrae M, Rollin PE, Pulendran B. Cutting Edge: Impairment of Dendritic Cells and Adaptive Immunity by Ebola and Lassa Viruses. The Journal of Immunology. 2003;170(6):2797-801.
135. Baize S, Kaplon J, Faure C, Pannetier D, Georges-Courbot M-C, Deubel V. Lassa Virus Infection of Human Dendritic Cells and Macrophages Is Productive but Fails to Activate Cells. The Journal of Immunology. 2004;172(5):2861-9.
136. Lukashevich IS, Maryankova R, Vladyko AS, Nashkevich N, Koleda S, Djavani M, Horejsh D, Voitenok NN, Salvato MS. Lassa and Mopeia virus replication in human monocytes/macrophages and in endothelial cells: different effects on IL-8 and TNF-alpha gene expression. J Med Virol. 1999;59(4):552-60. Epub 1999/10/27. PubMed PMID: 10534741; PubMed Central PMCID: PMC2391009.
137. Pannetier D, Faure C, Georges-Courbot M-C, Deubel V, Baize S. Human Macrophages, but Not Dendritic Cells, Are Activated and Produce Alpha/Beta Interferons in Response to Mopeia Virus Infection. Journal of virology. 2004;78(19):10516-24. doi: 10.1128/jvi.78.19.10516-10524.2004.
138. Groseth A, Hoenen T, Weber M, Wolff S, Herwig A, Kaufmann A, Becker S. Tacaribe Virus but Not Junin Virus Infection Induces Cytokine Release from Primary Human Monocytes and Macrophages. PLoS neglected tropical diseases. 2011;5(5):e1137. doi: 10.1371/journal.pntd.0001137.
139. Lukashevich IS. The search for animal models for Lassa fever vaccine development. Expert review of vaccines. 2013;12(1):71-86. doi: 10.1586/erv.12.139. PubMed PMID: 23256740; PubMed Central PMCID: PMC3564576.
140. Vela E. Animal models, prophylaxis, and therapeutics for arenavirus infections. Viruses. 2012;4(9):1802-29. Epub 2012/11/22. doi: 10.3390/v4091802. PubMed PMID: 23170184; PubMed Central PMCID: PMC3499831.

141. Safronetz D, Geisbert TW, Feldmann H. Animal models for highly pathogenic emerging viruses. Current opinion in virology. 2013;3(2):205-9. doi: 10.1016/j.coviro.2013.01.001. PubMed PMID: 23403208; PubMed Central PMCID: PMC3644300.
142. Jahrling PB, Smith S, Hesse RA, Rhoderick JB. Pathogenesis of Lassa virus infection in guinea pigs. Infection and immunity. 1982;37(2):771-8. PubMed PMID: 6749685.
143. Peters CJ, Jahrling PB, Liu CT, Kenyon RH, McKee KT, Jr., Barrera Oro JG. Experimental studies of arenaviral hemorrhagic fevers. Current topics in microbiology and immunology. 1987;134:5-68. PubMed PMID: 3034512.
144. Carrion R, Jr., Brasky K, Mansfield K, Johnson C, Gonzales M, Ticer A, Lukashevich I, Tardif S, Patterson J. Lassa virus infection in experimentally infected marmosets: liver pathology and immunophenotypic alterations in target tissues. Journal of virology. 2007;81(12):6482-90. doi: 10.1128/JVI.02876-06. PubMed PMID: 17409137; PubMed Central PMCID: PMC1900113.
145. Scott EP, Aronson JF. Cytokine patterns in a comparative model of arenavirus haemorrhagic fever in guinea pigs. J Gen Virol. 2008;89(Pt 10):2569-79. PubMed PMID: 18796726.
146. Liang Y, Lan S, Ly H. Molecular determinants of Pichinde virus infection of guinea pigs--a small animal model system for arenaviral hemorrhagic fevers. Annals of the New York Academy of Sciences. 2009;1171 Suppl 1:E65-74. doi: 10.1111/j.1749-6632.2009.05051.x. PubMed PMID: 19751405; PubMed Central PMCID: PMC2774822.
147. Jahrling PB, Hesse RA, Eddy GA, Johnson KM, Callis RT, Stephen EL. Lassa virus infection of rhesus monkeys: pathogenesis and treatment with ribavirin. The Journal of infectious diseases. 1980;141(5):580-9. PubMed PMID: 6768812.
148. Lange JV, Mitchell SW, McCormick JB, Walker DH, Evatt BL, Ramsey RR. Kinetic study of platelets and fibrinogen in Lassa virus-infected monkeys and early pathologic events in Mopeia virus-infected monkeys. The American journal of tropical medicine and hygiene. 1985;34(5):999-1007. PubMed PMID: 4037187.
149. Walker DH, McCormick JB, Johnson KM, Webb PA, Komba-Kono G, Elliot LH, Gardner JJ. Pathologic and virologic study of fatal Lassa fever in man. Am J Pathol. 1982;107(3):249-356.
150. Callis RT, Jahrling PB, DePaoli A. Pathology of Lassa virus infection in the rhesus monkey. The American journal of tropical medicine and hygiene. 1982;31(5):1038-45. PubMed PMID: 7125056.
151. Fisher-Hoch SP, Mitchell SW, Sasso DR, Lange JV, Ramsey R, McCormick JB. Physiological and immunologic disturbances associated with shock in a primate model of Lassa fever. The Journal of infectious diseases. 1987;155(3):465-74. PubMed PMID: 3543155.
152. Hensley LE, Smith MA, Geisbert JB, Fritz EA, Daddario-DiCaprio KM, Larsen T, Geisbert TW. Pathogenesis of Lassa fever in cynomolgus macaques. Virol J. 2011;8:205. Epub 2011/05/10. doi: 10.1186/1743-422X-8-205. PubMed PMID: 21548931; PubMed Central PMCID: PMC3104370.

153. Safronetz D, Strong JE, Feldmann F, Haddock E, Sogoba N, Brining D, Geisbert TW, Scott DP, Feldmann H. A recently isolated Lassa virus from Mali demonstrates atypical clinical disease manifestations and decreased virulence in cynomolgus macaques. The Journal of infectious diseases. 2013;207(8):1316-27. doi: 10.1093/infdis/jit004. PubMed PMID: 23303805; PubMed Central PMCID: PMC3603532.
154. Rasmussen AL, Tchitchek N, Safronetz D, Carter VS, Williams CM, Haddock E, Korth MJ, Feldmann H, Katze MG. Delayed inflammatory and cell death responses are associated with reduced pathogenicity in Lujo virus-infected cynomolgus macaques. Journal of virology. 2015;89(5):2543-52. doi: 10.1128/JVI.02246-14. PubMed PMID: 25520505; PubMed Central PMCID: PMC4325716.
155. Baize S, Marianneau P, Loth P, Reynard S, Journeaux A, Chevallier M, Tordo N, Deubel V, Contamin H. Early and Strong Immune Responses Are Associated with Control of Viral Replication and Recovery in Lassa Virus-Infected Cynomolgus Monkeys. Journal of virology. 2009;83(11):5890-903. doi: 10.1128/jvi.01948-08.
156. McLay L, Ansari A, Liang Y, Ly H. Targeting virulence mechanisms for the prevention and therapy of arenaviral hemorrhagic fever. Antiviral research. 2013;97(2):81-92. doi: 10.1016/j.antiviral.2012.12.003. PubMed PMID: 23261843; PubMed Central PMCID: PMC3563861.
157. Zapata JC, Salvato MS. Arenavirus variations due to host-specific adaptation. Viruses. 2013;5(1):241-78. doi: 10.3390/v5010241. PubMed PMID: 23344562; PubMed Central PMCID: PMC3564120.
158. Johnson KM, McCormick JB, Webb PA, Smith ES, Elliott LH, King IJ. Clinical virology of Lassa fever in hospitalized patients. The Journal of infectious diseases. 1987;155(3):456-64. PubMed PMID: 3805773.
159. McCormick JB, King IJ, Webb PA, Scribner CL, Craven RB, Johnson KM, Elliott LH, Belmont-Williams R. Lassa fever. Effective therapy with ribavirin. The New England journal of medicine. 1986;314(1):20-6. doi: 10.1056/NEJM198601023140104. PubMed PMID: 3940312.
160. Shao J, Liang Y, Ly H. Human hemorrhagic Fever causing arenaviruses: molecular mechanisms contributing to virus virulence and disease pathogenesis. Pathogens. 2015;4(2):283-306. doi: 10.3390/pathogens4020283. PubMed PMID: 26011826; PubMed Central PMCID: PMC4493475.
161. Beyer WR, Popplau D, Garten W, von Laer D, Lenz O. Endoproteolytic processing of the lymphocytic choriomeningitis virus glycoprotein by the subtilase SKI-1/S1P. Journal of virology. 2003;77(5):2866-72. PubMed PMID: 12584310; PubMed Central PMCID: PMC149737.
162. Lenz O, ter Meulen J, Klenk HD, Seidah NG, Garten W. The Lassa virus glycoprotein precursor GP-C is proteolytically processed by subtilase SKI-1/S1P. Proceedings of the National Academy of Sciences of the United States of America. 2001;98(22):12701-5. doi: 10.1073/pnas.221447598. PubMed PMID: 11606739; PubMed Central PMCID: PMC60117.
163. Saunders AA, Ting JP, Meisner J, Neuman BW, Perez M, de la Torre JC, Buchmeier MJ. Mapping the landscape of the lymphocytic choriomeningitis virus stable

signal peptide reveals novel functional domains. Journal of virology. 2007;81(11):5649-57. doi: 10.1128/JVI.02759-06. PubMed PMID: 17376927; PubMed Central PMCID: PMC1900251.
164. Eichler R, Lenz O, Strecker T, Eickmann M, Klenk HD, Garten W. Lassa virus glycoprotein signal peptide displays a novel topology with an extended endoplasmic reticulum luminal region. The Journal of biological chemistry. 2004;279(13):12293-9. PubMed PMID: 14709548.
165. Agnihothram SS, York J, Trahey M, Nunberg JH. Bitopic membrane topology of the stable signal peptide in the tripartite Junin virus GP-C envelope glycoprotein complex. Journal of virology. 2007;81(8):4331-7. doi: 10.1128/JVI.02779-06. PubMed PMID: 17267481; PubMed Central PMCID: PMC1866146.
166. Messina EL, York J, Nunberg JH. Dissection of the role of the stable signal peptide of the arenavirus envelope glycoprotein in membrane fusion. Journal of virology. 2012;86(11):6138-45. doi: 10.1128/JVI.07241-11. PubMed PMID: 22438561; PubMed Central PMCID: PMC3372177.
167. Burri DJ, da Palma JR, Kunz S, Pasquato A. Envelope glycoprotein of arenaviruses. Viruses. 2012;4(10):2162-81. doi: 10.3390/v4102162. PubMed PMID: 23202458; PubMed Central PMCID: PMC3497046.
168. Jahrling PB, Hesse RA, Rhoderick JB, Elwell MA, Moe JB. Pathogenesis of a pichinde virus strain adapted to produce lethal infections in guinea pigs. Infection and immunity. 1981;32(2):872-80. PubMed PMID: 6265367; PubMed Central PMCID: PMC351524.
169. Qian C, Jahrling PB, Peters CJ, Liu CT. Cardiovascular and pulmonary responses to Pichinde virus infection in strain 13 guinea pigs. Laboratory animal science. 1994;44(6):600-7. PubMed PMID: 7898034.
170. Lucia HL, Coppenhaver DH, Harrison RL, Baron S. The effect of an arenavirus infection on liver morphology and function. The American journal of tropical medicine and hygiene. 1990;43(1):93-8. PubMed PMID: 1974392.
171. Cosgriff TM, Jahrling PB, Chen JP, Hodgson LA, Lewis RM, Green DE, Smith JI. Studies of the coagulation system in arenaviral hemorrhagic fever: experimental infection of strain 13 guinea pigs with Pichinde virus. The American journal of tropical medicine and hygiene. 1987;36(2):416-23. PubMed PMID: 3030150.
172. Aronson JF, Herzog NK, Jerrells TR. Pathological and virological features of arenavirus disease in guinea pigs. Comparison of two Pichinde virus strains. The American journal of pathology. 1994;145(1):228-35. PubMed PMID: 8030751; PubMed Central PMCID: PMC1887300.
173. Lan S, McLay Schelde L, Wang J, Kumar N, Ly H, Liang Y. Development of infectious clones for virulent and avirulent pichinde viruses: a model virus to study arenavirus-induced hemorrhagic fevers. Journal of virology. 2009;83(13):6357-62. doi: 10.1128/JVI.00019-09. PubMed PMID: 19386714; PubMed Central PMCID: PMC2698569.
174. Leist TP, Ruedi E, Zinkernagel RM. Virus-triggered immune suppression in mice caused by virus-specific cytotoxic T cells. J Exp Med. 1988;167(5):1749-54. Epub 1988/05/01. PubMed PMID: 2966846; PubMed Central PMCID: PMC2188942.

175. York J, Nunberg JH. Role of the stable signal peptide of Junin arenavirus envelope glycoprotein in pH-dependent membrane fusion. Journal of virology. 2006;80(15):7775-80. doi: 10.1128/JVI.00642-06. PubMed PMID: 16840359; PubMed Central PMCID: PMC1563716.
176. York J, Nunberg JH. Distinct requirements for signal peptidase processing and function in the stable signal peptide subunit of the Junin virus envelope glycoprotein. Virology. 2007;359(1):72-81. doi: 10.1016/j.virol.2006.08.048. PubMed PMID: 17045626.
177. York J, Nunberg JH. Intersubunit interactions modulate pH-induced activation of membrane fusion by the Junin virus envelope glycoprotein GPC. Journal of virology. 2009;83(9):4121-6. doi: 10.1128/JVI.02410-08. PubMed PMID: 19224989; PubMed Central PMCID: PMC2668491.
178. Bederka LH, Bonhomme CJ, Ling EL, Buchmeier MJ. Arenavirus stable signal peptide is the keystone subunit for glycoprotein complex organization. mBio. 2014;5(6):e02063. doi: 10.1128/mBio.02063-14. PubMed PMID: 25352624; PubMed Central PMCID: PMC4217180.
179. Briknarova K, Thomas CJ, York J, Nunberg JH. Structure of a zinc-binding domain in the Junin virus envelope glycoprotein. The Journal of biological chemistry. 2011;286(2):1528-36. doi: 10.1074/jbc.M110.166025. PubMed PMID: 21068387; PubMed Central PMCID: PMC3020761.
180. Saunders AA, Ting JP, Meisner J, Neuman BW, Perez M, de la Torre JC, Buchmeier MJ. Mapping the landscape of the LCMV stable signal peptide reveals novel functional domains. J Virol. 2007. PubMed PMID: 17376927.
181. York J, Nunberg JH. Intersubunit interactions modulate pH-induced activation of membrane fusion by the Junin virus envelope glycoprotein GPC. J Virol. 2009. PubMed PMID: 19224989.
182. Naldini L, Blomer U, Gallay P, Ory D, Mulligan R, Gage FH, Verma IM, Trono D. In vivo gene delivery and stable transduction of nondividing cells by a lentiviral vector. Science. 1996;272(5259):263-7. PubMed PMID: 8602510.
183. Bergthaler A, Flatz L, Hegazy AN, Johnson S, Horvath E, Lohning M, Pinschewer DD. Viral replicative capacity is the primary determinant of lymphocytic choriomeningitis virus persistence and immunosuppression. Proceedings of the National Academy of Sciences of the United States of America. 2010;107(50):21641-6. doi: 10.1073/pnas.1011998107. PubMed PMID: 21098292; PubMed Central PMCID: PMC3003068.
184. York J, Nunberg JH. A novel zinc-binding domain is essential for formation of the functional Junin virus envelope glycoprotein complex. Journal of virology. 2007;81(24):13385-91. doi: 10.1128/JVI.01785-07. PubMed PMID: 17928348; PubMed Central PMCID: PMC2168868.
185. York J, Romanowski V, Lu M, Nunberg JH. The signal peptide of the Junin arenavirus envelope glycoprotein is myristoylated and forms an essential subunit of the mature G1-G2 complex. Journal of virology. 2004;78(19):10783-92. doi: 10.1128/JVI.78.19.10783-10792.2004. PubMed PMID: 15367645; PubMed Central PMCID: PMC516395.

186. Farazi TA, Waksman G, Gordon JI. The biology and enzymology of protein N-myristoylation. The Journal of biological chemistry. 2001;276(43):39501-4. doi: 10.1074/jbc.R100042200. PubMed PMID: 11527981.
187. Maniatis T, Fritsch, E.F. and Sambrook, J. Molecular Cloning: A Laboratory Manual. Cold Spring Harbor University Press, Cold Spring Harbor. 1982.
188. Frame JD, Baldwin JM, Jr., Gocke DJ, Troup JM. Lassa fever, a new virus disease of man from West Africa. I. Clinical description and pathological findings. The American journal of tropical medicine and hygiene. 1970;19(4):670-6. PubMed PMID: 4246571.
189. Knobloch J, McCormick JB, Webb PA, Dietrich M, Schumacher HH, Dennis E. Clinical observations in 42 patients with Lassa fever. Tropenmed Parasitol. 1980;31(4):389-98. PubMed PMID: 7233535.
190. de Bracco MM, Rimoldi MT, Cossio PM, Rabinovich A, Maiztegui JI, Carballal G, Arana RM. Argentine hemorrhagic fever. Alterations of the complement system and anti-Junin-virus humoral response. The New England journal of medicine. 1978;299(5):216-21. PubMed PMID: 207985.
191. Kenyon RH, Canonico PG, Green DE, Peters CJ. Effect of ribavirin and tributylribavirin on argentine hemorrhagic fever (Junin virus) in guinea pigs. Antimicrob Agents Chemother. 1986;29(3):521-3. PubMed PMID: 3013087.
192. Enria DA, Barrera Oro JG. Junin virus vaccines. Current topics in microbiology and immunology. 2002;263:239-61. PubMed PMID: 11987817.
193. Harrison LH, Halsey NA, McKee KT, Jr., Peters CJ, Barrera Oro JG, Briggiler AM, Feuillade MR, Maiztegui JI. Clinical case definitions for Argentine hemorrhagic fever. Clinical infectious diseases : an official publication of the Infectious Diseases Society of America. 1999;28(5):1091-4. doi: 10.1086/514749. PubMed PMID: 10452640.
194. Buchmeier MJ, De La Torre JC, Peters CJ. Arenaviridae: the viruses and their replication. In: Knipe DM, Howley PM, editors. Fields Virology. 5th ed. Philadelphia, PA: Lippincott Williams & Wilkins; 2007. p. 1791-827.
195. Meulen J, Badusche M, Satoguina J, Strecker T, Lenz O, Loeliger C, Sakho M, Koulemou K, Koivogui L, Hoerauf A. Old and New World arenaviruses share a highly conserved epitope in the fusion domain of the glycoprotein 2, which is recognized by Lassa virus-specific human CD4+ T-cell clones. Virology. 2004;321(1):134-43. Epub 2004/03/23. doi: 10.1016/j.virol.2003.12.013. PubMed PMID: 15033572.
196. Igonet S, Vaney MC, Vonhrein C, Bricogne G, Stura EA, Hengartner H, Eschli B, Rey FA. X-ray structure of the arenavirus glycoprotein GP2 in its postfusion hairpin conformation. Proceedings of the National Academy of Sciences of the United States of America. 2011;108(50):19967-72. Epub 2011/11/30. doi: 10.1073/pnas.1108910108. PubMed PMID: 22123988; PubMed Central PMCID: PMC3250147.
197. Shao J, Liu X, Ly H, Liang Y. Characterization of the Glycoprotein Stable Signal Peptide in Mediating Pichinde Virus Replication and Virulence. Journal of virology. 2016;90(22):10390-7. doi: 10.1128/JVI.01154-16. PubMed PMID: 27630230.

198. Enria DA, Briggiler AM, Sanchez Z. Treatment of Argentine hemorrhagic fever. Antiviral research. 2008;78(1):132-9. Epub 2007/12/07. doi: 10.1016/j.antiviral.2007.10.010. PubMed PMID: 18054395.
199. Meyer B, Ly H. Inhibition of Innate Immune Responses Is Key to Pathogenesis by Arenaviruses. Journal of virology. 2016;90(8):3810-8. doi: 10.1128/JVI.03049-15. PubMed PMID: 26865707; PubMed Central PMCID: PMC4810556.
200. Gack MU. Mechanisms of RIG-I-like receptor activation and manipulation by viral pathogens. Journal of virology. 2014;88(10):5213-6. doi: 10.1128/JVI.03370-13. PubMed PMID: 24623415; PubMed Central PMCID: PMC4019093.
201. Huang C, Kolokoltsova OA, Yun NE, Seregin AV, Poussard AL, Walker AG, Brasier AR, Zhao Y, Tian B, de la Torre JC, Paessler S. Junin Virus Infection Activates the Type I Interferon Pathway in a RIG-I-Dependent Manner. PLoS Negl Trop Dis. 2012;6(5):e1659. Epub 2012/05/26. doi: 10.1371/journal.pntd.0001659. PubMed PMID: 22629479; PubMed Central PMCID: PMC3358329.
202. Kell AM, Gale M, Jr. RIG-I in RNA virus recognition. Virology. 2015;479-480:110-21. doi: 10.1016/j.virol.2015.02.017. PubMed PMID: 25749629; PubMed Central PMCID: PMCPMC4424084.
203. Chiang JJ, Davis ME, Gack MU. Regulation of RIG-I-like receptor signaling by host and viral proteins. Cytokine Growth Factor Rev. 2014;25(5):491-505. doi: 10.1016/j.cytogfr.2014.06.005. PubMed PMID: 25023063.
204. Sun Z, Ren H, Liu Y, Teeling JL, Gu J. Phosphorylation of RIG-I by casein kinase II inhibits its antiviral response. Journal of virology. 2011;85(2):1036-47. doi: 10.1128/JVI.01734-10. PubMed PMID: 21068236; PubMed Central PMCID: PMC3020001.
205. Wies E, Wang MK, Maharaj NP, Chen K, Zhou S, Finberg RW, Gack MU. Dephosphorylation of the RNA sensors RIG-I and MDA5 by the phosphatase PP1 is essential for innate immune signaling. Immunity. 2013;38(3):437-49. doi: 10.1016/j.immuni.2012.11.018. PubMed PMID: 23499489; PubMed Central PMCID: PMC3616631.
206. Maharaj NP, Wies E, Stoll A, Gack MU. Conventional protein kinase C-alpha (PKC-alpha) and PKC-beta negatively regulate RIG-I antiviral signal transduction. Journal of virology. 2012;86(3):1358-71. doi: 10.1128/JVI.06543-11. PubMed PMID: 22114345; PubMed Central PMCID: PMC3264329.
207. Nistal-Villan E, Gack MU, Martinez-Delgado G, Maharaj NP, Inn KS, Yang H, Wang R, Aggarwal AK, Jung JU, Garcia-Sastre A. Negative role of RIG-I serine 8 phosphorylation in the regulation of interferon-beta production. The Journal of biological chemistry. 2010;285(26):20252-61. doi: 10.1074/jbc.M109.089912. PubMed PMID: 20406818; PubMed Central PMCID: PMC2888438.
208. Oshiumi H, Matsumoto M, Hatakeyama S, Seya T. Riplet/RNF135, a RING finger protein, ubiquitinates RIG-I to promote interferon-beta induction during the early phase of viral infection. The Journal of biological chemistry. 2009;284(2):807-17. doi: 10.1074/jbc.M804259200. PubMed PMID: 19017631.
209. Oshiumi H, Miyashita M, Inoue N, Okabe M, Matsumoto M, Seya T. The ubiquitin ligase Riplet is essential for RIG-I-dependent innate immune responses to RNA

virus infection. Cell Host Microbe. 2010;8(6):496-509. doi: 10.1016/j.chom.2010.11.008. PubMed PMID: 21147464.
210. Oshiumi H, Miyashita M, Matsumoto M, Seya T. A distinct role of Riplet-mediated K63-Linked polyubiquitination of the RIG-I repressor domain in human antiviral innate immune responses. PLoS pathogens. 2013;9(8):e1003533. doi: 10.1371/journal.ppat.1003533. PubMed PMID: 23950712; PubMed Central PMCID: PMC3738492.
211. Gack MU, Nistal-Villan E, Inn KS, Garcia-Sastre A, Jung JU. Phosphorylation-mediated negative regulation of RIG-I antiviral activity. Journal of virology. 2010;84(7):3220-9. doi: 10.1128/JVI.02241-09. PubMed PMID: 20071582; PubMed Central PMCID: PMC2838087.
212. Gack MU, Shin YC, Joo CH, Urano T, Liang C, Sun L, Takeuchi O, Akira S, Chen Z, Inoue S, Jung JU. TRIM25 RING-finger E3 ubiquitin ligase is essential for RIG-I-mediated antiviral activity. Nature. 2007;446(7138):916-20. doi: 10.1038/nature05732. PubMed PMID: 17392790.
213. Versteeg GA, Rajsbaum R, Sanchez-Aparicio MT, Maestre AM, Valdiviezo J, Shi M, Inn KS, Fernandez-Sesma A, Jung J, Garcia-Sastre A. The E3-ligase TRIM family of proteins regulates signaling pathways triggered by innate immune pattern-recognition receptors. Immunity. 2013;38(2):384-98. doi: 10.1016/j.immuni.2012.11.013. PubMed PMID: 23438823; PubMed Central PMCID: PMC3584420.
214. Jiang X, Kinch LN, Brautigam CA, Chen X, Du F, Grishin NV, Chen ZJ. Ubiquitin-induced oligomerization of the RNA sensors RIG-I and MDA5 activates antiviral innate immune response. Immunity. 2012;36(6):959-73. doi: 10.1016/j.immuni.2012.03.022. PubMed PMID: 22705106; PubMed Central PMCID: PMC3412146.
215. Yoneyama M, Kikuchi M, Natsukawa T, Shinobu N, Imaizumi T, Miyagishi M, Taira K, Akira S, Fujita T. The RNA helicase RIG-I has an essential function in double-stranded RNA-induced innate antiviral responses. Nat Immunol. 2004;5(7):730-7. doi: 10.1038/ni1087. PubMed PMID: 15208624.
216. Myong S, Cui S, Cornish PV, Kirchhofer A, Gack MU, Jung JU, Hopfner KP, Ha T. Cytosolic viral sensor RIG-I is a 5'-triphosphate-dependent translocase on double-stranded RNA. Science. 2009;323(5917):1070-4. Epub 2009/01/03. doi: 10.1126/science.1168352. PubMed PMID: 19119185.
217. Patel JR, Jain A, Chou YY, Baum A, Ha T, Garcia-Sastre A. ATPase-driven oligomerization of RIG-I on RNA allows optimal activation of type-I interferon. EMBO Rep. 2013;14(9):780-7. doi: 10.1038/embor.2013.102. PubMed PMID: 23846310; PubMed Central PMCID: PMC3790048.
218. Kok KH, Lui PY, Ng MH, Siu KL, Au SW, Jin DY. The double-stranded RNA-binding protein PACT functions as a cellular activator of RIG-I to facilitate innate antiviral response. Cell Host Microbe. 2011;9(4):299-309. doi: 10.1016/j.chom.2011.03.007. PubMed PMID: 21501829.
219. Patel RC, Sen GC. PACT, a protein activator of the interferon-induced protein kinase, PKR. EMBO J. 1998;17(15):4379-90. doi: 10.1093/emboj/17.15.4379. PubMed PMID: 9687506; PubMed Central PMCID: PMC1170771.

220. Siu KL, Yeung ML, Kok KH, Yuen KS, Kew C, Lui PY, Chan CP, Tse H, Woo PC, Yuen KY, Jin DY. Middle east respiratory syndrome coronavirus 4a protein is a double-stranded RNA-binding protein that suppresses PACT-induced activation of RIG-I and MDA5 in the innate antiviral response. Journal of virology. 2014;88(9):4866-76. doi: 10.1128/JVI.03649-13. PubMed PMID: 24522921; PubMed Central PMCID: PMC3993821.
221. Tawaratsumida K, Phan V, Hrincius ER, High AA, Webby R, Redecke V, Hacker H. Quantitative proteomic analysis of the influenza A virus nonstructural proteins NS1 and NS2 during natural cell infection identifies PACT as an NS1 target protein and antiviral host factor. Journal of virology. 2014;88(16):9038-48. doi: 10.1128/JVI.00830-14. PubMed PMID: 24899174; PubMed Central PMCID: PMC4136281.
222. Luthra P, Ramanan P, Mire CE, Weisend C, Tsuda Y, Yen B, Liu G, Leung DW, Geisbert TW, Ebihara H, Amarasinghe GK, Basler CF. Mutual antagonism between the Ebola virus VP35 protein and the RIG-I activator PACT determines infection outcome. Cell Host Microbe. 2013;14(1):74-84. doi: 10.1016/j.chom.2013.06.010. PubMed PMID: 23870315; PubMed Central PMCID: PMC3875338.
223. Kew C, Lui PY, Chan CP, Liu X, Au SW, Mohr I, Jin DY, Kok KH. Suppression of PACT-induced type I interferon production by herpes simplex virus 1 Us11 protein. Journal of virology. 2013;87(24):13141-9. doi: 10.1128/JVI.02564-13. PubMed PMID: 24067967; PubMed Central PMCID: PMC3838286.
224. Ho TH, Kew C, Lui PY, Chan CP, Satoh T, Akira S, Jin DY, Kok KH. PACT- and RIG-I-Dependent Activation of Type I Interferon Production by a Defective Interfering RNA Derived from Measles Virus Vaccine. Journal of virology. 2015;90(3):1557-68. doi: 10.1128/JVI.02161-15. PubMed PMID: 26608320; PubMed Central PMCID: PMC4719617.
225. Yuen CK, Chan CP, Fung SY, Wang PH, Wong WM, Tang HM, Yuen KS, Chan CP, Jin DY, Kok KH. Suppression of Type I Interferon Production by Human T-Cell Leukemia Virus Type 1 Oncoprotein Tax through Inhibition of IRF3 Phosphorylation. Journal of virology. 2016;90(8):3902-12. doi: 10.1128/JVI.00129-16. PubMed PMID: 26819312; PubMed Central PMCID: PMC4810532.
226. Ding Z, Fang L, Yuan S, Zhao L, Wang X, Long S, Wang M, Wang D, Foda MF, Xiao S. The nucleocapsid proteins of mouse hepatitis virus and severe acute respiratory syndrome coronavirus share the same IFN-beta antagonizing mechanism: attenuation of PACT-mediated RIG-I/ MDA5 activation. Oncotarget. 2017;8(30):49655-70. doi: 10.18632/oncotarget.17912. PubMed PMID: 28591694.
227. Martinez-Sobrido L, Zuniga EI, Rosario D, Garcia-Sastre A, de la Torre JC. Inhibition of the type I interferon response by the nucleoprotein of the prototypic arenavirus lymphocytic choriomeningitis virus. Journal of virology. 2006;80(18):9192-9. Epub 2006/08/31. doi: 10.1128/JVI.00555-06. PubMed PMID: 16940530; PubMed Central PMCID: PMC1563941.
228. Qi X, Lan S, Wang W, Schelde LM, Dong H, Wallat GD, Ly H, Liang Y, Dong C. Cap binding and immune evasion revealed by Lassa nucleoprotein structure. Nature. 2010;468(7325):779-83. doi: 10.1038/nature09605. PubMed PMID: 21085117; PubMed Central PMCID: PMC3057469.

229. Hastie KM, Kimberlin CR, Zandonatti MA, Macrae IJ, Saphire EO. Structure of the Lassa virus nucleoprotein reveals a dsRNA-specific 3' to 5' exonuclease activity essential for immune suppression. Proceedings of the National Academy of Sciences of the United States of America. 2011;108(6):2396-401. Epub 2011/01/26. doi: 1016404108 [pii]

10.1073/pnas.1016404108. PubMed PMID: 21262835.
230. Brunotte L, Kerber R, Shang W, Hauer F, Hass M, Gabriel M, Lelke M, Busch C, Stark H, Svergun DI, Betzel C, Perbandt M, Gunther S. Structure of the Lassa virus nucleoprotein revealed by X-ray crystallography, small-angle X-ray scattering, and electron microscopy. The Journal of biological chemistry. 2011;286(44):38748-56. Epub 2011/09/16. doi: 10.1074/jbc.M111.278838. PubMed PMID: 21917929; PubMed Central PMCID: PMC3207459.
231. Huang Q, Shao J, Lan S, Zhou Y, Xing J, Dong C, Liang Y, Ly H. In vitro and in vivo characterizations of pichinde viral nucleoprotein exoribonuclease functions. Journal of virology. 2015;89(13):6595-607. doi: 10.1128/JVI.00009-15. PubMed PMID: 25878103; PubMed Central PMCID: PMC4468471.
232. Harmon B, Kozina C, Maar D, Carpenter TS, Branda CS, Negrete OA, Carson BD. Identification of critical amino acids within the nucleoprotein of Tacaribe virus important for anti-interferon activity. The Journal of biological chemistry. 2013;288(12):8702-11. doi: 10.1074/jbc.M112.444760. PubMed PMID: 23382389; PubMed Central PMCID: PMC3605688.
233. Hastie KM, Liu T, Li S, King LB, Ngo N, Zandonatti MA, Woods VL, Jr., de la Torre JC, Saphire EO. Crystal structure of the Lassa virus nucleoprotein-RNA complex reveals a gating mechanism for RNA binding. Proceedings of the National Academy of Sciences of the United States of America. 2011;108(48):19365-70. Epub 2011/11/16. doi: 10.1073/pnas.1108515108. PubMed PMID: 22084115; PubMed Central PMCID: PMC3228486.
234. Loo YM, Fornek J, Crochet N, Bajwa G, Perwitasari O, Martinez-Sobrido L, Akira S, Gill MA, Garcia-Sastre A, Katze MG, Gale M, Jr. Distinct RIG-I and MDA5 signaling by RNA viruses in innate immunity. Journal of virology. 2008;82(1):335-45. doi: 10.1128/JVI.01080-07. PubMed PMID: 17942531; PubMed Central PMCID: PMCPMC2224404.
235. Rowe TM, Rizzi M, Hirose K, Peters GA, Sen GC. A role of the double-stranded RNA-binding protein PACT in mouse ear development and hearing. Proceedings of the National Academy of Sciences of the United States of America. 2006;103(15):5823-8. doi: 10.1073/pnas.0601287103. PubMed PMID: 16571658; PubMed Central PMCID: PMC1458657.
236. Marques JT, Devosse T, Wang D, Zamanian-Daryoush M, Serbinowski P, Hartmann R, Fujita T, Behlke MA, Williams BR. A structural basis for discriminating between self and nonself double-stranded RNAs in mammalian cells. Nat Biotechnol. 2006;24(5):559-65. Epub 2006/05/02. doi: 10.1038/nbt1205. PubMed PMID: 16648842.
237. Pichlmair A, Schulz O, Tan CP, Naslund TI, Liljestrom P, Weber F, Reis e Sousa C. RIG-I-mediated antiviral responses to single-stranded RNA bearing 5'-phosphates.

Science. 2006;314(5801):997-1001. doi: 10.1126/science.1132998. PubMed PMID: 17038589.
238. Louber J, Brunel J, Uchikawa E, Cusack S, Gerlier D. Kinetic discrimination of self/non-self RNA by the ATPase activity of RIG-I and MDA5. BMC biology. 2015;13:54. doi: 10.1186/s12915-015-0166-9. PubMed PMID: 26215161; PubMed Central PMCID: PMC4517655.
239. Anchisi S, Guerra J, Garcin D. RIG-I ATPase activity and discrimination of self-RNA versus non-self-RNA. mBio. 2015;6(2):e02349. doi: 10.1128/mBio.02349-14. PubMed PMID: 25736886; PubMed Central PMCID: PMC4358010.
240. Kowalinski E, Lunardi T, McCarthy AA, Louber J, Brunel J, Grigorov B, Gerlier D, Cusack S. Structural basis for the activation of innate immune pattern-recognition receptor RIG-I by viral RNA. Cell. 2011;147(2):423-35. Epub 2011/10/18. doi: 10.1016/j.cell.2011.09.039. PubMed PMID: 22000019.
241. Jiang F, Ramanathan A, Miller MT, Tang GQ, Gale M, Jr., Patel SS, Marcotrigiano J. Structural basis of RNA recognition and activation by innate immune receptor RIG-I. Nature. 2011;479(7373):423-7. Epub 2011/09/29. doi: 10.1038/nature10537. PubMed PMID: 21947008.
242. Luo D, Ding SC, Vela A, Kohlway A, Lindenbach BD, Pyle AM. Structural insights into RNA recognition by RIG-I. Cell. 2011;147(2):409-22. doi: 10.1016/j.cell.2011.09.023. PubMed PMID: 22000018; PubMed Central PMCID: PMC3222294.
243. Leung DW, Amarasinghe GK. Structural insights into RNA recognition and activation of RIG-I-like receptors. Curr Opin Struct Biol. 2012;22(3):297-303. Epub 2012/05/09. doi: 10.1016/j.sbi.2012.03.011. PubMed PMID: 22560447; PubMed Central PMCID: PMC3383332.
244. Nunberg JH, York J. The curious case of arenavirus entry, and its inhibition. Viruses. 2012;4(1):83-101. Epub 2012/02/23. doi: 10.3390/v4010083. PubMed PMID: 22355453; PubMed Central PMCID: PMC3280523.
245. York J, Dai D, Amberg SM, Nunberg JH. pH-induced activation of arenavirus membrane fusion is antagonized by small-molecule inhibitors. Journal of virology. 2008;82(21):10932-9. doi: 10.1128/JVI.01140-08. PubMed PMID: 18768973; PubMed Central PMCID: PMC2573205.
246. Lee SM, Yen HL. Targeting the host or the virus: current and novel concepts for antiviral approaches against influenza virus infection. Antiviral research. 2012;96(3):391-404. Epub 2012/10/02. doi: 10.1016/j.antiviral.2012.09.013. PubMed PMID: 23022351.
247. Lee AM, Rojek JM, Spiropoulou CF, Gundersen AT, Jin W, Shaginian A, York J, Nunberg JH, Boger DL, Oldstone MB, Kunz S. Unique small molecule entry inhibitors of hemorrhagic fever arena viruses. The Journal of biological chemistry. 2008. PubMed PMID: 18474596.
248. Thomas CJ, Casquilho-Gray HE, York J, DeCamp DL, Dai D, Petrilli EB, Boger DL, Slayden RA, Amberg SM, Sprang SR, Nunberg JH. A specific interaction of small molecule entry inhibitors with the envelope glycoprotein complex of the Junin hemorrhagic fever arenavirus. The Journal of biological chemistry. 2011;286(8):6192-

200. Epub 2010/12/17. doi: 10.1074/jbc.M110.196428. PubMed PMID: 21159779; PubMed Central PMCID: PMC3057843.
249. Hope TJ, McDonald D, Huang XJ, Low J, Parslow TG. Mutational analysis of the human immunodeficiency virus type 1 Rev transactivator: essential residues near the amino terminus. Journal of virology. 1990;64(11):5360-6. PubMed PMID: 2120472.
250. Hastie KM, King LB, Zandonatti MA, Saphire EO. Structural Basis for the dsRNA Specificity of the Lassa Virus NP Exonuclease. PLoS ONE. 2012;7(8):e44211. Epub 2012/09/01. doi: 10.1371/journal.pone.0044211. PubMed PMID: 22937163; PubMed Central PMCID: PMC3429428.
251. Chiang JJ, Sparrer KMJ, van Gent M, Lassig C, Huang T, Osterrieder N, Hopfner KP, Gack MU. Viral unmasking of cellular 5S rRNA pseudogene transcripts induces RIG-I-mediated immunity. Nat Immunol. 2018;19(1):53-62. doi: 10.1038/s41590-017-0005-y. PubMed PMID: 29180807; PubMed Central PMCID: PMC5815369.
252. Kato H, Takeuchi O, Sato S, Yoneyama M, Yamamoto M, Matsui K, Uematsu S, Jung A, Kawai T, Ishii KJ, Yamaguchi O, Otsu K, Tsujimura T, Koh CS, Reis e Sousa C, Matsuura Y, Fujita T, Akira S. Differential roles of MDA5 and RIG-I helicases in the recognition of RNA viruses. Nature. 2006;441(7089):101-5. PubMed PMID: 16625202.